Structure and Ozone Decomposition Reactivity of Supported Manganese Oxide Catalysts

Rakesh Radhakrishnan

Dissertation submitted to the Faculty of the
Virginia Polytechnic Institute and State University
in partial fulfillment of the requirements for the degree of

DOCTOR OF PHILOSOPHY
in
Chemical Engineering

Dr. S. Ted Oyama, Chair
Dr. Gerald V. Gibbs
Dr. David F. Cox
Dr. Richey M. Davis
Dr. John G. Dillard

January 18, 2001
Blacksburg, Virginia

Keywords: Manganese Oxides,
Ozone, Oxygen Chemisorption, Temperature Programmed Desorption, Kinetics,
Mechanism, Decomposition, Raman Spectroscopy, X-ray Absorption Fine Structure
Spectroscopy, Ab initio

Structure and Ozone Decomposition Reactivity of Supported Manganese Oxide Catalysts

Rakesh Radhakrishnan

(Abstract)

Manganese oxide catalysts supported on Al_2O_3, ZrO_2, TiO_2 and SiO_2 supports were used to study the effect of support on ozone decomposition kinetics. X-ray diffraction (XRD), *in-situ* laser Raman spectroscopy, temperature programmed oxygen desorption, surface area measurements, extended and near edge x-ray absorption fine structure (EXAFS and NEXAFS) showed that the manganese oxide was highly dispersed on the surface of the supports. EXAFS spectra suggest that the manganese active centers on all of the surfaces were surrounded by five oxygen atoms. These metal centers were of a mononuclear type for the Al_2O_3 supported catalyst and multinuclear for the other supports. NEXAFS spectra for the catalysts showed a chemical shift to lower energy and an intensity change in the L-edge features which followed the trend $Al_2O_3 > ZrO_2 > TiO_2 > SiO_2$. The trends provided insights into the positive role of available empty electronic states required in the reduction step of a redox reaction.

The catalysts were tested for their ozone decomposition reactivity and reaction rates had a fractional order dependency ($n < 1$) with ozone partial pressure. The apparent activation energies for the reaction was low (3 – 15 kJ/mol). The support influenced the desorption step (a reduction step) and this effect manifested itself in the pre-exponential

factor of the rate constant for desorption. Trends for this pre-exponential factor correlated with trends in NEXAFS features and reflected the ease of electron donation from the adsorbed species to the active center.

ACKNOWLEDGEMENTS

First and foremost I would like to express my sincere gratitude to my advisor and committee chair Dr S. Ted Oyama for giving me the opportunity of being involved with several research projects during my tenure here at Virginia Tech. I greatly appreciated his patience, astute observations and unique motivational skills. Furthermore, his emphasis on creative thinking and willigness to share knowledge have helped mould me into a better scientist.

Special thanks go to Dr K. Asakura at Hokkaido University in Japan for the EXAFS measurements and to Dr J. G. Chen at the University of Delaware for the NEXAFS measurements. Thanks also for financial support from the Director, Division of Chemical and Thermal Systems of the National Science Foundation, under Grant CTS-9712047.

I thank all of my committee members for their suggestions and assistance. They have played an integral part in my completing this project. I am particularly grateful to Dr G. V. Gibbs for introducing me to the area of *ab initio* calculations. I am confident that this will be a useful tool I can employ in all of my future research endeavors.

I have had the great pleasure of working with several talented people in a highly collaborative and friendly atmosphere at the Environmental Catalysis and Materials Laboratory here in the chemical engineering department at Virginia Tech. I would like to thank Bala Dhandapani, Anil Prabhu, Rajat Kapoor and Wei Li for training me in various experimental methods used in the laboratory. Thanks also go out to all other group members and colleagues, V. T da Silva, Todd S. t Clair, Viviane Schwartz, Paul Clark, Doo Hwan Lee, Mark Abee, Chad Byrd, Corey Reed, Xianqin Wang, Toby Lucy, Celine Sayag, Yong Kul Lee, Lixiong Zhang and others for the stimulating discussions we've had over the years.

I thank the staff in the chemical engineering department for their help with various matters over the years. Thanks go out to all of my room mates past and present, along with, my martial arts teacher Dr Ed Hampton of the American Martial Arts Center and my friends there, who have made for a very enjoyable living experience here in Blacksburg. I am thankful to my friends from my undergraduate days at the University of Virginia who have made my stay in the United States memorable.

Last but not least I would like to thank my family for their love, patience and encouragement over the years. Thanks go out to my sister Reshma Radhakrishnan for being a great friend over the years. I would like to express my admiration and respect for my parents Mr P. P. Radhakrishnan and Mrs Radhamani Radhakrishnan. They have been the most important people in my life and without their unconditional support and unfettering confidence in me, this dissertation would not have been possible. It is my privelege to be able to dedicate this work to them.

TABLE OF CONTENTS

LIST OF FIGURES

LIST OF TABLES

CHAPTER 1

LITERATURE REVIEW AND OBJECTIVES

1.1 Introduction

Ozone is a chemical compound that has gained a lot of attention in the past few years. It occurs naturally in the stratosphere 15 to 50 km above the earth's surface in concentrations of 1-10 ppm[1]. This layer of ozone in the stratosphere is generated through the action of solar radiation on molecular oxygen. The layer of ozone protects biological organisms on the planet from harmful ultra-violet radiation, which it absorbs. Recently, a lot of concern has been raised about the depletion of the ozone layer due to CFCs (chlorofluorocarbons) released from aerosol cans and refrigeration systems. In addition, there is also concern about increasing ground level ozone released from copiers, printers and water purification systems. This ground level ozone is responsible for nausea, headaches and other respiratory problems especially in work environments. OSHA has thereby declared a permissible exposure limit (PEL) of 0.08 ppm to ozone for a period of eight hours at ground level.

1.2 Literature review

1.2.1 Properties of ozone

Ozone (O_3) is an allotropic form of oxygen. It is a pale blue gas at ambient conditions and it condenses into an indigo blue liquid (-112 ^oC) and freezes to a deep blue-violet solid (-192.5 ^oC). Ozone is the simplest combustible and explosive system, a function of its thermodynamic instability (ΔG^o_{298} = -163 kJ/mol). Ozone decomposes very slowly at temperatures up to 250 ^oC. This slow decomposition is represented well by the fact that 1 mol% of pure gaseous ozone diluted with oxygen at 25 ^oC and atmospheric pressure has a half life of 19.3 yr[2]. The ozone structure is resonance stabilized which is one of the reasons for its resistance against decomposition at low temperatures.

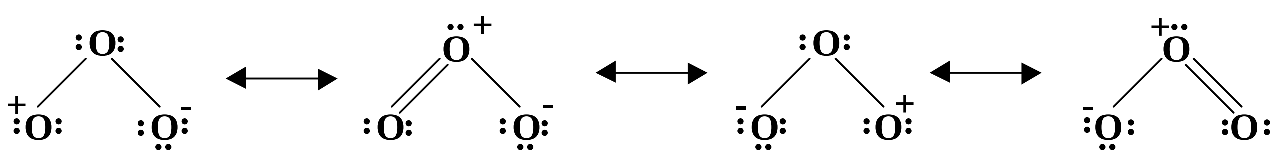

Figure 1. Resonance structures of ozone

1.2.2 Manganese oxide catalysts

There have been several characterization and reactivity studies conducted on supported manganese oxides. Manganese oxides have been used for catalyzing several chemical reactions including the decomposition of nitrous oxide[3, 4, 5], isopropanol[5, 6] ; oxidation of methanol[7], ethanol[8], benzene[9], CO[5, 6, 10], propane[11] and reduction of nitric oxide[12] and nitrobenzene[13]. Oxides of manganese are also being applied in air pollution control technology particularly the decomposition of ozone[14] and volatile organic compounds (VOCs)[15].

Alumina supported manganese oxide is the most frequently studied catalyst appearing in literature. The popular techniques used to characterize the catalyst have been Raman spectroscopy[16, 17], X-ray photoelectron spectrscopy (XPS)[6, 16], X-ray diffraction

(XRD)[3, 17], magnetic susceptibility[3, 18, 19] and electron spin resonance (ESR)[19, 20]. Limited work done has been done on other supports[5, 6, 21, 22] .

1.2.3 Ozone decomposition

Ozone decomposition has been studied extensively as reported in the patent[14] literature. The catalysts used for this process have been noble metals like Pt or Pd, or transition metal oxides of metals like Mn, Co, Ni and Mg. These catalysts have been supported on a range of supports like γ-Al_2O_3, TiO_2, SiO_2, zeolites and activated carbon (AC). The commercial catalysts used for removal of ozone need to be replaced periodically, due to catalyst deactivation. Improving the performance of ozone decomposition catalysts is an important research goal. It was found that *p*-type oxides were active in the ozone decomposition process[23]. Among some of the major *p*-type oxides, MnO_2 has been identified as the best catalyst for ozone decomposition[14].The kinetics and mechanism for MnO_2 supported on Al_2O_3 have been studied in detail using *in-situ* laser Raman spectroscopy [24, 25]. The effect of support on the structure and ozone decomposition activity of manganese oxide has not been explored.

1.3 Objectives, methodology and organization

The previous work[24, 25] on Al_2O_3 supported manganese oxide catalyst did not evaluate the effect of support on the ozone decomposition activity and kinetic parameters. Another problem not solved in the previous work was determination of the structure and concentration of manganese active sites on the surface of the catalyst. The dissertation objectives are based upon addressing these problems.

1.3.1 Objectives

The main objective of this project is to better understand the effect of support on the ozone decomposition activity of manganese oxides. The specific objectives are:

1) Determine the structure and oxidation state of manganese for Al_2O_3, ZrO_2, TiO_2 and SiO_2 supported manganese oxides.
2) Estimate the active site density for the supported manganese oxide catalysts.
3) Evaluate the effect of support on the kinetic parameters for ozone decomposition for the manganese oxide catalysts.

1.3.2 Methodology

The methodology used to complete project objectives are summarized below :

1) Study catalyst structure using XRD, Raman spectroscopy and EXAFS (extended x-ray absorption fine structure) spectroscopy.
2) Determine manganese oxidation state using NEXAFS (near edge x-ray absorption fine structure) spectroscopy.
3) Evaluate manganese active site density on the catalysts using oxygen chemisorption and oxygen desorption techniques.
4) Compare EXAFS and Raman spectroscopy data to *ab initio* quantum calculations to determine the validity of predicted structural paprameters.
5) Examine the effect of support on ozone decomposition activity using kinetic measurements at varying ozone partial pressures and temperatures.
6) Use *in situ* laser Raman spectroscopy to monitor changes in adsorbed species concentration during ozone decomposition reaction.

7) Incorporate the surface coverage of the adsorbed species in the analysis, thereby allowing the evaluation of kinetic parameters for ozone adsorption and desorption.

1.3.3 Organization

The rest of the dissertation is organized as follows :

a) Chapter 2, “Preparation and characterization”, discusses the methods used to determine the structure and oxidation state of the supported manganese oxides.

b) Chapter 3, “*Ab initio* calculations of the structure of alumina supported manganese oxide”, determines the validity of the structures determined in Chapter 2 using theoretical quantum chemical calculations.

c) Chapter 4, “Active site titration for supported manganese oxide catalysts”, presents and evaluates techniques used to measure the number of active manganese sites on the surface of the supports.

d) Chapter 5, “Ozone decomposition studies”, shows how the effect of support on the kinetic parameters for ozone reactivity can be determined.

REFERENCES:

[1] *Ulmann's Encyclopedia of Industrial Chemistry*, Vol A18, **1991**, 349.

[2] Wojtowicz, J. A.; "Ozone", *Kirk-Othmer, Encyclopedia Chem. Technol.*, 4th Ed., John Wiley, **1996**, *17*, 953.

[3] Lo Jacano, M., and Schiavello, M., in *Preparation of Catalysts,* B. Delmon, P. A. Jacobs, and G. Poncelet (Eds.), **1976**, Elsevier, 474.

[4] Yamashita, T.; Vannice, A.; *J. Catalysis.* **1996**, *161*, 254.

[5] Ma, J.; Chuah, G. K.; Jaenicke, S.; Gopalakrishnan, R.; Tan, K. L.; *Ber.Bunsenges. Phys. Chem.* **1995**, *100*, 585.

[6] Ma, J.; Chuah, G. K.; Jaenicke, S.; Gopalakrishnan, R.; Tan, K. L.; *Ber.Bunsenges. Phys. Chem.* **1995**, *99*, 184.

[7] Baltanas, M. A., Stiles, A. B., and Katzer, J. R., *Appl. Catal.* **1986**, *28*, 13.

[8] Li, Wei; Oyama, S. T.; in *Heterogeneous Hydrocarbon Oxidation*, B. K. Warren and S. T. Oyama (Eds.), *ACS Symp. Ser.* 638; ACS: Washington, DC, **1996**, 364.

[9] Naydenov, A.; Mehandjiev, D. *Appl. Catal. A. : General.* **1993**, *97*, 17.

[10] Boreskov, G. K., *Adv. Catal.* **1964**, *15*, 285.

[11] Baldi, M.; Finochhio, E.; Pistarino, C.; Busca, G.; *J. Appl.Catal. A: General*. **1998**, *173*, 61.

[12] Kapteijn, F.; Singoredjo, L.; Andreini, A.; Moulijn, J. A.; *J. Appl.Catal. B: Environmental*. **1994**, *3*, 173.

[13] Maltha, A.; Favre, L. F. T.; Kist, H. F.; Zuur, A. P.; Ponec, V.; *J. Catal.* **1994**, *149*, 364.

[14] Dhandapani,, B.; Oyama, S. T.; *J. Appl. Catal. B: Environmental.* **1997**, *11*, 129.

[15] Hunter, P; Oyama, S. T; *Control of Volatile Organic Compound Emissions*, **2000**, John Wiley & Sons, Inc.

[16] Kapteijn, F.; van Langeveld, A. D.; Moulijn, J. A.; Andreini, A; Vuurman, M. A.; Turek, M. A.; Jehng, J.M; Wachs, I. E.; *J. Catal.* **1994**, *150*, 94.

[17] Buciuman, F; Patcas, F; Cracium, R; Zhan, R. T. D; *Phys. Chem. Chem. Phys.* **1999**, *1*, 185.

[18] Selwood, P. W.; Moore, T. E.; Ellis, M.; *J. Am. Chem. Soc.*, **1949**, *71*, 693.

[19] Plot, G. T.; Mcnicol, B. D.; *Discuss. Faraday Soc.*, **1971**, *52*, 121.

[20] Burlamacchi, L.; Villa, P. L.; *React. Kinet. Catal. Lett.*, **1975**, *3*, 199.

[21] Brown, N. M. D.; Mcmonagle, J. B.; Greaves, G. N.; *J. Chem. Soc. Faraday. Trans. 1*, **1984**, *80*, 589.

[22] Baltanas, M. A.; Stiles, A. B.; Katzer, J. R.; *J. Catalysis.*, **1984**, *88*, 362.

[23] Imamura, S.; Ikebata, M.; Ito, T.; Ogita, T.; *Ind. Eng. Chem. Res.*, **1991**, *30*, 217.

[24] Li, Wei; Oyama, S. T.; Gibbs, G. V.; *J. Am. Chem. Soc.*, **1998**, *120*, 9041.

[25] Li, Wei; Oyama, S. T.; *J. Am. Chem. Soc.*, **1998**, *120*, 9047.

CHAPTER 2

CATALYST PREPARATION AND STRUCURE CHARACTERIZATION

2.1 Introduction

A common method for the preparation of supported metal oxide catalysts is the incipient wetness technique[1]. The procedure involves a support (e.g. Al_2O_3) with a metal precursor solution using a quantity of liquid just sufficient to fill the pores of the support. This impregnation is followed by a drying and calcination procedure to obtain the final catalyst. These catalysts are then characterized to obtain information about their bulk and surface properties.

The two bulk properties of interest are a) the phase structure, b) the composition. The phase structure is typically determined through diffraction techniques and the composition is determined through spectroscopic methods. A brief discussion of the various methods used in this manuscript are presented below.

XRD (x-ray diffraction) provides information about the crystallinity and particle size of catalytic materials[2]. Previous XRD work[3] on MnO_x / Al_2O_3 and MnO_x / SiO_2 has found this as an effective method for determining the identity of the manganese oxide phase at high loadings (> 6%).

Raman spectroscopy is a powerful technique that provides the structural information about materials through their vibrational signatures. It has been widely used in heterogeneous catalysis[4] to study supported transition metal oxide systems including oxides of Mo[5,6], V[4,7,] Cr[8], Nb[9], W[10] and Re[11]. Few Raman studies have presented spectra for supported manganese[3, 12, 13], and these studies have concentrated on manganese oxide supported on alumina oxide[12, 13] or silica[3].

X-ray absorption fine structure (XAFS) has emerged as an effective technique for directly probing the structure of surface sites in catalysis. Extended x-ray absorption fine structure (EXAFS)[14, 15, 16] and near-edge x-ray absorption fine structure (NEXAFS)[16, 17, 18] provide information about the local coordination and electronic properties of the catalyst active centers. The majority of x-ray absorption work on manganese oxides has been done on bulk materials[19, 20, 21]. The only supported manganese oxide catalyst studied using these techniques is MnO_2/SiO_2[22].

2.2 Catalyst Preparation

Manganese oxide catalysts (3 wt%) were prepared using aqueous solutions of manganese acetate ($Mn(CH_3COO)_2 \bullet 4H_2O$, Aldrich > 99.99%). The supports used were Al_2O_3 (Degussa, Aluminium oxide C), ZrO_2 (Degussa, VP ZrO_2), TiO_2 (Degussa, Titanoxid P25) and SiO_2 (Cabosil, L-90). The 3 wt% basis translated to molar percentages of manganese at 3.5 %, 4.2 %, 2.8 % and 2.1 % respectively on the Al_2O_3, ZrO_2, TiO_2 and SiO_2 supports. These values were calculated based on the assumption that MnO_2 was formed on the support surfaces.

The supports were impregnated with the precursor solution to the point of incipient wetness determined in separate measurements. For example, 1.69 g of manganese acetate was dissolved in 4 cm^3 of distilled water and this solution was added dropwise to 20 g of Al_2O_3. After impregnation, the sample was heated at 393 K for 6 h and calcined at 773 K for 6 h to produce 3 wt% MnO_x/Al_2O_3. A similar method was used to prepare the other catalysts. A single batch of 20 g of catalyst was prepared with each support and samples from this batch were used for all the experiments.

2.3 Catalyst Structure Characterization – Experimental

The supported manganese oxides were characterized using XRD, Raman spectroscopy and EXAFS spectroscopy to determine the structure of the manganese active center. NEXAFS spectroscopy was used to determine the oxidation state of the manganese.

2.3.1 X-ray diffraction (XRD)

X-ray diffraction (XRD) analysis was used to determine the crystalline manganese oxide phases for the supported catalysts. An ASC (0007 model) diffractometer using Cu K_α radiation source was used. The samples were scanned from 2θ angles of 10^o to 110^o at a rate of 0.03^o s^{-1} (1^o min^{-1}). The x-ray power was operated with a current of 40 mA and a voltage of 45 kV.

2.3.2 In situ Laser Raman spectroscopy

The schematic of the *in situ* laser Raman apparatus used to run characterization and reactivity tests on the catalyst is shown in Fig 2.1. The system used an argon ion laser (514.5 nm, Spex Lexel 95), as a light source, a holographic notch filter (Kaiser, Super Notch Plus) for removing Rayleigh scattering, a single stage monochromator (Spex, 500 M) for energy dispersions and a CCD detector (Spex, Spectrum One) for spectral acquistion. The laser was operated at 200 mW and the detector slit width was set at 100 μm. The resolution of the Raman spectrometer was 6 cm^{-1}. The catalysts were pelletized into thin cylindrical wafers of 0.1 cm thickness and 1.5 cm diameter. These were then mounted onto a ceramic rod sample holder, and held in place by a stainless steel cap. The rod was rotated at 1500 rpm to prevent sample heating by the laser. The temperature of the sample was measured through a thermocouple placed in a well 3 mm from the sample. The samples were pre-treated at 773 K for 2 hours in oxygen (Air products, > 99.6%) flow prior to spectral acquisition.

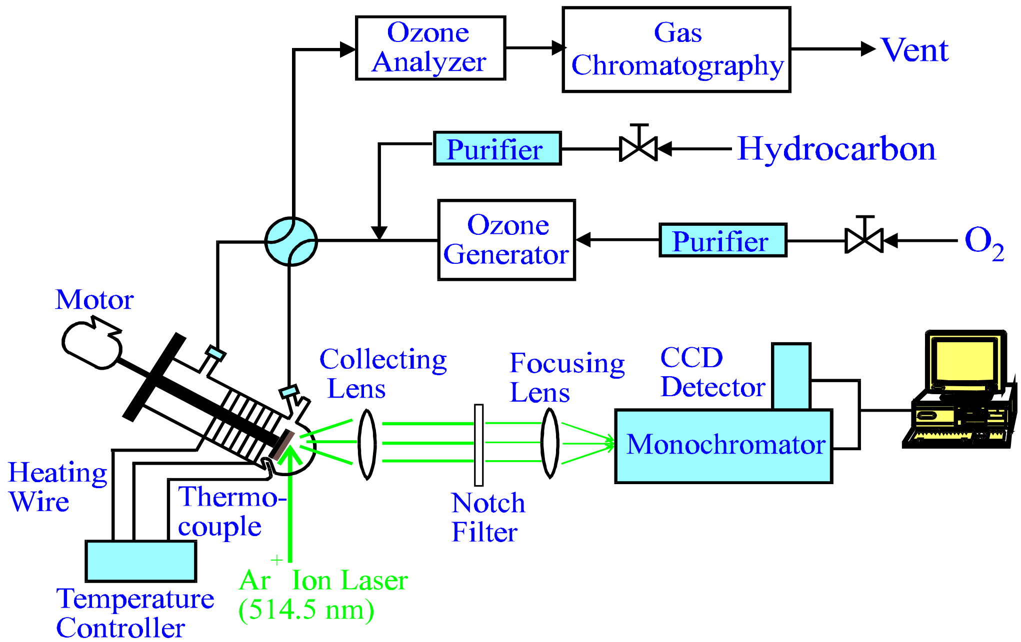

Figure 2.1 Schematic of *in situ* laser Raman spectroscopy system

2.3.3 Extended x-ray absorption fine structure (EXAFS) spectroscopy

The catalysts (0.13 g for SiO_2 and Al_2O_3 supported samples and 0.065 g for TiO_2 supported samples) were pretreated in oxygen at 723 K for 1 h and transferred into *in situ* cells with Kapton windows without exposure to the atmosphere. The measurements were carried out in a transmission mode at the BL10B beam line of the Photon Factory, Institute for Material Science (Japan), (KEK-PF) with a 2.5 GeV ring energy and a 300-

200 mA ring current. The monochromator used a Si(311) channel cut single crystal and had an energy resolution of about 1eV. The incident and transmitted X-rays were detected by N_2- filled ionization chambers with lengths of 14 cm and 28 cm respectively. The samples were measured twice with a total accumulation time 4-6 s. The scan range for EXAFS was 6186.1-7539.7 eV(step = 2-3 eV). These measurements were made in collaboration with Prof. Kiyotaka Asakura of the Catalysis Research Center at Hokkaido University in Japan.

2.3.4 Near edge x-ray absorption fine structure (NEXAFS) spectroscopy

The NEXAFS measurements for the catalysts were carried out at the NSLS (National Synchrotron Light Source) using the Exxon Mobil U1A beamline. Details about the experimental setup can be found elsewhere[18]. Briefly, the powder samples of the catalyst were loaded into a sample holder cup with dimensions 1 cm diameter and 0.1 cm depth. The synchrotron radiation was monochromatized using a spherical grating monochromator (SGM). The energy range of the incident photons was set between 630 eV to 680 eV with an energy resolution $\Delta E/E$ of approximately 0.0025. These measurements were made in collaboration with Prof. Jinguang Chen of the Materials Science department at the University of Delaware.

2.4 Catalyst Structure Characterization – Results

2.4.1 XRD results

The x-ray diffraction results for the samples are compared to those for the supports in Fig 2.2. There were no differences between the supported samples and the pure supports presented. The diffractograms for the Al_2O_3 and MnO_x / Al_2O_3 samples showed peaks with the three largest intensities at 2θ angle values of 67°, 46° and 37°. The diffractograms for the ZrO_2 and MnO_x / ZrO_2 samples showed peaks with the three largest intensities at 2θ angle values of 26°, 28° and 48°. The diffractograms for the TiO_2 and MnO_x / TiO_2 samples showed peaks with the three largest intensities at 2θ angle values of 28°, 32° and 35°. Finally, the diffractograms for the SiO_2 and MnO_x / SiO_2 samples showed only a very broad feature at a 2θ angle value of 28° .

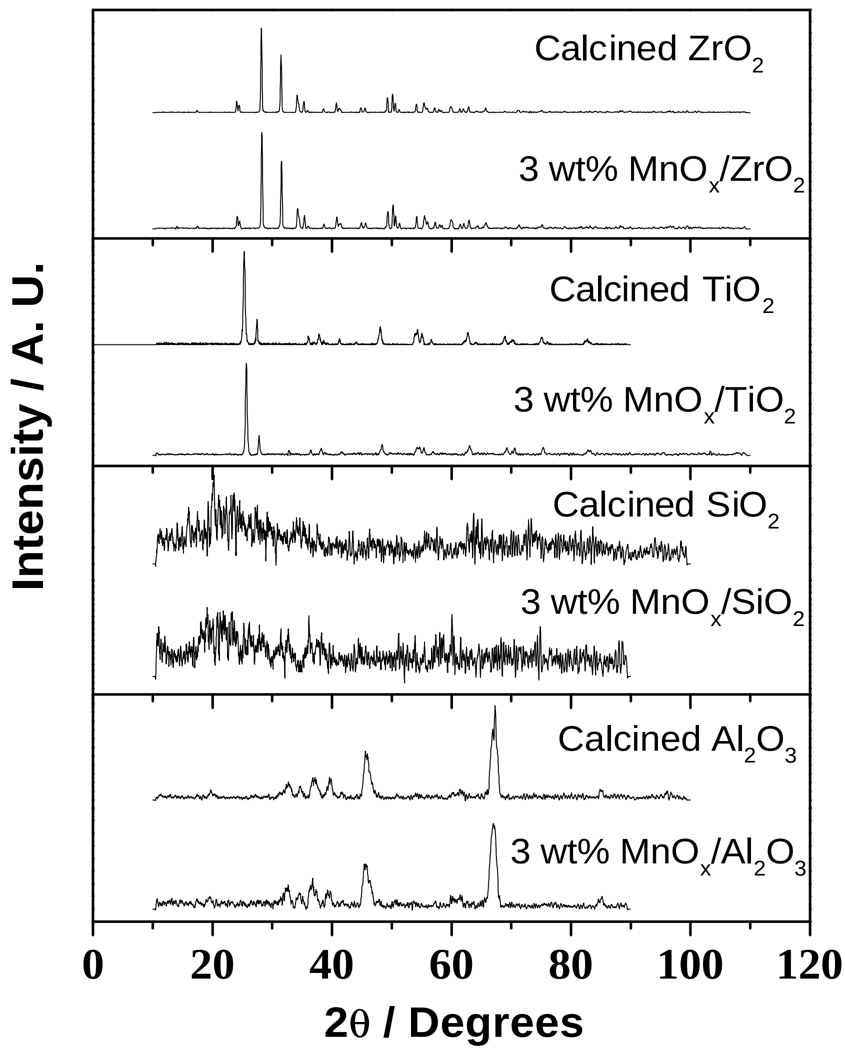

Figure 2.2 X-ray diffractograms for the manganese oxide catalysts and supports

2.4.2 Raman spectroscopy results

The MnO_x / SiO_2 sample had a simple spectrum consisting of one band at 664 cm^{-1} (Fig. 2.3a). The MnO_x / TiO_2 catalyst showed two bands at 510 cm^{-1} and 632 cm^{-1} (Fig. 2.3b). The MnO_x / ZrO_2 had a complex spectrum with peaks at 532 cm^{-1}, 552 cm^{-1}, 618 cm^{-1} and 638 cm^{-1} (Fig. 2.3c). Finally, the MnO_x / Al_2O_3 sample also presented a simple spectrum (Fig. 2.3d) with a band at 661 cm^{-1}. As will be discussed, the peaks in the SiO_2 and Al_2O_3 supported samples correspond to dispersed manganese oxide species while those for the ZrO_2 and TiO_2 are due to the support. The spectra for the ZrO_2 and TiO_2 supported manganese oxide species were reduced in scale due to the large intensities of the support peaks.

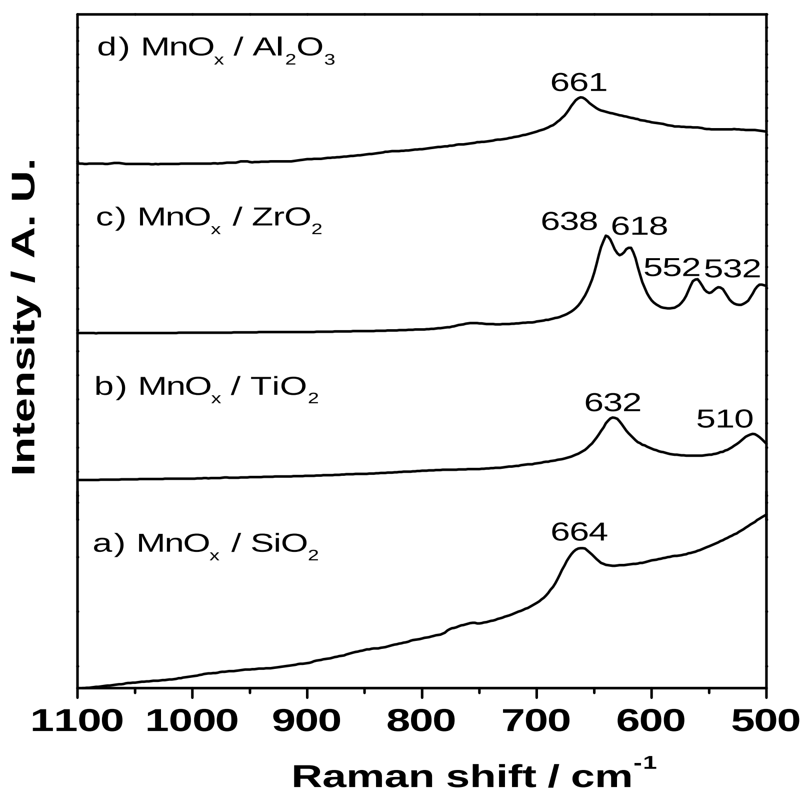

Figure 2.3 Raman spectra for the supported manganese oxide catalysts

2.4.3 EXAFS spectroscopy results

Figure 2.4, shows the x-ray absorption spectra for Mn_3O_4 (Fig 2.4a), β-MnO_2 (Fig 2.4b), MnO_x / SiO_2 (Fig 2.4c), MnO_x / TiO_2 (Fig 2.4d) and MnO_x / Al_2O_3 (Fig 2.4e).

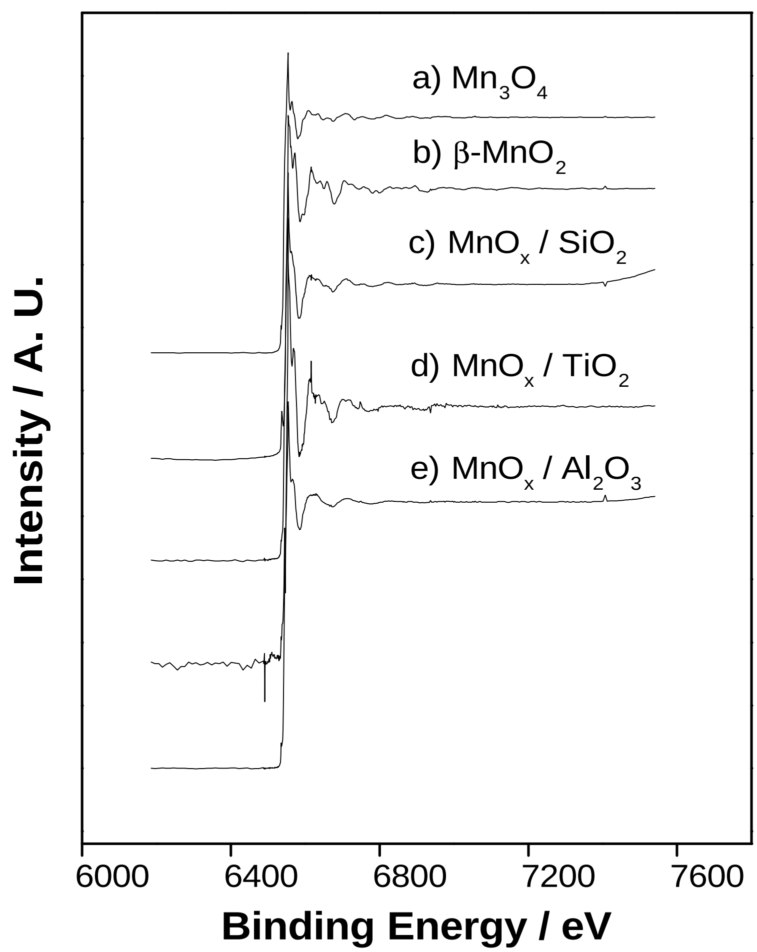

Figure 2.4 EXAFS spectra for the supported manganese oxide catalysts

The EXAFS oscillations after background subtraction in k space are shown in Fig 2.5. The dotted lines in the figure represent the fitting functions used to evaluate interatomic distances.

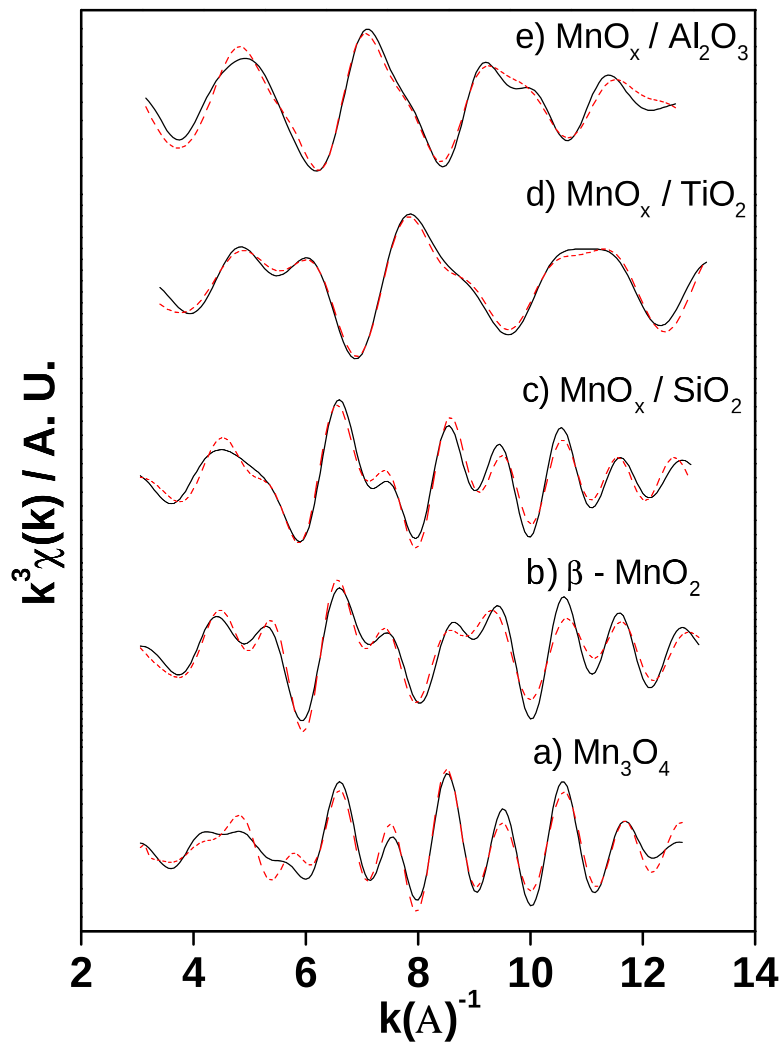

Figure 2.5 EXAFS spectra (in k – space) for the catalysts compared to bulk manganese oxides

The Fourier transforms of these lines are plotted in Fig 2.6. The transforms for Mn_3O_4 (Fig 2.6a), β-MnO_2 (Fig 2.6b), γ-MnO_2 (Fig 2.6c), MnO_x / SiO_2 (Fig 2.6d), MnO_x

/ TiO_2 (Fig 2.6e) and MnO_x / Al_2O_3 (Fig 2.6f) all have a broad feature at 2.0 Å (0.20 nm). The spectrum for the MnO_x / ZrO_2 could not be obtained because of interference from the ZrO_2 support. The transforms for all the samples except the MnO_x / Al_2O_3 have features around 2.9 Å (0.29 nm) and 3.5 Å (0.35 nm). These results are discussed in detail later in the chapter. All of the data presented for the EXAFS spectra were drawn to scale.

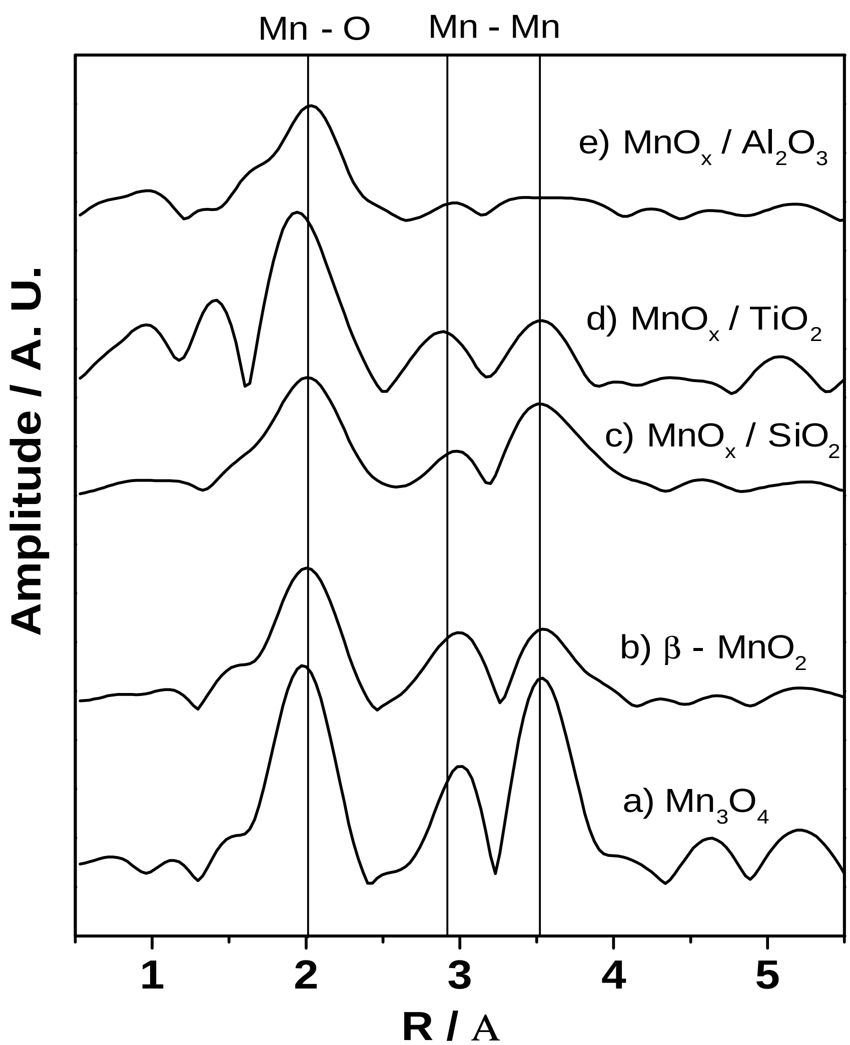

Figure 2.6 Fourier transforms of the EXAFS spectra for the catalysts compared to bulk manganese oxides

2.4.4 NEXAFS spectroscopy results

Figure 2.7, presents the Mn L-edge NEXAFS spectra for all of the catalysts compared to β-MnO_2. The peak at 655 eV for the MnO_2 represents the L_{II} peak while the peaks at 645 eV and 643 eV represent the L_{III} peaks. There is a shift in both the L_{II} and L_{III} edge features for the various supports which follows the trend Al_2O_3 > ZrO_2 > TiO_2 > SiO_2. The positions of the peaks are 653.5 eV and 641.5 eV respectively for the L_{II} and L_{III} features on the alumina supported manganese oxide. The spectra presented below were drawn to scale.

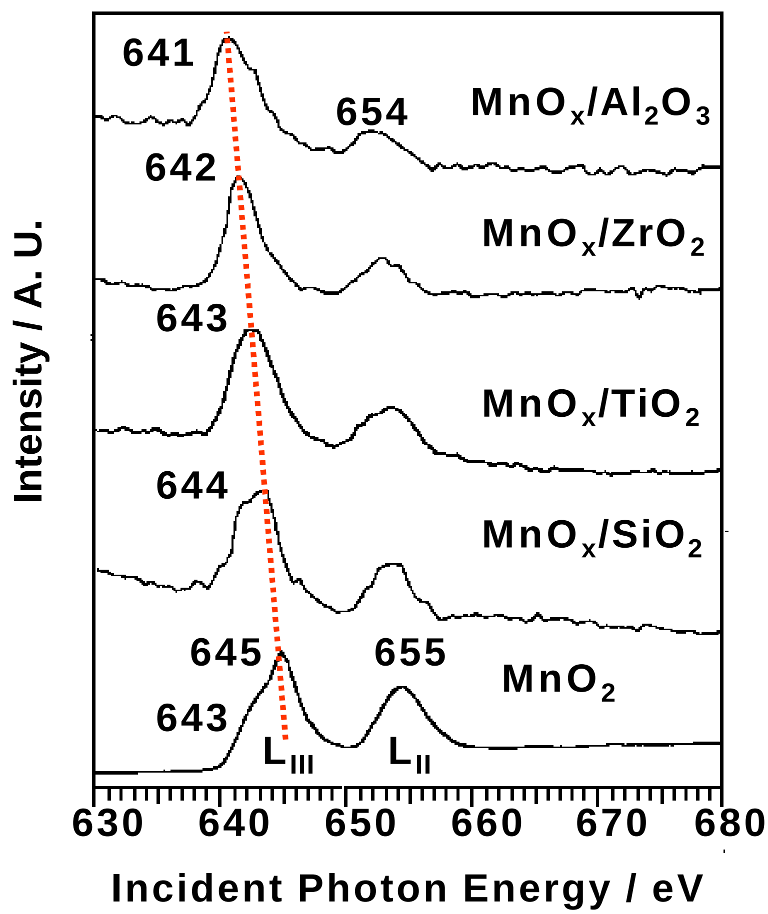

Figure 2.7 Mn L-edge NEXAFS spectra for β-MnO_2 and the supported manganese oxide catalysts

2.5 Discussion

2.5.1 X-ray diffractograms

The peaks at 67^o, 47^o and 37^o for the Al_2O_3 support and MnO_x / Al_2O_3 catalyst correspond to γ-Al_2O_3. The broad diffraction feature for the SiO_2 and MnO_x / SiO_2 catalyst at 20^o is indicative of amorphous silica as was found earlier on supported MoO_3 catalysts[23]. The TiO_2 and MnO_x / TiO_2 catalyst sample peaks at 28^o, 32^o and 35^o are due to a mixture of rutile and anatase TiO_2. Finally, the ZrO_2 and MnO_x / ZrO_2 diffraction peaks at 26^o, 28^o and 48^o are due to monoclinic ZrO_2.

Ma et al.[24,25] have studied manganese oxides supported on Al_2O_3 and ZrO_2 using XRD. These studies found that at low loadings (< 6 wt%), the XRD patterns for the catalysts matched those of the support. It was suggested in their studies that this is indicative of well dispersed manganese oxide species on the catalyst surface. Kapteijn et al.[13] studied MnO_x / Al_2O_3 using XRD and they suggested that the manganese oxide at low loadings (< 6 wt%) was a well dispersed species. In conclusion, the only information which can be deduced from the XRD patterns for our catalysts is that the manganese oxide is also a well dispersed species. Crystallites of some bulk oxide species are possible, but if present would be of size smaller than 4 nm.

2.5.2 Raman spectra

The Raman spectra for the Al_2O_3 and SiO_2 supported catalysts had peaks at 661 cm^{-1} and 664 cm^{-1} respectively (Fig. 2.3). Since SiO_2 has very weak spectral features[26] at 604 cm^{-1}, 804 cm^{-1}, 974 cm^{-1} and Al_2O_3 does not have any features in the region scanned, it can be concluded that the peaks observed were due to the manganese oxide species. Buciuman et al.[3] , investigated manganese oxide species with Raman spectroscopy and found vibrational frequencies in the range of 659 cm^{-1} – 650 cm^{-1} for Mn_3O_4 species. They also observed vibrational frequencies for α-Mn_2O_3 at 650 cm^{-1} and 680 cm^{-1} and a frequency of 633 cm^{-1} for γ-Mn_2O_3. Wachs et al.[13] , in their studies on Al_2O_3 supported manganese oxide, observed Raman peaks in the range of 637 cm^{-1} – 647 cm^{-1} for catalysts with manganese loadings between 1 – 8.4 wt%. In their work, XPS revealed an average stoichiometry corresponding to a highly dispersed Mn_2O_3 phase. Although Wachs et al. did not observe any vibrational frequencies for β-MnO_2, Buciuman et al. have observed weak vibrational features for this compound at 510 cm^{-1}, 580 cm^{-1} and 640 cm^{-1}. It can be concluded that the peaks in the 650 – 660 cm^{-1} wavenumber region confirm the presence of a manganese oxide species but do not provide enough information to ascertain the Mn oxidation state. It is likely that the manganese oxide species bands result from Mn – O bonds. This has been independently confirmed through *ab-initio* calculations as will be presented in the next chapter.

In the case of the ZrO_2 sample, the peaks at 532 cm^{-1}, 552 cm^{-1}, 618 cm^{-1} and 638 cm^{-1} are support peaks. Similarly for the TiO_2 sample, the peaks at 632 cm^{-1} and 510 cm^{-1} are TiO_2 peaks. The large intensity of the support peaks in the scanned region precluded the observation of any supported manganese oxide peaks on these supports.

During ozone decomposition, the presence of an adsorbed species is indicated by the appearance of a band in the 876 – 880 cm^{-1} wavenumber region in the Raman spectra for the catalysts[27]. This feature is not found in the Raman spectra of any of the pure supports exposed to ozone. The adsorbed species has been identified as a peroxide type (O_2^{2-}) oxygen species based on its band position[28] and *ab-initio* calculations. Heating the catalysts to 500 K, led to the disappearence of this peak. This observation was consistent with the oxygen TPD results to be presented in Chapter 4.

2.5.3 EXAFS spectra

The relevant Mn-O and Mn-Mn distances, r, obtained from the EXAFS measurements for supported and reference Mn oxide species are presented in Table 2.1. The co-ordination numbers, N, indicate that there are five Mn-O bonds on each of the supported manganese active centers. In the case of the TiO_2 and SiO_2 supported manganese oxides an N value > 1 is observed for a Mn-Mn distance of 0.350 nm (Fig 2.6). This seems to suggest the presence of multiple manganese atoms attached through bridging oxygen atoms on these surfaces. The MnO_x / Al_2O_3 sample, however, does not have this feature, which suggests it alone has mononuclear manganese sites. Figure 2.8, presents a structural representation of the manganese sites on each of the supports. Strong absorption from the ZrO_2 support prevented the use of EXAFS analysis on the MnO_x / ZrO_2 catalyst.

Table 2.1 : EXAFS Results

Bond	β-MnO_2	Mn_3O_4	MnO_x / Al_2O_3	MnO_x / TiO_2	MnO_x / SiO_2
Mn-O	N – 6.1	N – 2.4	N – 5	N – 4.5	N – 5
	r – 0.192 nm	r – 0.200 nm	r – 0.195 nm	r – 0.195 nm	r – 0.195 nm
Mn-Mn	N – 1.3	N – 1.6	N – 0.2	N – 0.8	N – 0.37
	r – 0.293 nm	r – 0.320 nm	r – 0.282 nm	r – 0.290 nm	r – 0.287 nm
Mn-Mn	N – 1.3	N – 3.2	N – 0.8	N – 1.7	N – 2.1
	r – 0.348 nm	r – 0.350 nm	r – 0.350 nm	r – 0.350 nm	r – 0.350 nm

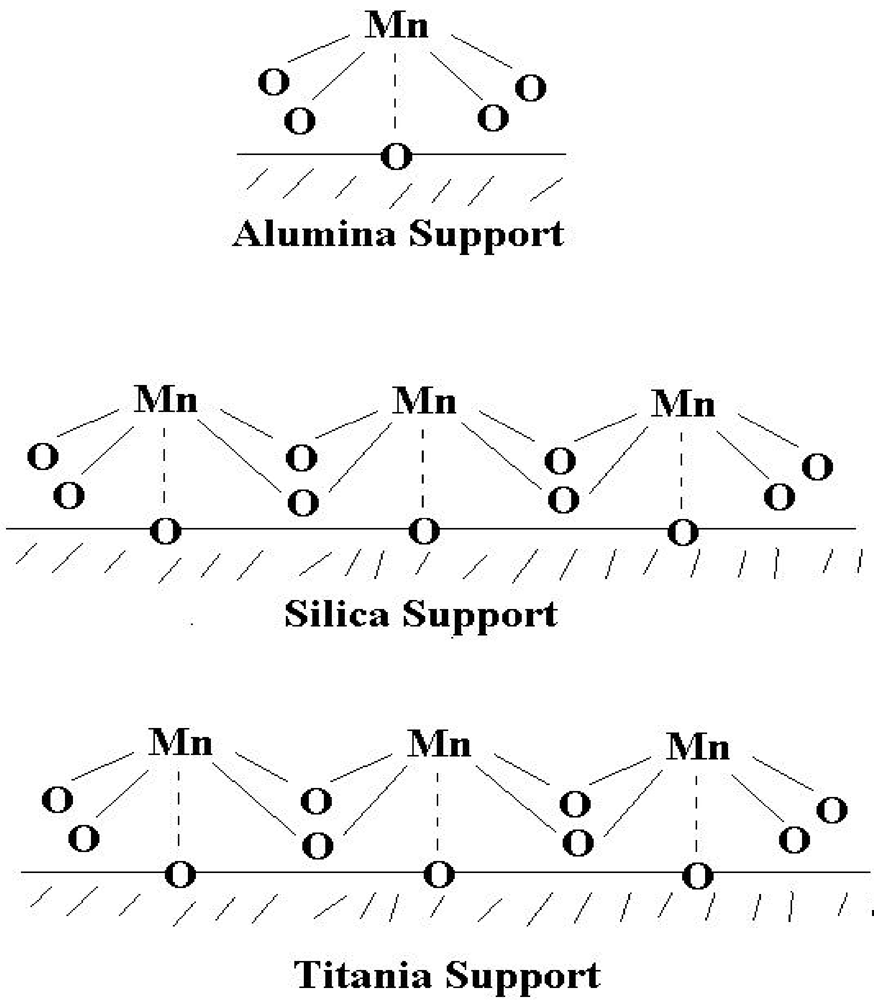

Figure 2.8 Structure of manganese active sites for the supported manganese oxide catalysts

Brown et al.[22] , have studied a MnO_2/SiO_2 catalyst prepared from permanganate solution using EXAFS spectroscopy. This study concluded that the manganese metal center was closer to a +5 oxidation state as opposed to the expected +4 value. EXAFS studies in this dissertation suggest a manganese center surrounded by five oxygen atoms, but do not allow a definitive determination of oxidation state. This information is provided by the NEXAFS measurements.

2.5.4 NEXAFS spectra

The Mn L-edge features for the various supported catalysts can give information regarding the oxidation state and the electronic structure of the manganese empty electronic states. The oxidation state information is obtained from the chemical shift and the L_{III}/L_{II} white line intensity ratio. Table 2.2 summarizes the ratios obtained for bulk oxides in the literature[29, 30, 31] compared with those obtained for our supported catalysts[32].

Table 2.2 : L_{III}/L_{II} Intensity Ratios

Oxide	Ratio	Mn oxidation state
MnO	4.8[29], 5.3[30], 3.3[31] (Avg 4.5)	2
Mn_3O_4	2.9[29], 2.6[31] (Avg 2.8)	2 2/3
Mn_2O_3	2.5[29], 2.6[30], 2.7[31] (Avg 2.6)	3
MnO_2	2.3[29], 2.1[30], 2.0[31], 1.9[32] (Avg 2.1)	4
MnO_x / Al_2O_3	3.4	2.4*
MnO_x / ZrO_2	3.2	2.5*
MnO_x / TiO_2	2.7	2.8*
MnO_x / SiO_2	2.2	3.8*

* Calculated by extrapolation between values of the MnO_x references.

According to the L_{III} / L_{II} intensity ratio studies reported in the literature, the ratios tend to decrease as the manganese oxidation state increases. De Groot et al.[33], have studied L_{III} and L_{II} edges for 3d and 4d transition metal complexes in octahedral symmetry. Their studies attributed varying intensities in L_{III} and L_{II} ratios for 3d complexes to multiplet effects resulting from the coupling of 2p core and 3d valence wave functions. The ratio of the intensities were found to correlate to the degree of occupancy of the 3d level thereby suggesting a direct relationship between oxidation state and L_{III} / L_{II} ratios for 3d metal complexes.

Comparing the intensity ratios for the supported catalysts to the bulk oxides and interpolating (Table 2.2) suggests that the Mn in MnO_x / Al_2O_3 is in an oxidation state of 2.4, the MnO_x / ZrO_2 in an oxidation state of 2.5, the MnO_x / TiO_2 catalyst in an oxidation state of 2.8, while in the MnO_x / SiO_2 in an oxidation state of 3.8. EXAFS results suggest a manganese site surrounded by five oxygen atoms in the case of MnO_x / Al_2O_3, MnO_x / TiO_2 and MnO_x / SiO_2 catalysts. This co-ordination is not necessarily related to the oxidation state of the manganese center. For example, in MnO_2 of the rutile structure, the coordination number of 6 is higher than the oxidation state of 4.

The chemical shift of the L-edge features also provides information on the oxidation state. This also follows the trend : $Al_2O_3 < ZrO_2 < TiO_2 < SiO_2$ found with the L_{III} / L_{II} ratio. A higher oxidation state suggests a large number of empty d-states and greater reducibility (electron accepting nature) of the active center[34]. This trend in catalyst reducibility can be directly correlated to catalyst activity for ozone decomposition, as will be shown in Chapter 5.

2.6 Conclusions

1) X-ray diffractograms for the supported manganese oxide catalysts showed peak features which could be attributed to the support. It can be deduced from these results that the manganese oxide species are well dispersed.
2) Raman spectra taken on supported manganese oxide catalysts revealed the presence of Mn – O bands due to a dispersed species on Al_2O_3 and SiO_2 supported catalysts.

The large intensities of the support peaks precluded the observation of these bands for the ZrO_2 and TiO_2 supported catalysts.

3) EXAFS analysis revealed that the manganese active center on the Al_2O_3 support was likely a mononuclear species coordinated to five oxygen atoms, while on the other supported catalysts it was multinuclear, but with similar oxygen co-ordination.

4) The Mn L-edge features observed through NEXAFS showed a shift to lower energy in the positions of the L_{II} and L_{III} edge features whose magnitude followed the trend : $Al_2O_3 > ZrO_2 > TiO_2 > SiO_2$. The L_{III} / L_{II} ratios for the catalysts indicated that the Mn oxidation state followed the trend : $Al_2O_3 < ZrO_2 < TiO_2 < SiO_2$.

REFERENCES:

[1] Richardson, J. T.; *Principles of Catalyst Development*, **1989**, Plenum Press.

[2] Thomas, J. M.; Thomas, W. J.; *Principles and Practice of Heterogeneous Catalysis*, **1997**, VCH Publishers Inc.

[3] Buciuman, F.; Patcas, F.; Craciun, R.; Zhan, D. R. T.; *Phys. Chem. Chem. Phys.*; **1999**, *1*, 185.

[4] Wachs, I. E.; *Catalysis Today*. **1996**, *27*, 437.

[5] Hu, H.; Wachs, I. E.; Bare, S.; *J. Phys. Chem.* **1995**, *99*, 10903.

[6] Oyama, S. T.; Zhang, W.; *J. Am. Chem. Soc.* **1996**, *118*, 7173.

[7] Went, G. T.; Oyama, S. T.; *J. Phys. Chem.* **1990**, *94*, 4240.

[8] Weckhuysen, B. M.; Wachs, I. E.; .; *J. Phys. Chem.* **1996**, *100*, 14437.

[9] Hardcastle, F. D.; Wachs, I. E.; *Solid State Ionics.* **1991**, *45*, 201.

[10] Ostromecki, M. M.; Burcham, L. J.; Wachs, I. E.; Ramani, N.; Ekerdt, J. G.; *J. Mol. Catal. (A): Chemical*. **1998**, *132*, 43.

[11] Deo, G.; Wachs, I. E.; *J. Phys. Chem.* **1991**, *95*, 5889.

[12] Stroheimer, B. R.; Hercules, D. M.; *J. Phys. Chem.* **1991**, *95*, 5889.

[13] Kapteijn, F.; van Langeveld, A. D.; Moulijn, J. A.; Andreini, A; Vuurman, M. A.; Turek, M. A.; Jehng, J.M; Wachs, I. E.; *J. Catal.* **1994**, *150*, 94.

[14] Teo, B. K.; Joy, D. C. (Eds.); *EXAFS Spectrscopy Techniques and Applications.*, **1981**, Plenum Press.

[15] Teo, B. K.; *EXAFS: Basic Principles and Data Analysis.*, **1986**, Springer-Verlag.

[16] Koningsberger, D. C.; Prins, R. (Eds.); *Principles, Applications and Techniques of EXAFS, SEXAFS and XANES.*, **1988**, Wiley.

[17] Stöhr, J.; *NEXAFS Spectroscopy*, Springer Series in Surface Science, **1992**, *25*, Springer.

[18] Chen, J. G.; *Surf. Sci. Rep.*, **1997**, *30(1-3)*, 1.

[19] Mande, C.; Deshpande, A. P.; *Phys. Stat. Sol. (b)*, **1990**, *158*, 737.

[20] Godart, C.; Latroche, M.; Fretigny, C.; Levy-Clement, C.; *Phys. Stat. Sol. (b)*, **1992**, *132*, 253.

[21] Sankar, G.; Sarode, P. R.; Rao, C. N. R.; *Chemical Physics*, **1983**, *76*, 435.

[22] Brown, N. M. D.; Mcmonagle, J. B.; Greaves, G. N.; *J. Chem. Soc. Faraday. Trans. 1*, **1984**, *80*, 589.

[23] Desikan, A. N.; Huang, L.; Oyama, S. T.; *J. Phys. Chem.*, **1991**, *95*, 10050.

[24] Ma, J.; Chuah, G. K.; Jaenicke, S.; Gopalakrishnan, R.; Tan, K. L.; *Ber.Bunsenges. Phys. Chem.* **1995**, *99*, 184.

[25] Ma, J.; Chuah, G. K.; Jaenicke, S.; Gopalakrishnan, R.; Tan, K. L.; *Ber.Bunsenges. Phys. Chem.* **1995**, *100*, 585.

[26] Oyama, S. T.; Zhang, W.; *J. Am. Chem. Soc.*, **1996**, *118*, 7173.

[27] Radhakrishnan, R.; Oyama, S. T.; Submitted *J. Catal*.

[28] Che, M.; Tench, A. J.; *Advances in Catalysis*; **1983**, *32*, 1.

[29] Sparrow, T. G.; Williams, B. G.; Rao, C. N. R.; Thomas, J. M.; *Chemical Physics Letters.*, **1984**, *108(6)*, 547.

[30] Rask, J. H.; Miner, B. A.; Buseck, P. R.; *Ultramicroscopy.*, **1987**, *21*, 321.

[31] Paterson, J. H.; Krivanek, O. L.; *Ultramicroscopy.*, **1990**, *32*, 319.

[32] Present work.

[33] De Groot, F. M. F.; Hu Z. W.; Lopez, M. F.; Kaindl, G.; Guillot, F., Tronc, M.; *J. Chem. Phys.*, **1994**, *101*, 6570.

[34] Zhang, W.; Desikan, A.; Oyama, S. T.; *J. Phys. Chem.*, **1995**, *99*, 14468.

CHAPTER 3

AB INITIO CALCULATIONS OF THE STRUCTURE OF ALUMINA SUPPORTED MANGANESE OXIDE

3.1 Introduction

Ab intio quantum chemical methods are being applied in heterogeneous catalysis for evaluating activation energies and reaction mechanisms[1]. A majority of such studies have concentrated on adsorption of molecules over well defined face planes of metal surfaces[1, 2]. Studies have also been conducted on surfaces of bulk metal oxides[3, 4, 5].

The ozone decomposition reaction mechanism and kinetics have been studied in detail for the MnO_x / Al_2O_3 catalyst[6, 7]. Several different spectroscopy[8] techniques have been used to study manganese oxides but the structure of these oxides at low metal oxide loadings (<6 wt%) is not clearly understood.

The previous chapter presented EXAFS and *in situ* laser Raman spectroscopy measurements which were used to evaluate the structure of the manganese active center for a MnO_x / Al_2O_3 catalyst. These studies provided bond distances and vibrational frequencies which can be directly compared to results obtained from *ab initio* calculations.

The EXAFS measurements have revealed the possibility of a manganese center surrounded by four or five oxygen atoms with a Mn – O bond distance of 0.20 nm (Fig.

2.8). In this chapter, these structural possibilities for the manganese active center in MnO_x / Al_2O_3 catalysts are explored using the Hartree – Fock *ab initio* method. Earlier work using isotope shift experiments has confirmed the presence of an adsorbed peroxide species on the catalyst surface during ozone decomposition[6]. The experimental Raman vibrational frequencies obtained for the Mn – O bonds and the peroxide species bands can be compared to those predicted by *ab initio* calculations; to better understand the molecular structures involved in the ozone decomposition process.

3.2 Experimental

3.2.1 Raman spectroscopy

The *in situ* Raman spectroscopy system used for catalyst characterization was permitted the observation of changes on the catalyst surface during the ozone decomposition reaction. The catalyst sample was pre-treated at 773 K for 2 hours in oxygen flow prior to spectral measurements. Spectra were acquired under oxygen flow and under ozone / oxygen mixture flows at 298 K and ozone partial pressure of 3000 Pa. The ozone was generated by passing filtered oxygen through a high-voltage silent-discharge ozone generator (OREC, V5-0). The laser was operated at 200 mW and the detector slit width was set at 100 μm. The resolution of the Raman spectrometer was 6 cm^{-1}. Spectra were acquired for 30 minutes using 60 second scans.

3.2.2 Ab initio calculations

All of the calculations were performed using a Gaussian 98 program on an IBM RS6000 machine. The geometry optimization of manganese – aluminum oxide clusters MnO_4Al_2O and $(MnO_4Al_2OO_2)^+$ were carried out using the Hartree – Fock method with all electrons treated explicitly; the vibrational frequencies of the compounds were computed by determining the second derivatives of the energy. The frequencies values estimated at the Hartree – Fock level were scaled using an empirical factor 0.8929[9]. This was done because of overestimates of frequencies resulting from the neglect of electron correlation by the Hartree – Fock method. The effect of four different basis sets (6-31G, 6-31G(d), 6-311G and 6-311G(d)) were used to determine the best converged geometries that compared well with both Raman and EXAFS results. The 6-31G method is a split valence basis set while the 6-311G method is a triple split valence basis set. Both methods model the valence shell using the *p* orbitals for oxygen and aluminum and the *d* orbitals for manganese. In the split valence basis set, two different sizes are used for the valence orbitals while in the triple split valence basis set three different sizes for these orbitals are employed. The 6-31G(d) and 6-311G(d) are similar to the previous basis sets except for the addition of polarized *d* functions for the oxygen and aluminum atoms and *f* functions for the manganese atoms. Ideally, the addition of polarized basis functions should improve the accuracy of the calculations being carried out.

3.3 Results

3.3.1 Raman spectra

The Raman spectra for the MnO_x / Al_2O_3 catalyst acquired under oxygen flow showed a feature at 660 cm^{-1} (Fig. 3.1a). The introduction of ozone led to the appearance of a peak at 880 cm^{-1} and a weak band at 930 cm^{-1} (Fig. 3.1b).

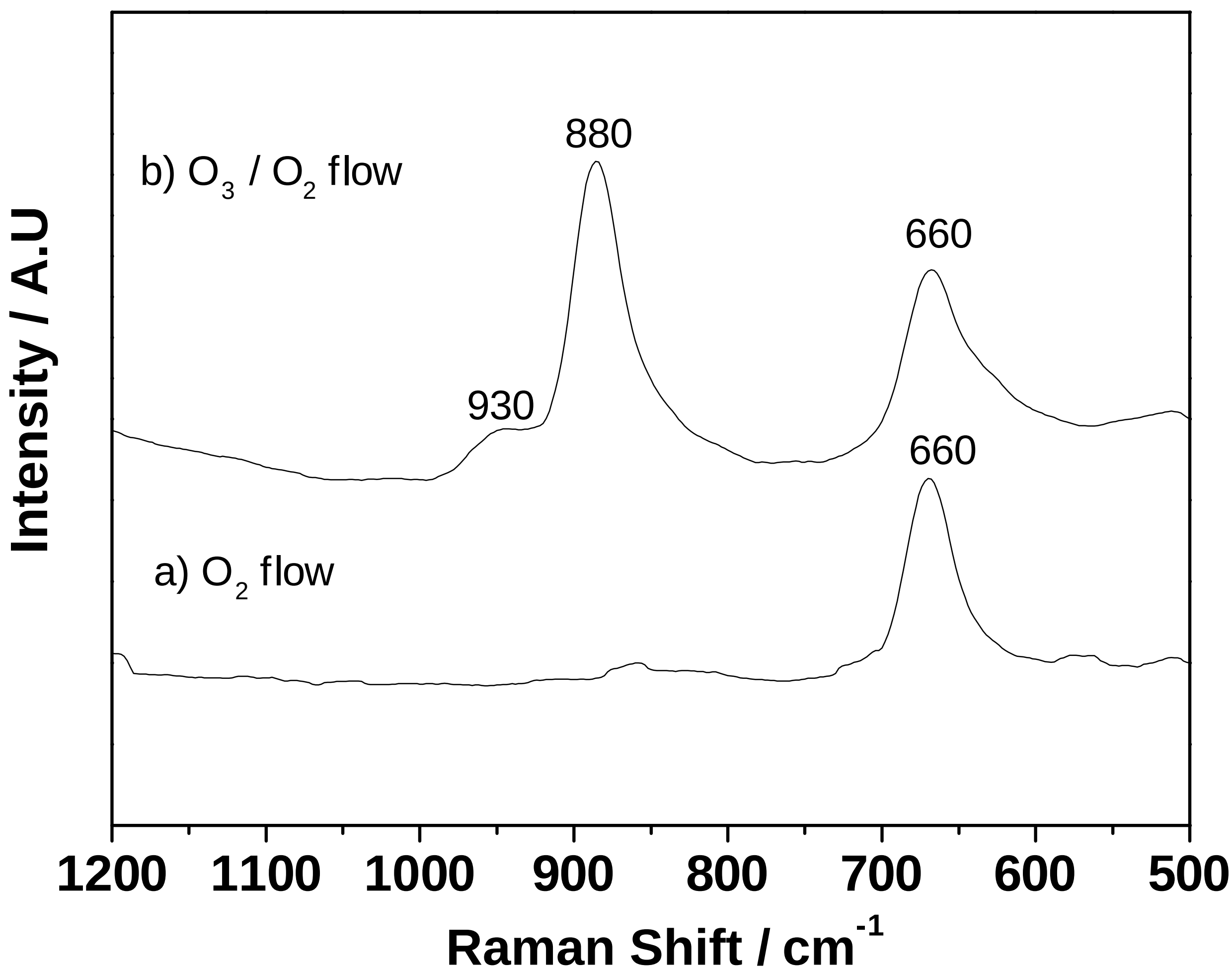

Figure 3.1 ***In situ*** **Raman spectra for MnO_x / Al_2O_3 catalyst at 298 K, 1 atm : a) O_2 flow, b) O_3/O_2 flow**

3.3.2 Ab initio calculations

Fig. 3.2 and Table 3.1 present the energy optimized geometry for the manganese center surrounded by five oxygen atoms using the HF / 6-31G(d) method.

MnO_4Al_2O

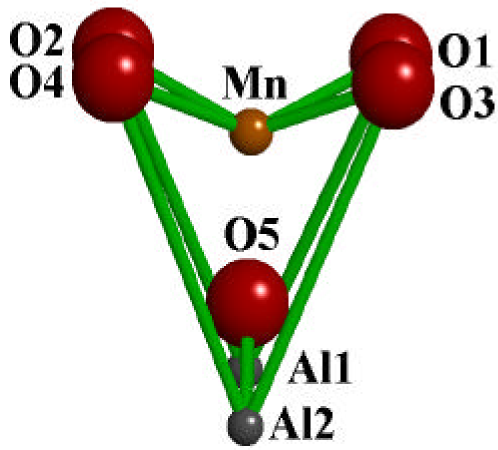

HF / 6-31G(d)

Figure 3.2 Energy optimized five oxygen co-ordinated manganese structure

Table 3.1 : Final structural parameters for five co-ordinate Mn species

Bond	Bond length / nm	Angle	Bond angle / ^{o}
Mn – O1(O2,O3,O4)	0.21	O1-Mn-O2	137.2
Mn – O5	0.21	O2-Mn-O4	71.4
Al1 – O1(O3)	0.38	Mn-O5-Al1	113.2
Al2 – O2(O4)			
Al1 – O5	0.18	Al1-O5-Al2	133.6
Al2 – O5			

Fig. 3.3 and Table 3.2 present similar results for the four co-ordinate manganese species using the HF / 6-311G basis set.

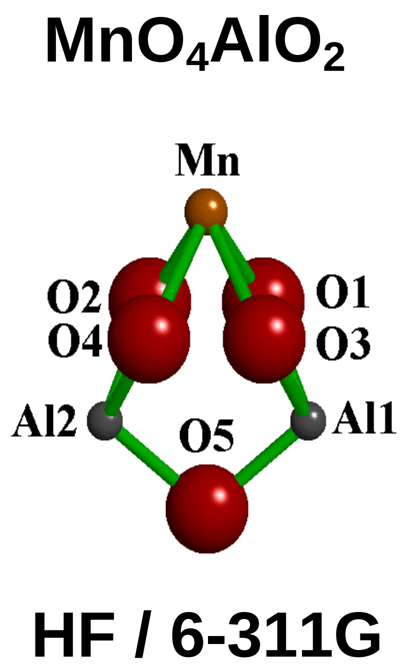

Figure 3.3 Energy optimized four oxygen co-ordinated manganese structure

Table 3.2 : Final structural parameters for four co-ordinate Mn species

Bond	Bond length / nm	Angle	Bond angle / ^{o}
Mn – O1(O2,O3,O4)	0.20	O1-Mn-O2	76.3
Mn – O5	0.35	O2-Mn-O4	65.8
Al1 – O1(O3)	0.18	Mn-O2-Al2	91.5
Al2 – O2(O4)			
Al1 – O5	0.17	Al1-O5-Al2	99.9
Al2 – O5			

Finally, Fig. 3.4 and Table 3.3 presents results for the four co-ordinate manganese center with an adsorbed peroxide species on top. This structure was again optimized using the HF / 6-311G method.

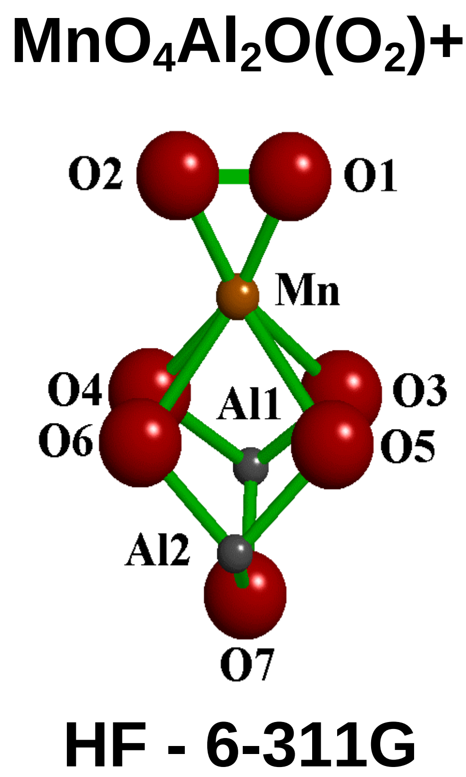

Figure 3.4 Energy optimized structure for manganese active site with a peroxide species

Table 3.3 : Final structural parameters for Mn active site with the peroxide group

Bond	Bond length / nm	Angle	Bond angle / ^{o}
Mn – O3(O4,O5,O6)	0.22	O4-Mn-O6	69.8
Mn – O7	0.40	O2-Mn-O4	69.9
Mn – O1(O2)	0.18	O1-Mn-O2	65.2
Al1 – O3(O5)	0.18	Mn-O6-Al2	102.1
Al2 – O4(O6)			
Al1 – O7	0.17	Al1-O7-Al2	97.6
Al2 – O7			
O1 – O2	0.15		

The choice of the basis sets and the relevant Raman vibrational frequency results will be discussed later in this chapter. Appendix A1 and A2 present the Gaussian input and a section of the output files for the structures represented in Fig. 3.3 and Fig. 3.4.

3.4 Discussion

3.4.1 Raman spectra

The Raman spectra for the catalyst acquired under oxygen flow shows a feature at 660 cm^{-1} (Fig. 3a). Work on supported manganese oxides indicated that the band does not provide insights into the local coordination or oxidation state of the manganese. The only information provided by this spectra was the presence of Mn-O bonds on the catalyst surface[8].

The introduction of an O_3/O_2 mixture lead to the appearance of a band at 880 cm^{-1} assigned to an adsorbed peroxide species (Fig. 3b). Earlier work using model Mn compounds and isotope shift experiments has confirmed this assignment[6].

3.4.2 Ab initio calculations

Tables 3.4 and 3.5 present a summary of the relevant Mn – O bond distances and Raman vibrational frequencies for the five and four coordinated manganese structures, respectively. The interatomic distances for both the four and five co-ordinate structures for all of the basis sets were between 0.20 and 0.22 nm. These were obtained as averages over all the Mn-O bonds and were close to the 0.20 nm value as determined through EXAFS.

A study on the Raman spectra of supported manganese oxides has identified Mn – O vibrational frequencies lower than 700 cm^{-1}[10]. The Mn – O bond vibrational frequency in this study was at 660 cm^{-1}. The smallest errors in vibrational frequency and bond length measurements for the five co-ordinate structure were obtained with the HF / 6-31G(d) method. The predicted vibrational frequency was 655 cm^{-1} (~ 1% error) with Mn – O distances of 0.21 nm. In the case of the four co-ordinate structure, the smallest errors in Mn – O vibrational frequency and bond length were predicted by the HF / 6-311G method. The predicted vibrational frequency was 638 cm^{-1} (~ 3% error) with Mn – O distances of 0.20 nm.

Table 3.4 : Results for the five co-ordinate Mn structure

Basis set	Mn – O distances / nm	Mn – O Raman frequency / cm^{-1}
6-31G	0.22	636
6-31G(d)	0.21	655
6-311G	0.21	1126
6-311G(d)	0.22	599

Table 3.5 : Results for the four co-ordinate Mn structure

Basis set	Mn – O distances / nm	Mn – O Raman frequency / cm^{-1}
6-31G	0.23	897
6-31G(d)	0.22	816
6-311G	0.20	638
6-311G(d)	0.20	699

Pott et. al[11] have determined that manganese in a +2 oxidation prefers a tetrahedral site. NEXAFS (Near edge x-ray absorption fine structure) studies[8] conducted for the MnO_x / Al_2O_3 catalysts have revealed that the oxidation state of Mn in this catalyst is close to +2. This suggests the four co-ordinate manganese structure is the more likely of the two structures, although the tetrahedral geometry is not reproduced. Attempts to geometry-optimize a tetrahedral structure were unsuccessful.

Table 3.6 presents a summary of Mn-O distances and vibrational frequencies for the manganese active center with the adsorbed peroxide species (O_2^{2-}). The vibrational frequencies for these O_2^{2-} species fall in the range 640 cm^{-1} – 970 cm^{-1}[12]. Only the structure predicted by the HF / 6-311G method gives an O-O frequency in this region. Additionally, the error of the predicted (903 cm^{-1}) and experimental (880 cm^{-1}) vibrational frequencies is < 3%.

Table 3.6 : Results for the four co-ordinate Mn structure with peroxide species

Basis set	Mn – O distances / nm	Mn – O Raman frequency / cm^{-1}
6-31G	0.24	1555
6-31G(d)	0.23	1023
6-311G	0.22	903
6-311G(d)	0.22	1013

Raman work using oxygen isotopes[6] has provided distinct vibrational frequency values for ^{16}O – ^{16}O, ^{16}O – ^{18}O and ^{18}O – ^{18}O. These represent three different peroxide groups on the catalyst surface in the presence of $^{18}O_3$ and $^{16}O_3$. The HF / 6-311G method was used to predicted vibrational frequencies for the various oxygen isotope combinations and the results are presented in Table 3.7.

The Raman vibrational frequencies predicted by the *ab-initio* method were corrected by a scaling factor. This scaling factor for vibrational frequencies was determined by Pople et al.[13] for the HF / 6-31G(d) method to be 0.8929. The value may not be readily applicable for the HF / 6-311G as scaling factors vary with basis set[9]. In this work we explored a scaling factor of 0.8724 based to provide a result which would agree with the observed $^{16}O - {}^{16}O$ frequency . Using this scaling factor for the other two peroxide species gave reasonable agreement between predicted and experimentally observed vibrational frequencies.

Table 3.7 : Raman frequency comparisons for adsorbed peroxide species isotopes

Isotope	Experimental / cm^{-1}	Predicted / cm^{-1}
$^{16}O - {}^{16}O$	886	882
$^{16}O - {}^{18}O$	860	861
$^{18}O - {}^{18}O$	836	840

3.5 Conclusions

EXAFS and Raman spectroscopy coupled with complementary *ab initio* calculations suggested that the structure of the manganese active center in MnO_x / Al_2O_3 catalysts is likely a four coordinate mononuclear species. The presence of an adsorbed peroxide species at 880 cm^{-1} during ozone decomposition on the surface of the MnO_x / Al_2O_3 catalyst was confirmed using Raman spectroscopy. The HF / 6-311G method provided the best estimates of bond lengths and Raman vibrational frequencies.

REFERENCES:

[1] Neurock, M.; *Studies in Surface Science and Catalysis.* **1997**, *109*, 3.

[2] Salazar, M. R.; Saravanan, C.; Kress, J. D.; Redondo, A.; *Surface Science*. **2000**, *449*, 75.

[3] Witko, M.; Hermann, K.; Tokarz, R.; *Catalysis Today.* **1999**, *50*, 553.

[4] Papakondylis, A.; Sautet, P.; *J. Phys. Chem.***1996**, *100*, 10681.

[5] Witko, M.; Hermann, K.; Michalak, A.; *Surface Science*. **1996**, *366*, 323.

[6] Li, Wei; Oyama, S. T.; *J. Am. Chem. Soc.*, **1998**, *120*, 9041.

[7] Li, Wei; Oyama, S. T.; *J. Am. Chem. Soc.*, **1998**, *120*, 9047.

[8] Radhakrishnan, R.; Oyama, S. T.; *J. Phys. Chem.*, Submitted.

[9] Foresman, J. B.; Frisch, A; *Exploring Chemistry with Electronic Structure Methods*. 2nd edition., **1993**, Gaussian, Inc.

[10] Buciuman, F; Patcas, F; Craciun, R; Zhan, R. T. D; *Phys. Chem. Chem. Phys.* **1999**, *1*, 185.

[11] Pott, G. T.; McNicol, B. D.; *Discuss. Faraday. Soc.* **1971**, *52*, 121.

[12] Che, M.; Tench, A. J.; *Advances in Catalysis*. **1983**, *32*, 1.

[13] Pople, J. A.; Scott, A. P.; Wong, M. W.; Radom, L.; *Israel J. Chem*. **1993**, *33*, 345.

CHAPTER 4

ACTIVE SITE TITRATION FOR SUPPORTED MANGANESE OXIDE CATALYSTS

4.1 Introduction

The dispersion of an active phase on a support surface metal and the total surface area of the sample are important catalyst properties estimated through chemisorption and physisorption techniques[1]. Counting the number of active sites on a catalyst surface is of particular importance because this value is used to obtain turnover rates for reactions. The turnover rates provide an accurate measure of comparing catalytic activity of different catalysts for the same reaction[2].

A method for estimating the number of active metal sites for supported molybdenum oxide catalysts was developed earlier[3]. The procedure involved carrying out oxygen chemisorption on the catalyst sample after pre-reduction at an elevated temperature. This elevated temperature, designated as T_{red}, was a temperature prior to bulk catalyst reduction, and was estimated using a temperature programmed reduction (TPR) technique. The same experimental procedure was applied to calculate the number of surface manganese sites on the supported manganese oxide catalysts. Alternatively, the number of active sites may also be estimated using a reactant probe technique. The procedure was developed specifically to measure active sites during the ozone decomposition reaction and utilizes the reactant itself as a probe. Temperature programmed desorption (TPD) traces (for oxygen) taken from MnO_x / Al_2O_3 catalysts after ozone adsorption[4] reveal peaks due to chemisorbed oxygen species. Quantifying the amount of these adsorbed oxygen species gives a direct estimate of the number of active manganese sites involved in the reaction. The two methods are compared to confirm the validity of the site densities obtained by the reaction probe method.

4.2 Active site density estimation – Experimental

4.2.1 Temperature programmed reduction (TPR) and oxygen chemisorption

The system used to measure oxygen chemisorption was a standard flow adsorption system using a computer interfaced mass spectrometer (Dycor / Ametek Model MA100)[3]. The TPR experimental procedure typically involved pre-treatment of the sample at 773 K for 2 hours in O_2 flow (Air Products > 99.6%) to remove accumulated moisture and other impurities. The reduction temperature of the bulk catalyst was determined by reducing the sample in H_2 flow (Air Products > 99.6%) from room temperature to 1073 K at a heating rate of 10 K/min. The mass spectrometer signal m/e of 18 corresponding to H_2O^+, was monitored during the reduction process. The onset of bulk reduction was the temperature at which the intensity of this signal increased dramatically.

The temperature at the point right before the onset of bulk reduction (T_{red}) was the temperature at which the oxygen chemisorption experiments were performed. This procedure involved pre-treatment of the sample at 773 K for 2 hours in O_2 flow (Air Products > 99.6%) followed by the reduction of the sample in H_2 flow (Air Products > 99.6%) at T_{red} for 2 hours. Following reduction, helium (Air Products > 99.6%) was introduced while monitoring the mass spectrometer signal m/e of 32, corresponding to O_2^+. Periodic pulses (5.6 μmol) of oxygen (Grade 4.4) were introduced into the reactor while monitoring the peak area and intensity of the O_2^+ signal. At saturation, the area under the oxygen peak was designated as A_{sat} (corresponding to 5.6 μmol). The difference in the area of the saturation peaks compared to the other oxygen peaks gave an estimate of the total amount of oxygen adsorbed by the sample. The oxygen chemisorption value was estimated using the expression : Uptake = $\Sigma 5.6((A_{sat}-A_I)/A_{sat})/$ mass of catalyst, where A_I is the area of each of the individual peaks. An example of the spectra used to estimate oxygen chemisorption values is presented in Fig 4.1.

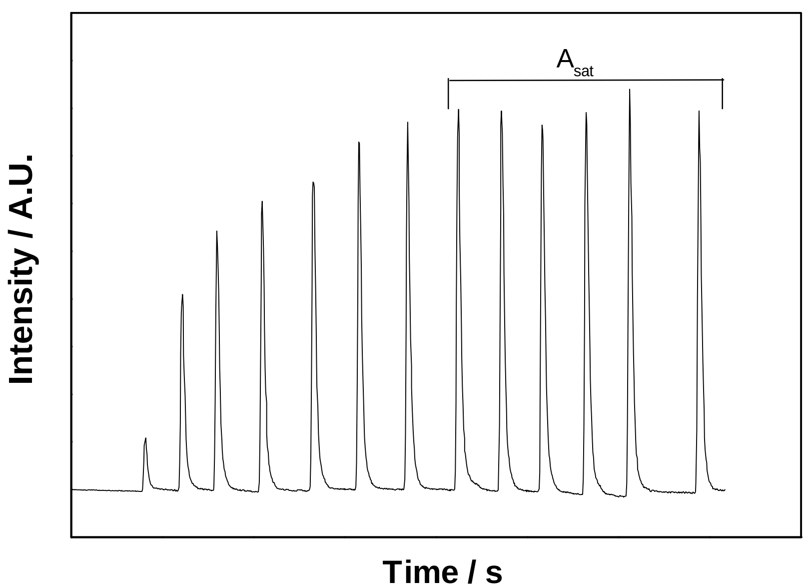

Figure 4.1 Oxygen peaks obtained during pulse flow chemisorption measurements

4.2.2 Temperature programmed oxygen desorption (TPD) and surface area estimation

This experiment was conducted in the same flow apparatus used in the oxygen chemisorption experiments. The catalyst (0.9 g) was loaded in a quartz reactor and pretreated in oxygen (Air products, Grade 2.6) flow for 2 hours. The sample was then cooled to 233 K using an isopropanol – liquid nitrogen gel. Ozone generated from oxygen using an ozone generator (OREC, V5-0) was introduced into the reactor and the sample was exposed to a 2 mol% O_3/O_2 mixture for 2 hours. The temperature programmed desorption was carried out in helium (Air products, Grade 5.0) flow by heating the sample to 1273 K at 0.17 K s^{-1} while monitoring the m/e signal 32, corresponding to molecular oxygen (O_2^+). Finally, the sample was cooled down to room temperature and 39 μmol pulses of oxygen were injected in order to calibrate the peaks corresponding to the adsorbed species. These calibrated values provided the required site densities (sites / g catalyst) for turnover rate calculations.

The surface area measurements were carried out in a Micromeritics ASAP 2000 unit. The sample (0.5 g) was loaded into a quartz reactor and degassed at 473 K in vacuum prior to all measurements. A five-point N_2 (Air products > 99.6%), BET analysis was used to measure the specific surface area (S_g) of each sample. All of the measurements were repeated twice.

4.3 Active site density estimation - Results

4.3.1 TPR and oxygen chemisorption results

Figure 4.2, shows the H_2O (m/e = 18) TPR traces for the Al_2O_3 support and the MnO_x / Al_2O_3 catalysts. There was a very weak increase in the H_2O signal observed at 863 K in the trace taken for the Al_2O_3 support. The H_2O signal increased sharply at 623 K for the trace taken for the MnO_x / Al_2O_3 catalyst and the signal peaked at 768 K. The signal intensity then dropped slightly and subsequently increased again at 863 K.

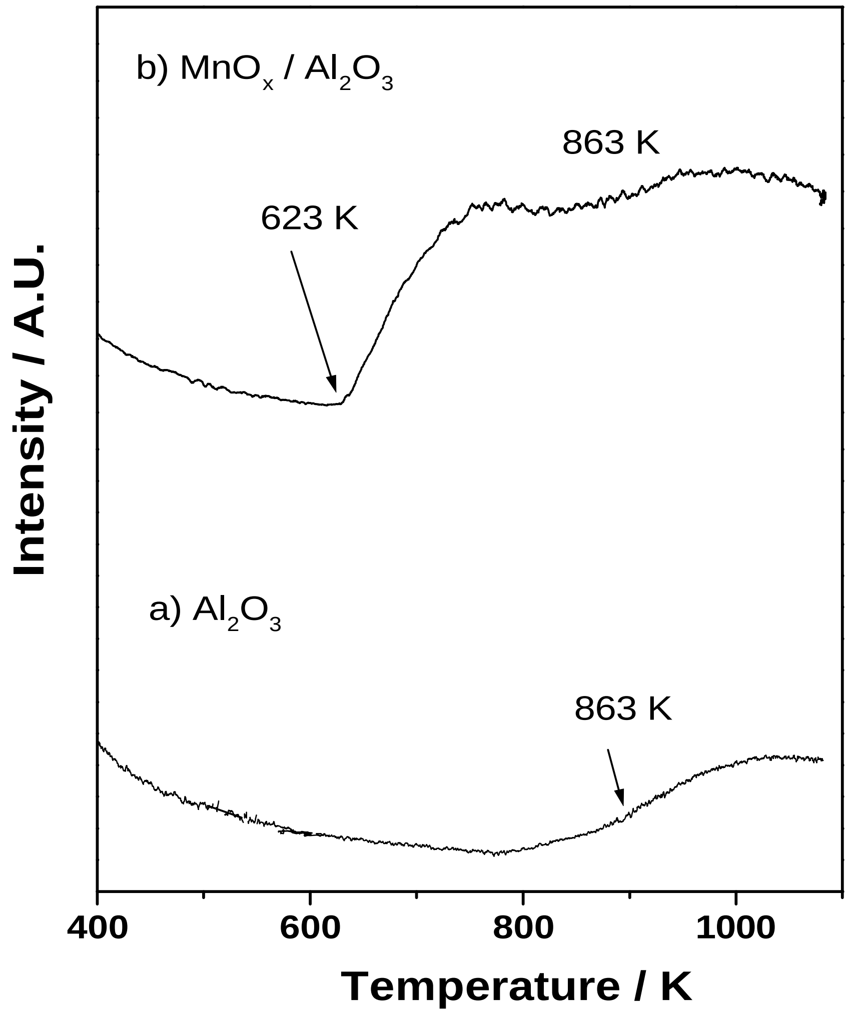

Figure 4.2 TPR trace (m / e = 18) for Al_2O_3 support and MnO_x / Al_2O_3 in hydrogen flow

Figure 4.3, shows the H_2O (m/e = 18) TPR traces for the ZrO_2 support and the MnO_x / ZrO_2 catalysts. There was no substantial increase in the H_2O signal in the trace taken for the ZrO_2 support. The H_2O signal increased sharply at 558 K for the trace taken for the MnO_x / ZrO_2 catalyst and the signal peaked at 673 K.

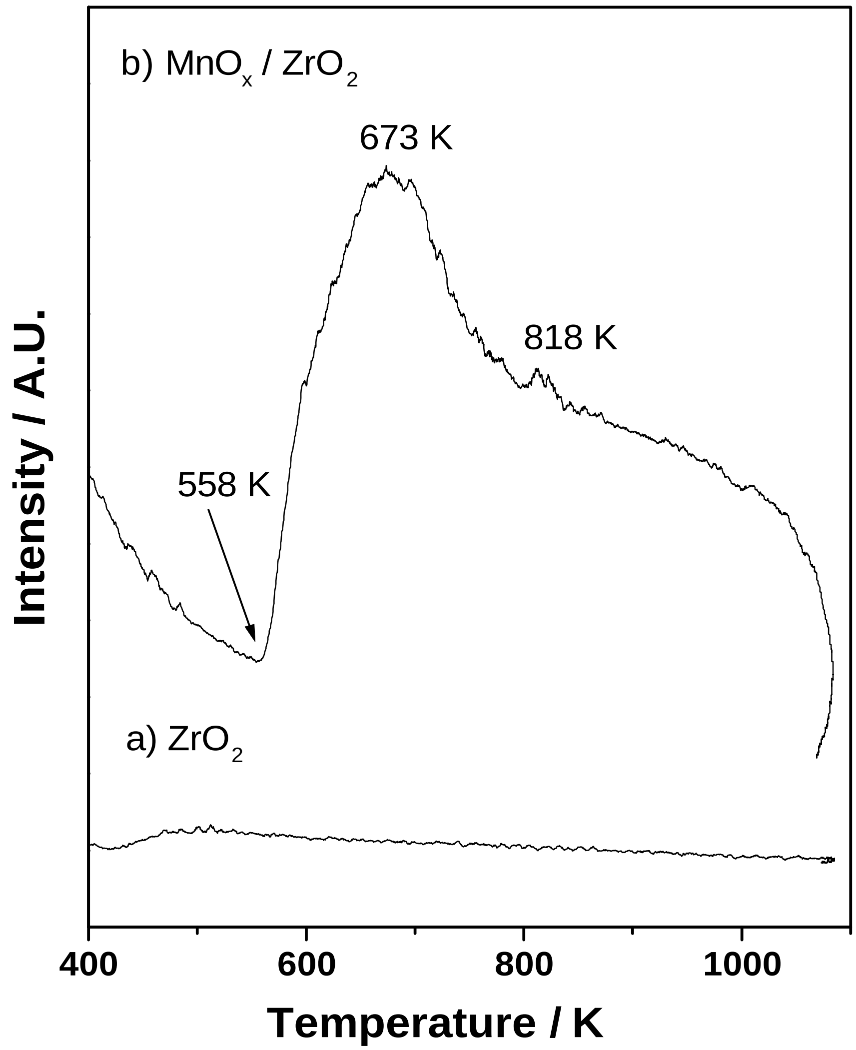

Figure 4.3 TPR trace (m / e = 18) for ZrO_2 support and MnO_x / ZrO_2 in hydrogen flow

Figure 4.4, shows the H_2O (m/e = 18) TPR traces for the TiO_2 support and the MnO_x / TiO_2 catalysts. There was a slight increase in the H_2O signal in the trace taken for the TiO_2 support at 711 K. The signal peaked at 908 K and eventually dropped off to a steady baseline. The H_2O signal increased sharply at 513 K for the trace taken for the

MnO_x / TiO_2. Two features for the H_2O signal at 603 K and 705 K were observed in the trace.

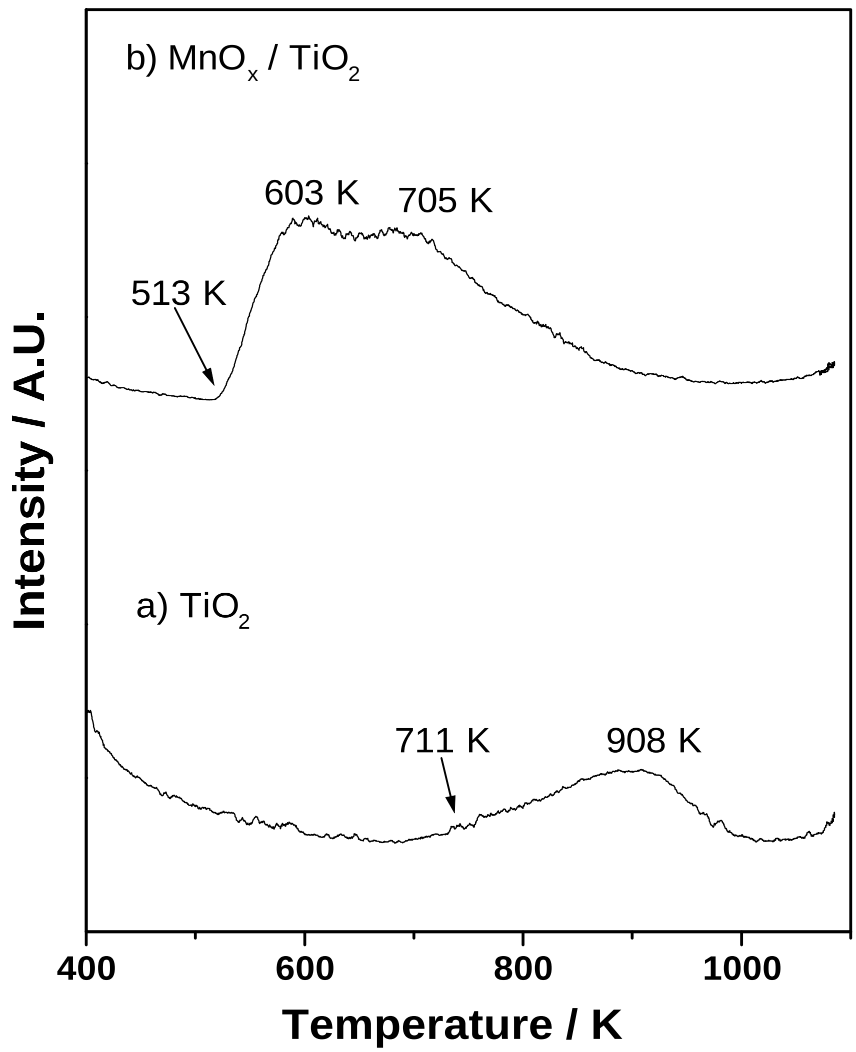

Figure 4.4   TPR trace (m / e = 18) for TiO_2 support and MnO_x / TiO_2 in hydrogen flow

Figure 4.5, shows the H_2O (m/e = 18) TPR traces for the SiO_2 support and the MnO_x / SiO_2 catalysts. There was an increase in the H_2O signal in the trace taken for the SiO_2 support at 655 K. The H_2O signal increased sharply at 498 K for the trace taken for the MnO_x / SiO_2. Two features for the H_2O signal at 535 K and 620 K were observed in the trace.

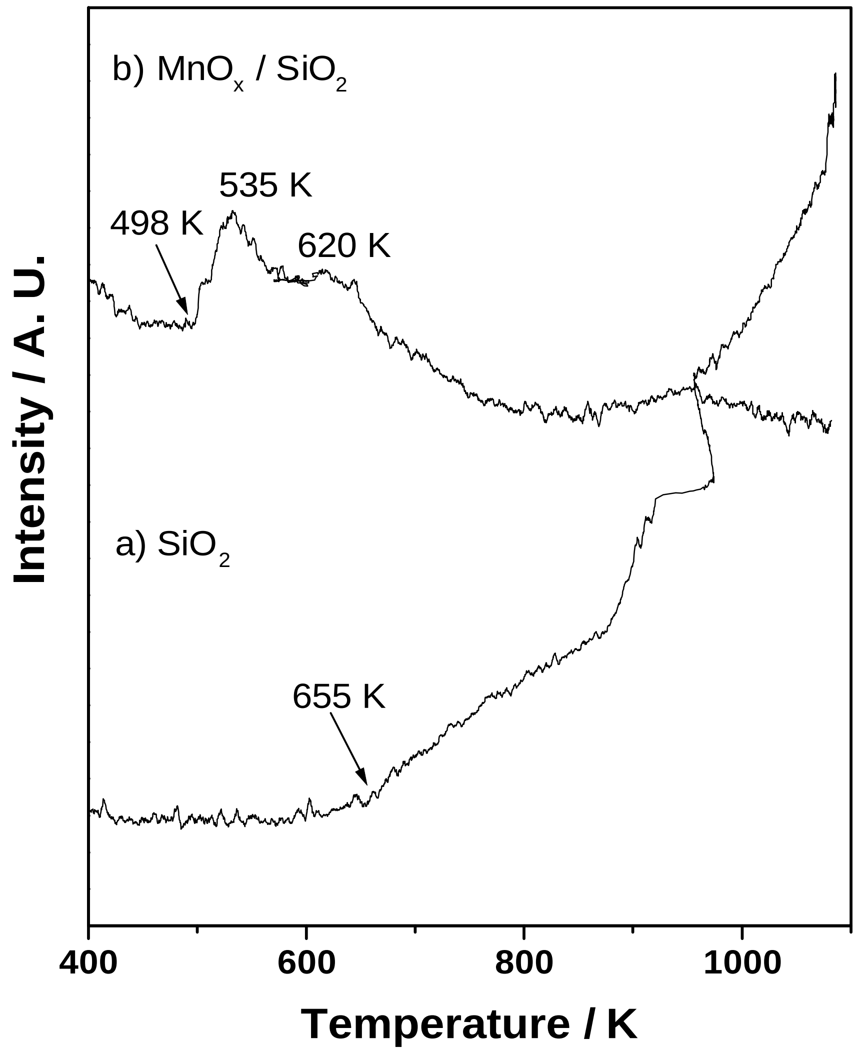

Figure 4.5 TPR trace (m / e = 18) for SiO_2 support and MnO_x / SiO_2 in hydrogen flow

Oxygen chemisorption experiments were conducted at the point of sharp H_2O signal increase (designated as the reduction temperature T_{red}) for each of the four catalysts. These chemisorption values are summarized along with the reduction temperature T_{red} in Table 4.1.

Table 4.1 : TPR and oxygen chemisorption results

Catalyst	Wt / Mol %	T_{red} / K	Uptake / μmol g^{-1}
MnO_x / Al_2O_3	1 / 0.42	623	44
MnO_x / ZrO_2	1 / 0.54	558	87
MnO_x / TiO_2	1 / 0.56	513	28
MnO_x / SiO_2	1 / 0.85	498	31

4.3.2 Oxygen TPD and surface area results

Figures 4.6-4.9 show oxygen (m/e = 32) TPD traces for the various Mn catalysts and supports. Signals due to ozone (m/e = 48) were not detected at any time in the experiments.

Figure 4.6 presents the oxygen TPD traces for the Al_2O_3 support and the MnO_x / Al_2O_3 catalyst. For the Al_2O_3 support alone, no peaks were observed in the TPD traces taken for the cases with and without ozone adsorption (Fig. 4.6a, 4.6b). Peaks at 830 K and 1095 K were observed for the MnO_x / Al_2O_3 catalyst when the sample was not exposed to ozone (Fig. 4.6c). Oxygen peaks at 410 K, 537 K, 830 K and 1095 K were recorded for the same sample after ozone adsorption (Fig. 4.6d).

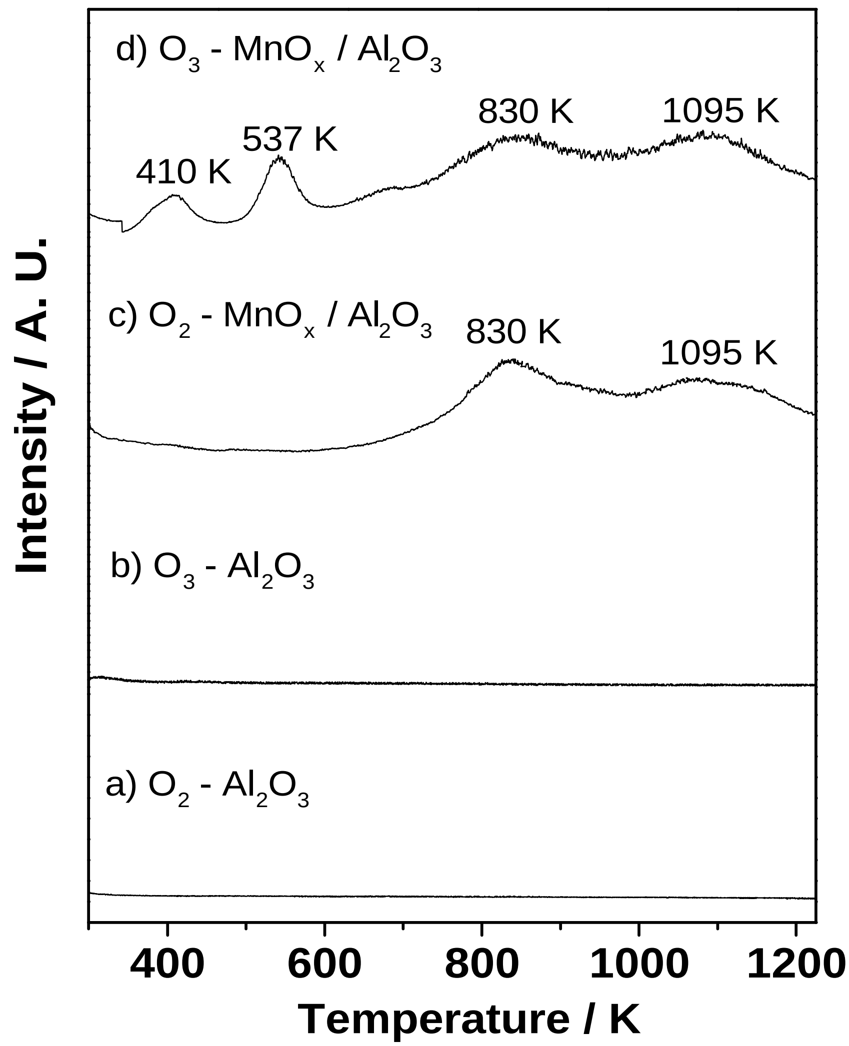

Figure 4.6 TPD traces (m/e = 32) for Al_2O_3 support and MnO_x / Al_2O_3 catalyst taken after O_3/O_2 and O_2 adsorption

Figure 4.7 shows similar TPD traces for the ZrO_2 support and the MnO_x / ZrO_2 catalyst. The ZrO_2 support trace showed no peaks without prior ozone adsorption (Fig. 4.7a). The MnO_x / ZrO_2 catalyst TPD trace without ozone adsorption showed oxygen peaks at 560 K, 775 K, 790 K and 1050 K (Fig. 4.7c) while the trace with ozone adsorption showed oxygen peaks at 370 K, 410 K, 549 K, 780 K, 790 K and 1060 K (Fig.

4.7d). After ozone adsorption, the trace from this support showed a mass 32 peak at 532 K (Fig. 4.7b).

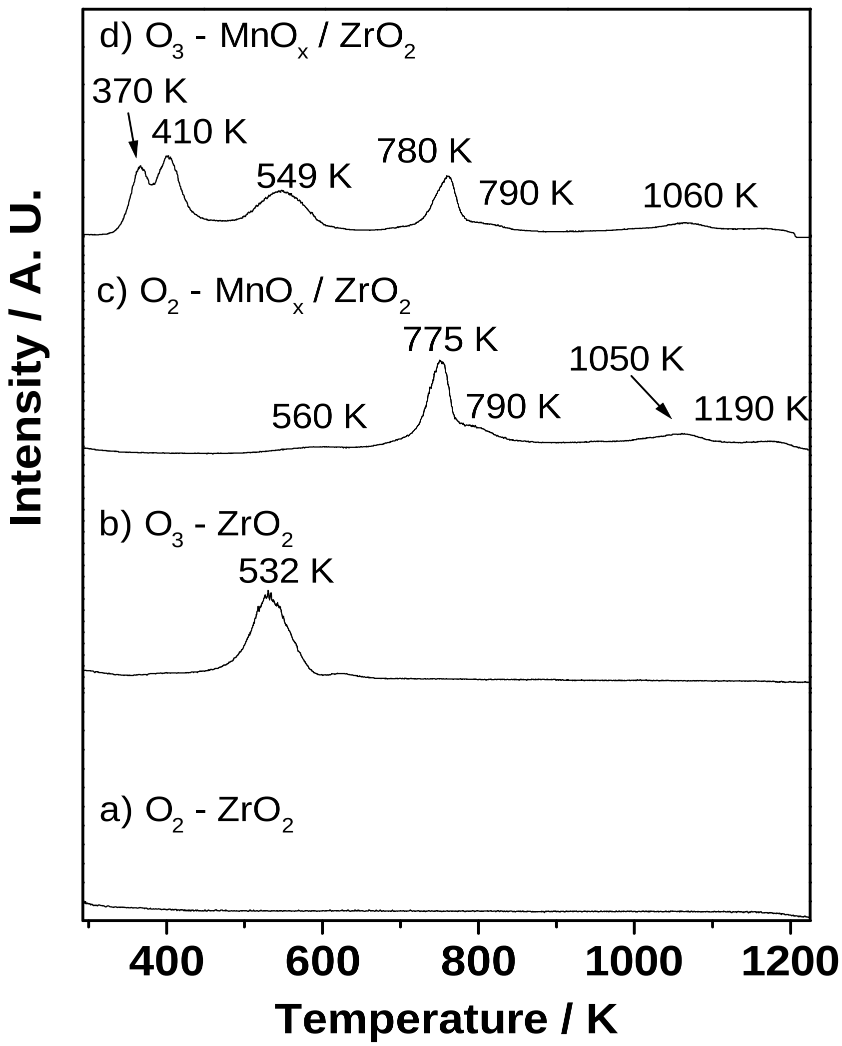

Figure 4.7 TPD traces (m/e = 32) for ZrO_2 support and MnO_x / ZrO_2 catalyst taken after O_3/O_2 and O_2 adsorption

Figure 4.8 shows the corresponding TPD traces for the TiO_2 support and the MnO_x / TiO_2 catalyst. The trace taken from the MnO_x / TiO_2 catalyst without ozone adsorption showed oxygen peaks at 770 K, 836 K and 1005 K (Fig. 4.8c) while the trace taken after ozone adsorption showed peaks at 378 K, 830 K and 995 K (Fig. 4.8d). Again, no peaks were observed for TPD traces taken from the TiO_2 support for cases with and without ozone adsorption (Fig. 4.8a, 4.8b).

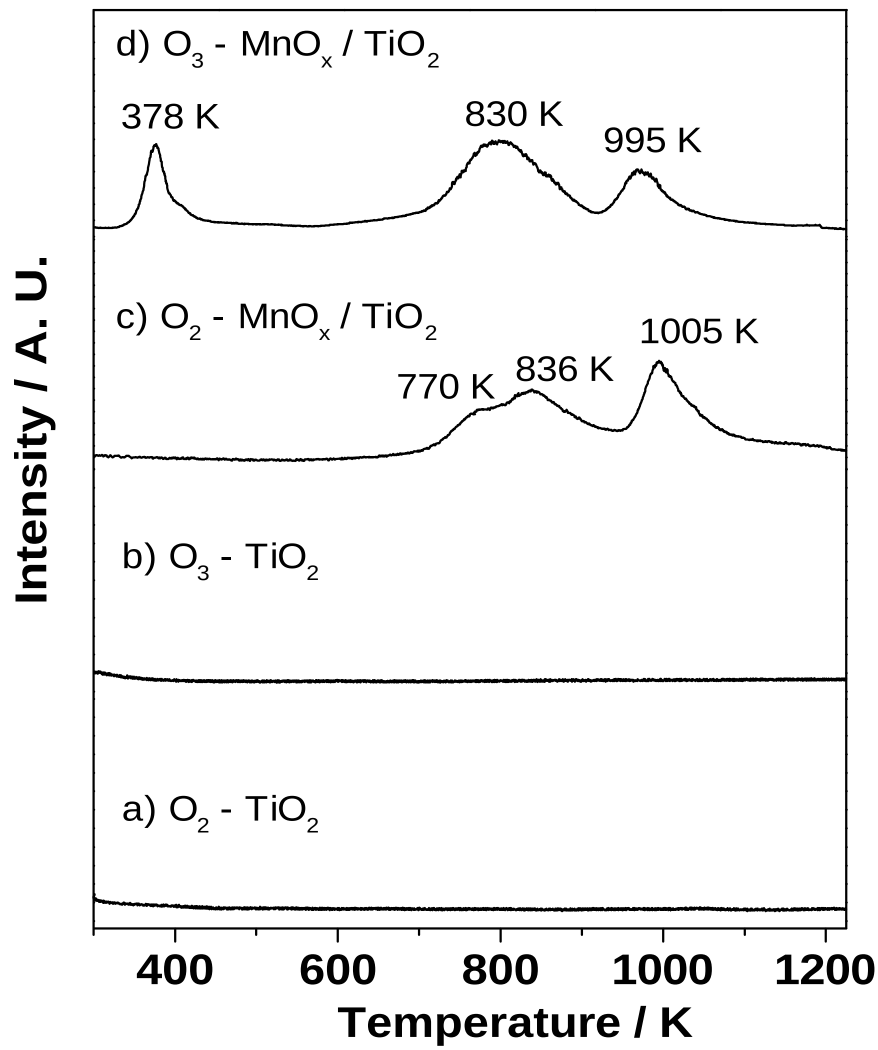

Figure 4.8 TPD traces (m/e = 32) for TiO_2 support and MnO_x / TiO_2 catalyst taken after O_3/O_2 and O_2 adsorption

Figure 4.9 shows the TPD traces for the SiO_2 support and the MnO_x / SiO_2 catalyst. Oxygen peaks at 755 K, 865 K and 1225 K were observed when the trace was taken without ozone adsorption on the MnO_x / SiO_2 catalyst (Fig. 4.9c). After ozone adsorption, oxygen peaks at 363 K, 548 K, 760 K, 870 K and 1230 K were identified (Fig. 4.9d). For the SiO_2 support, TPD traces revealed no peaks with and without ozone adsorption (Fig. 4.9a, 4.9b).

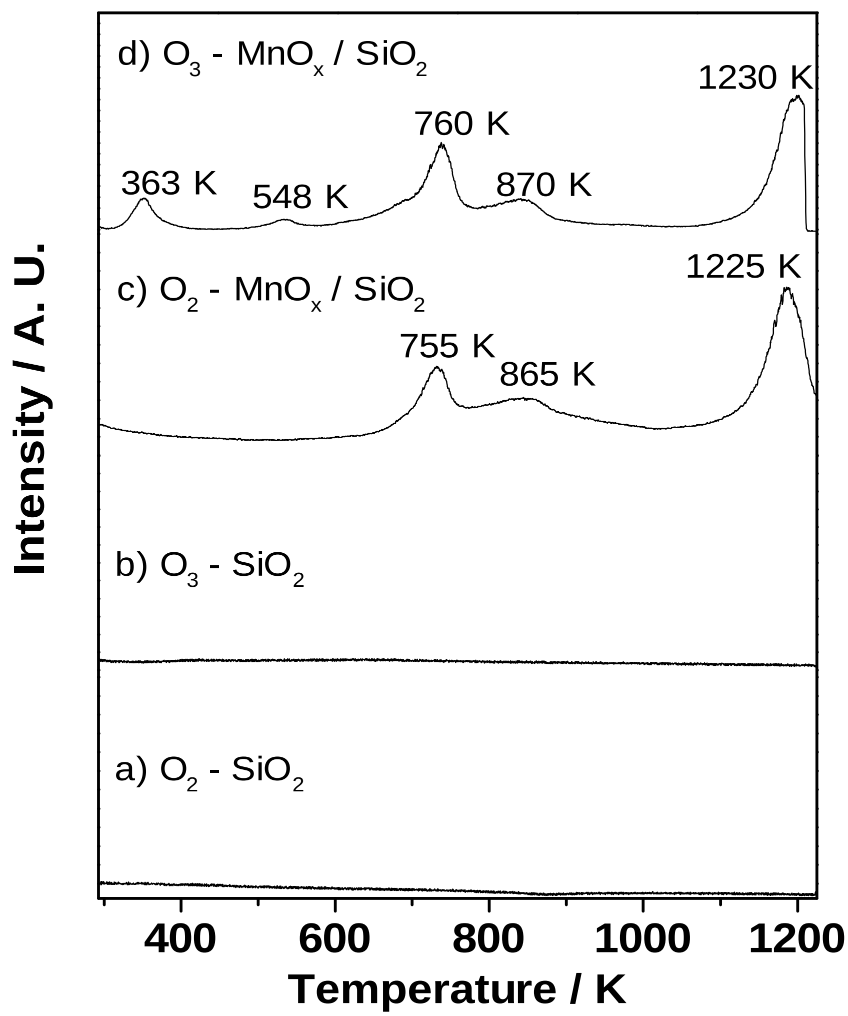

Figure 4.9 TPD traces (m/e = 32) for SiO_2 support and MnO_x / SiO_2 catalyst taken after O_3/O_2 and O_2 adsorption

Integration of the TPD peak areas corresponding to the desorption of molecular oxygen allowed the determination of the active site density and corresponding dispersion values for the catalysts. The surface areas for the supports and the catalysts followed the trend $Al_2O_3 \sim SiO_2 > TiO_2 \sim ZrO_2$. These values have been summarized along with the corresponding catalyst active site concentrations in Table 4.2.

Table 4.2 : Active site densities and surface areas

Catalyst	Wt / mol %	S_g / $m^2\ g^{-1}$	Total / μmol g^{-1}	Dispersion / %
MnO_x / Al_2O_3	3 / 3.5	92	40	12
MnO_x / ZrO_2	3 / 4.2	45	163	47
MnO_x / TiO_2	3 / 2.8	47	31	9
MnO_x / SiO_2	3 / 2.1	88	13	4
Al_2O_3		96	-	-
ZrO_2		50	25	0.3
TiO_2		52	-	-
SiO_2		95	-	-

4.4 Discussion

4.4.1 TPR spectra

The slight increase in the H_2O signal (m/e = 18) in the case of the TPR traces taken from all of the supports (Fig. 4.2a, Fig. 4.3a, Fig 4.4a, Fig. 4.5a) is probably due to support dehydroxylation. The H_2O peaks obtained for the traces taken for each of the catalysts (Fig. 4.2b, Fig. 4.3b, Fig 4.4b, Fig. 4.5b) are an indication of bulk reduction of manganese oxide.

Kapteijn et. al[5] studied MnO_x / Al_2O_3 catalyst using TPR. Their studies identified two bulk reduction peaks at 650 K and 840 K for 1 wt% MnO_x / Al_2O_3. They concluded that greater interaction with the support led to a larger bulk reduction temperature. The point at which bulk reduction begins, T_{red}, for catalysts in this work, followed the trend $Al_2O_3 > ZrO_2 > TiO_2 > SiO_2$. This trend is comparable to the trend in pH at the point of zero charge (PZC) for the various supports where the strongest interaction is expected between the Al_2O_3 and the acidic manganese acetate solution. Since the oxidation state of manganese is the lowest for MnO_x / Al_2O_3 (Chapter 2), it can be deduced that greater interaction with the support leads to a lower oxidation state and a larger bulk reduction temperature for the supported manganese oxides. This may also be the reason for the mononuclear structure of the manganese center in MnO_x / Al_2O_3.

4.4.2 TPD spectra

The absence of oxygen (m/e = 32) desorption peaks in the TPD trace of pure alumina without ozone adsorption indicated, as is well known, that the support does not undergo bulk reduction at elevated temperatures (Fig. 4.6a). The absence of desorption peaks after the alumina is exposed to ozone indicated that no adsorbed species are formed on this support, a result that is consistent with its lack of activity for the ozone decomposition reaction (Fig. 4.6b). The peaks at 830 K and 1095 K in the TPD trace of MnO_x / Al_2O_3 (without ozone adsorption) indicated reduction of bulk manganese oxide at these temperatures (Fig. 4.6c). The TPD trace for the catalyst after ozone adsorption showed desorption peaks at 410 K and 537 K, both indicating the presence of adsorbed oxygen species. Raman spectroscopy indicated the presence of peroxide species on the catalyst surface which desorbed at temperatures < 500 K. This suggests that the peak observed at 410 K was likely due to the peroxide species while the peak observed at 537 K resulted from the recombination and desorption of another species, most probably adsorbed atomic oxygen[4].

It is likely that the pure zirconia did not undergo bulk reduction at elevated temperatures because of the absence of oxygen desorption peaks in the TPD trace taken without ozone adsorption (Fig. 4.7a). As with the Al_2O_3 support, the desorption peak at 532 K on the TPD trace taken after ozone adsorption (Fig. 4.7b) on zirconia was indicative of adsorbed atomic oxygen on the support surface during ozone decomposition. The recombination and desorption reaction of the adsorbed atomic oxygen probably did not occur under the ozone decomposition reaction conditions tested for the catalysts (T < 350 K).

The peaks at 775 K and 1050 K in the TPD trace of MnO_x / ZrO_2 (without ozone adsorption) indicated bulk manganese oxide reduction at these temperatures (Fig. 4.7c). After ozone adsorption (Fig. 4.7d), the desorption peaks at 370 K and 410 K were due to decomposing peroxide groups on the catalyst surface while the peak at 549 K was due to the recombination and desorption of adsorbed atomic oxygen. The same TPD experiment for the MnO_x / ZrO_2 catalyst was repeated at 193 K and the active site concentration was calculated by integrating the areas under the desorption peaks. This concentration was the same at both 193 K and 233 K suggesting that the surface active sites were already saturated by adsorbed species at 233 K.

The TPD trace taken for pure titania with (Fig. 4.8a) and without (Fig. 4.8b) ozone adsorption showed no desorption features from bulk reduction or adsorbed oxygen species. Bulk manganese oxide reduction peaks at 770 K, 836 K and 1005 K were observed in the TPD trace of MnO_x / TiO_2 catalyst taken without ozone adsorption (Fig. 4.8c). There was only one desorption peak at 378 K for the TPD trace taken after ozone adsorption on the MnO_x / TiO_2 catalyst (Fig. 4.8d), indicative of an adsorbed peroxide species. The absence of a peak due to adsorbed atomic oxygen in this trace suggested that the recombination and desorption reaction of this species for the catalyst did not occur under the measurement conditions.

Finally, the TPD trace taken for pure silica with (Fig. 4.9a) and without (Fig. 4.9b) ozone adsorption showed no desorption features from bulk reduction or adsorbed oxygen species. Bulk manganese oxide reduction peaks at 755 K, 865 K and 1225 K were observed in the TPD trace of MnO_x / SiO_2 catalyst taken without ozone adsorption (Fig. 4.9c). These desorption features shifted to 760 K, 870 K and 1230 K when the trace was taken after ozone adsorption on the MnO_x / SiO_2 catalyst (Fig. 4.9d). The trace also had weak desorption features at 378 K and 548 K indicative of adsorbed peroxide and atomic oxygen species, respectively.

4.4.3 Manganese active site density estimation

Table 4.3 presents a comparison of the manganese active site density values obtained for the catalysts, obtained using oxygen chemisorption and oxygen TPD methods. The average percentage error in these measurements is about 10% based on repeated experiments.

Table 4.3 : Comparison of active site density estimates

Catalyst	Oxygen chemisorption $\mu mol\ g^{-1}$	Oxygen TPD $\mu mol\ g^{-1}$
MnO_x / Al_2O_3	44	40
MnO_x / ZrO_2	87	163
MnO_x / TiO_2	28	31
MnO_x / SiO_2	31	13

The largest difference in the measurements is seen for the MnO_x / ZrO_2 catalyst. The oxygen chemisorption measurements in this case could be measuring only the manganese sites involved in the reaction. The presence of two distinct peroxide species peaks in the TPD measurements for ZrO_2 suggested the presence of a second site possibly at the interface of the manganese and the support. It is therefore likely that the reactant probe method in this case is counting sites which are not measured by the oxygen chemisorption technique. This indicates that the reactant probe method gives a better estimate of all the active sites involved in the ozone decomposition reaction. Furthermore, the two methods can be used to complement one another and confirm the accuracy of active site density measurements.

4.5 Conclusions

The supported manganese oxide catalysts were reduced in hydrogen flow and it was determined that the reducibility of the catalysts followed the trend MnO_x / Al_2O_3 < MnO_x / ZrO_2 < MnO_x / TiO_2 < MnO_x / SiO_2. This followed trends predicted by NEXAFS measurements and showed that smaller metal oxide – support interactions lead to greater reducibility. The manganese site densities estimated through oxygen chemisorption (at T_{red}) and oxygen TPD showed very good agreement except in the case of the ZrO_2 supported catalyst. The TPD seemed to be a better method of estimating all of the active sites involved in the ozone decomposition reaction.

REFERENCES:

[1] Richardson, J. T.; *Principles of Catalyst Development*, **1989**, Plenum Press.

[2] Boudart, M.; Mariadassou, G. D.; *Kinetics of Heterogeneous Catalytic Reactions*, **1984**, *Princeton University Press*.

[3] Desikan, A. N.; Huang, L.; Oyama, S. T.; *J. Phys. Chem.*, **1991**, *95*, 10050.

[4] Oyama, S. T.; Li, Wei; *Topics in Catalysis.* **1999**, 75.

[5] Kapteijn, F.; van Langeveld, A. D.; Moulijn, J. A.; Andreini, A; Vuurman, M. A.; Turek, M. A.; Jehng, J.M; Wachs, I. E.; *J. Catal.* **1994**, *150*, 94.

CHAPTER 5

OZONE DECOMPOSITION STUDIES

5.1 Introduction

Catalytic activity is often influenced by the structure and electronic properties of the support[1]. Considerable work has been done in examining the effect of support on the reactivity of transition metal oxides. Previous studies of ethanol oxidation over MoO_3 catalysts has shown that metal oxide - support interactions are responsible for changing activities and selectivities[2]. The difference in the activities of the various supported MoO_3 catalysts for ethanol oxidation studies is reported to have resulted from a difference in the pre-exponential term in the reaction rate constant (because there was little activation energy variation among the catalysts). The reactivity trend in this case followed $TiO_2 > Al_2O_3 > SiO_2$. Similar trends in activity were observed for methanol oxidation on supported MoO_3[3] and V_2O_5[4] catalysts. The greater lability of the metal – oxygen – support bridging bond for ZrO_2 and TiO_2 supported catalysts was given as a reason for their higher activities.

Previous work done helped elucidate a mechanism and reaction kinetics for the ozone decomposition reaction on a MnO_x / Al_2O_3 catalyst[5, 6]. The effect of support on ozone decomposition activity and reaction kinetics were not studied. In this chapter ozone decomposition reactivity and kinetic work on the supported manganese oxides are presented. A detailed study was conducted on MnO_x / ZrO_2 and MnO_x / TiO_2 catalyst using *in-situ* laser Raman spectroscopy to quantify reaction intermediates on the surface of the working catalysts. The study confirmed the involvement of an adsorbed peroxide species on the two catalysts and the applicability of the non-uniform surface kinetics proposed earlier[6]. The result was a set of kinetic parameters that were compared to those obtained in the previous work (on MnO_x / Al_2O_3) and which help explain ozone decomposition activity differences for the various manganese oxide catalysts.

5.2 Experimental

The kinetic experiments were conducted in the *in situ* laser Raman spectroscopy system described in Chapter 2. The unique feature of this system was its ability to simultaneous measure both steady state kinetic data and coverages of the adsorbed species under actual reaction conditions. The reactor used was a low volume Suprasil quartz *in situ* cell (volume < 25 cm^3), which allowed effective investigation of surface reactions under varying partial pressure and temperature conditions. The temperature of the sample was monitored through a thermocouple placed 3 mm from the sample in a thermocouple well. The sample (0.3 g) was pressed into a thin cylindrical wafer with a diameter of about 15 mm and a thickness of 1 mm, which was rotated at approximately 1500 rpm to prevent local overheating due to the laser. The wafer was pretreated in flowing oxygen (Airco, >99.6%) at 773 K for 2 h. Ozone was generated by passing filtered oxygen through a high-voltage silent-discharge ozone generator (OREC, V5-0). The total pressure in the system was maintained at 101 kPa and the generated ozone/oxygen mixture was introduced into the cell with ozone partial pressures varying from 0.4 kPa to 3 kPa. The reaction temperature was varied from 293 K to 340 K and the flow rate of the ozone/oxygen mixture was maintained at 744 μmol s^{-1} (1000 cm^3 min^{-1}). The inlet and outlet ozone concentrations were monitored using a UV absorption-type ozone analyzer (IN-USA, AFX-H1). Steady state turnover rates were based on ozone conversions and the number of Mn active sites calculated from the ozone desorption experiments (Chapter 2), using the expression, rate = (conversion × flow rate) × (ozone concentration)/number of sites.

Simultaneous *in situ* Raman spectra for the adsorbed species were acquired using the argon ion laser, single stage monochromator and CCD detector. The laser was operated at 200 mW and the detector slit width was set at 100 μm. The resolution of the Raman spectrometer was 6 cm^{-1}. Heating was carried out using heating tape around the samples. Cooling of the samples was achieved by passing chilled water through Teflon tubing wrapped around the cell.

The kinetic parameters like activation energies and pre-exponentials for the MnO_x / ZrO_2 and MnO_x / TiO_2 catalysts were obtained by incorporating the coverage of the adsorbed species obtained from the *in situ* Raman spectra for the catalysts under reaction conditions. These coverage values were obtained by quantifying the area of the adsorbed species peaks and normalizing them based on areas obtained at the lowest temperature (293 K) and largest ozone partial pressure (3000 Pa), where saturation was expected.

5.3 Ozone decomposition mechanism and kinetics

The proposed ozone decomposition mechanism from the studies on an Al_2O_3 supported manganese oxide catalyst is presented in Scheme 1. The symbol * is used to denote surface sites. Briefly, experiments involving isotope ($^{18}O_3$)[5] substitution ruled out the possibility of oxygen atom recombination, and the finding that the adsorbed ozone never desorbed established the irreversibility of steps (i) and (ii). Furthermore, the finding that the peroxide species could not be formed from molecular oxygen at any conditions showed the irreversibility of step (iii).

Scheme 1. Proposed Ozone Decomposition Mechanism

$$O_3 + * \longrightarrow O_2 + O* \qquad \text{(i)}$$

$$O_3 + O* \longrightarrow O_2* + O_2 \qquad \text{(ii)}$$

$$O_2* \longrightarrow O_2 + * \qquad \text{(iii)}$$

The acquired steady state reaction rate and coverage data were analyzed using : a) a uniform surface kinetic treatment; b) a non uniform surface kinetic treatment.

5.3.1 Uniform surface kinetics

The uniform surface kinetic treatment is generally applied to catalysts when the active sites on the surface have the same thermodynamic and kinetic properties[7]. This treatment is also applied to cases where there are no interactions between the adsorbed species.

This method uses the Langmuir relationship[8] between surface coverage and reactant partial pressure (Eqn. 1). The reaction rate is expressed as a rate constant multiplied by the surface coverage θ_{SS} (Eqn. 2).

$$\theta_{ss} = \frac{K(O_3)}{1 + K(O_3)} \qquad (1)$$

$$r_{ss} = k\theta_{ss} \qquad (2)$$

In these equations, K is an equilibrium constant and k is the reaction rate constant.

5.3.2 Non uniform surface kinetics

A non uniform surface kinetic treatment is used when the surface is made up of several different active sites, or when there are interactions between adsorbed species. This method treats the surface a collection of sites of different properties[7].

The non-uniform analysis used here is taken from the classic case of ammonia synthesis on iron catalyst[9, 10] with an adsorption activation energy which increases linearly with coverage ($E_a = E_a^0 + gRT\theta$) and a desorption activation energy that decreases linearly with coverage ($E_d = E_d^0 - hRT\theta$). Equations 3 and 4 are the resulting rate expressions obtained for adsorption and desorption, respectively.

$$r_a = k_a^o (O_3) e^{-g\theta} \tag{3}$$

$$r_d = k_d^o e^{h\theta} \tag{4}$$

In these expressions, k_a^0 and k_d^0 are the adsorption and desorption rate constants at zero coverage.

Setting the adsorption and desorption rate expressions equal provides equations for both the steady state rate and the steady state coverage, equations 5 and 6.

$$r_{ss} = k_d^o \left[\frac{k_a^o}{k_d^o} (O_3) \right]^{\frac{h}{g+h}} \tag{5}$$

$$\theta_{ss} = \frac{1}{g+h} \ln \left[\frac{k_a^o}{k_d^o} (O_3) \right] \tag{6}$$

The rate expression indicates that a fractional order dependency on ozone partial pressure (h/ (g+h) < 1) is anticipated.

5.4 Results

5.4.1 In situ Raman spectra

Figure 5.1, shows the Raman spectra at room temperature (293 K) for manganese oxide on ZrO_2, under both oxygen flow and ozone/oxygen flow. Under oxygen flow (Fig. 5.1a), there were peaks at 336 cm^{-1}, 383cm^{-1}, 470 cm^{-1}, 552 cm^{-1} and 626 cm^{-1}. The introduction of ozone (Fig. 5.1b) resulted in the appearance of a very intense peak at 880 cm^{-1} along with a shoulder feature at 852 cm^{-1} and a broad band at 930 cm^{-1}.

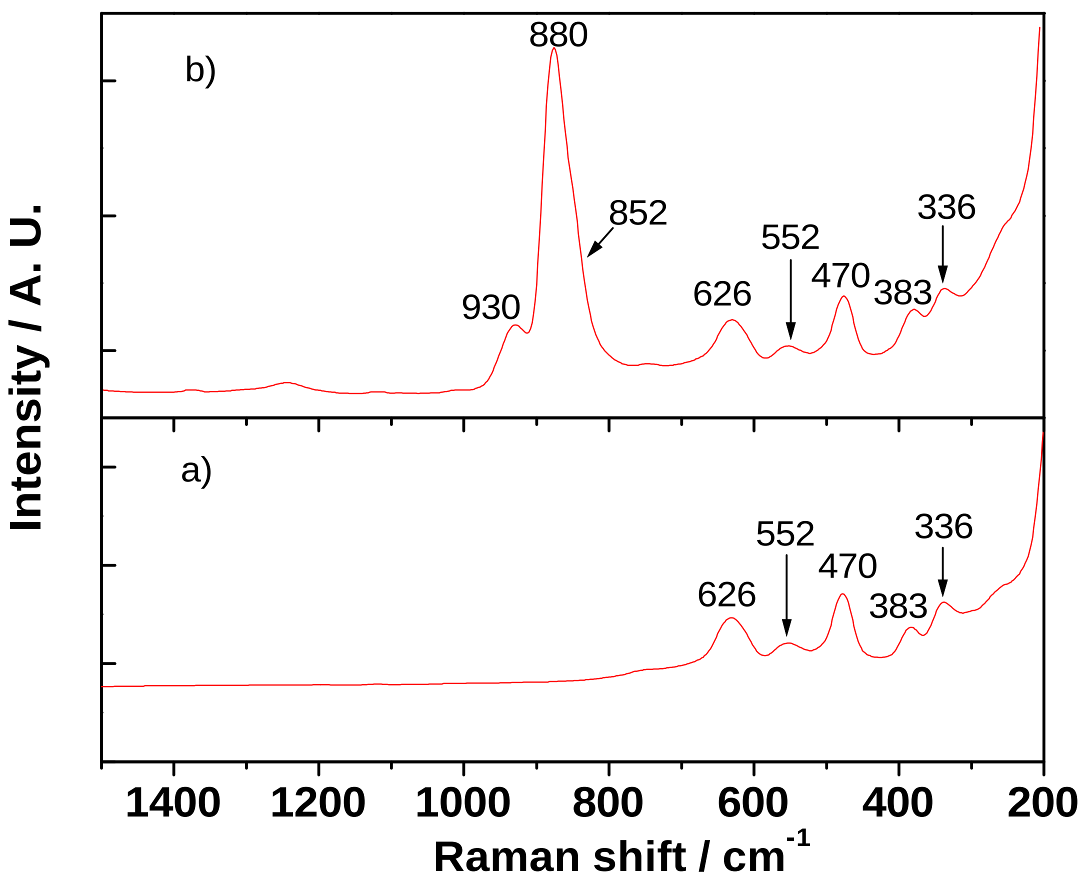

Figure 5.1 ***In situ*** **Raman spectra for MnO_x / ZrO_2 catalyst at 298 K, 1 atm : a) O_2 flow, b) O_3/O_2 flow**

This peak at 880 cm^{-1} was accompanied by two overtone peaks at 1754 cm^{-1} and 2615 cm^{-1}(not shown). All the new peaks (Fig. 5.1b) slowly disappeared once ozone flow was cut off. Similar measurements were carried out at different temperatures (273, 313, 328 and 343 K). It was found that the maximum peak intensity for the adsorbed species did not change for the 273 K and 293 K measurements.

Figure 5.2, presents the Raman spectra for TiO_2 supported manganese oxide under similar conditions, again at room temperature (293 K). Spectra presented in figures 5.1 and 5.2 are drawn to scale.

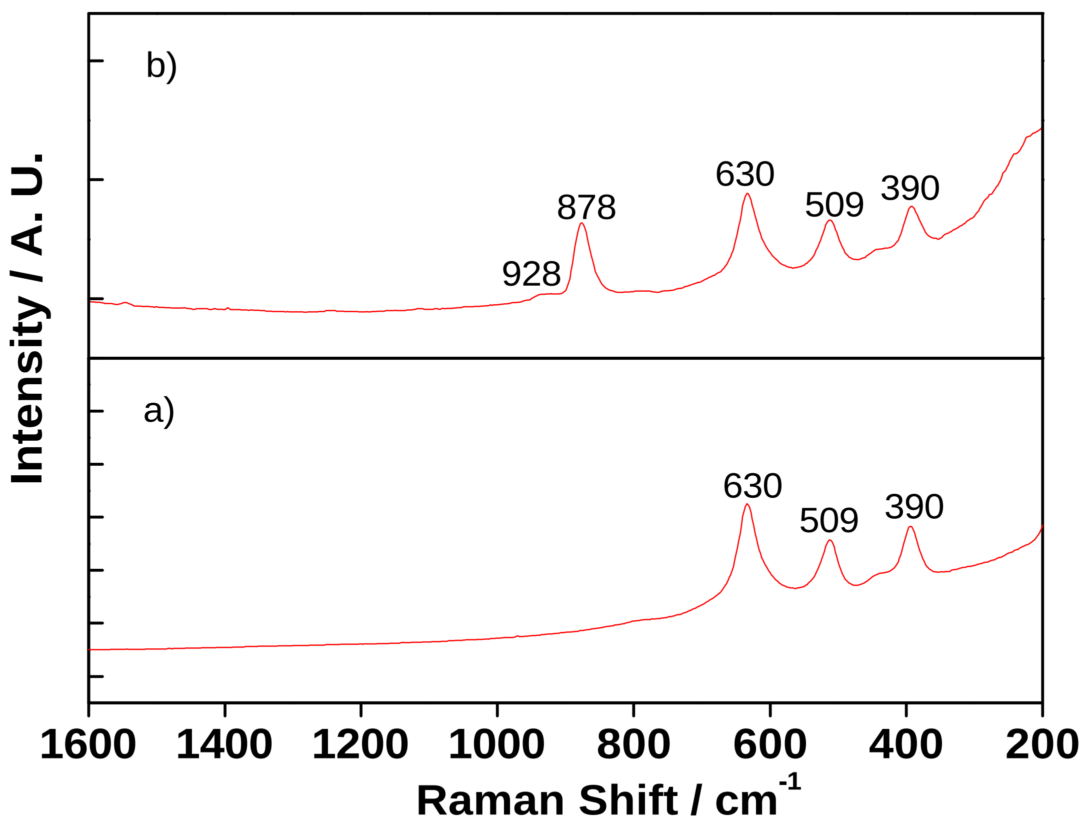

Figure 5.2 ***In situ*** **Raman spectra for MnO_x / TiO_2 catalyst at 298 K, 1 atm : a) O_2 flow, b) O_3/O_2 flow**

In oxygen flow (Fig. 5.2a), peaks appeared at 390 cm^{-1}, 509 cm^{-1} and 630 cm^{-1}. Under continuous ozone flow (Fig. 5.2b), a peak at 878 cm^{-1} appeared along with a very weak feature at 928 cm^{-1}. The first and second overtone peaks in this case were at 1750 cm^{-1} and 2614 cm^{-1}, respectively. Similar measurements were made at different temperatures (273, 313, 328 and 343 K).

Blank experiments conducted with the supports indicated that the presence of ozone did not result in a decrease in the intensity of the support peaks. The intense support peaks for the ZrO_2 and TiO_2 supported manganese oxide prevented the observation of any manganese oxide peak or changes to it during the course of the reaction.

5.4.2 Reaction orders and apparent activation energies

The turnover rates for ozone decomposition for each catalyst were measured at varying temperature (293 K – 343 K) and ozone partial pressure (600 Pa – 3000 Pa) conditions. The decomposition rates increased with increasing ozone partial pressure and temperature (Fig 5.3 – 5.6). A fractional reaction order was observed for all four catalysts and this order was found to be independent of temperature. The turnover rate measurements were repeated twice and the average error was determined to be about 10%.

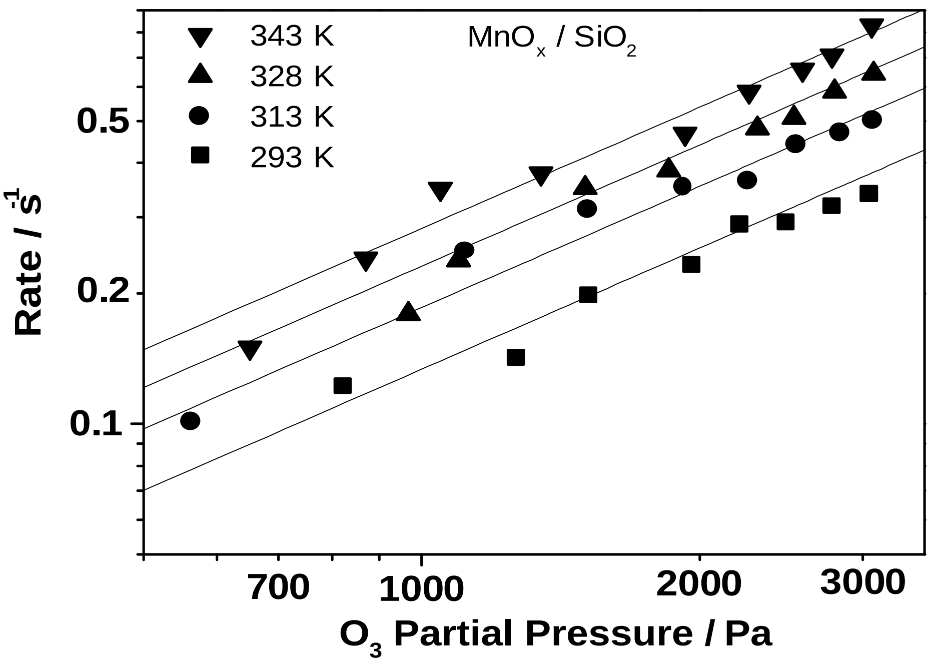

Fig 5.3 Rate vs ozone partial pressure – MnO_x / SiO_2 – Total O_3/O_2 flow rate = 670 μmol s^{-1}

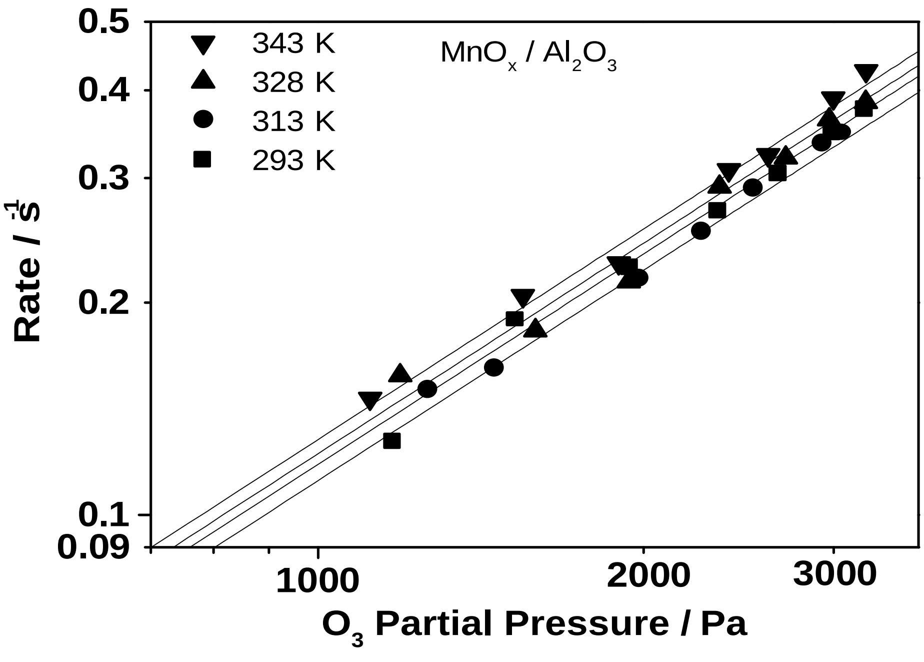

Fig 5.4 Rate vs ozone partial pressure – MnO_x / Al_2O_3 – Total O_3/O_2 flow rate = 670 μmol s^{-1}

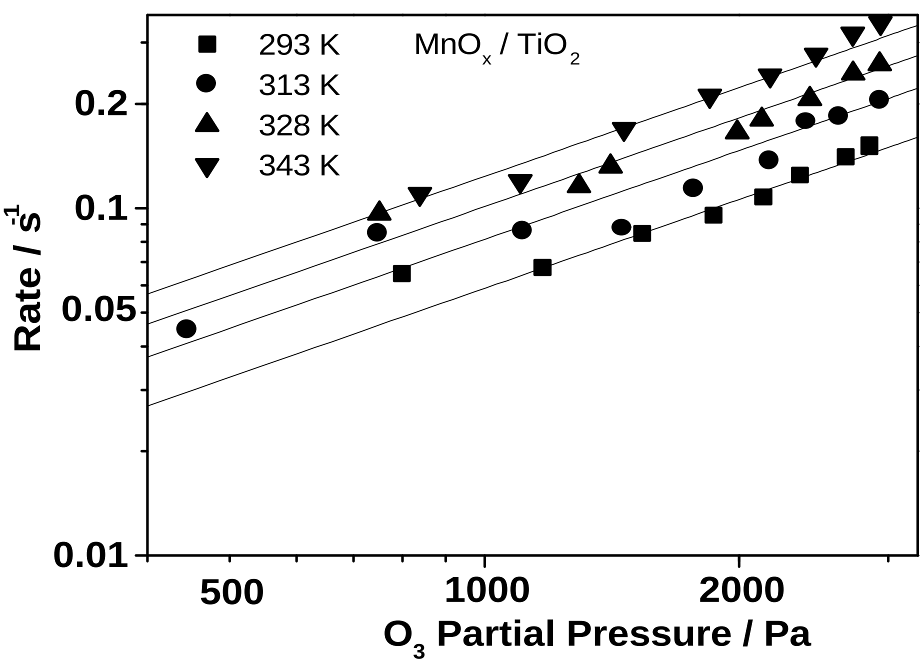

Fig 5.5 Rate vs ozone partial pressure – MnO$_x$ / TiO$_2$ – Total O$_3$/O$_2$ flow rate = 670 μmol s^{-1}

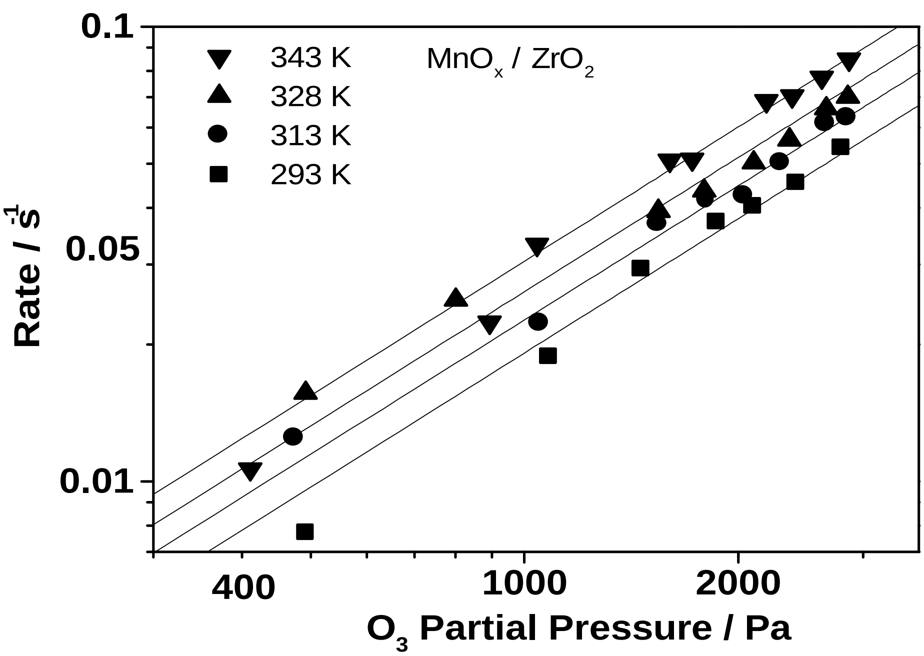

Fig 5.6 Rate vs ozone partial pressure – MnO$_x$ / ZrO$_2$ – Total O$_3$/O$_2$ flow rate = 670 μmol s^{-1}

Table 5.1, presents a summary of the turnover rates (TOR) at two different ozone partial pressures and four different temperatures for the catalysts.

Table 5.1 : Summary of turnover rates

T / K	Ozone Partial Pressure / kPa	Mn/SiO_2 (TOR/ s^{-1})	Mn/Al_2O_3 (TOR/ s^{-1})	Mn/TiO_2 (TOR/ s^{-1})	Mn/ZrO_2 (TOR/ s^{-1})
293	1.5	0.21	0.16	0.085	0.031
313		0.24	0.19	0.099	0.035
328		0.31	0.18	0.150	0.037
343		0.35	0.20	0.190	0.047
293	3.0	0.39	0.35	0.150	0.058
313		0.47	0.38	0.200	0.059
328		0.59	0.39	0.260	0.066
343		0.77	0.43	0.340	0.079

5.4.3 Peroxide species coverage results

The peak at 880 cm^{-1} for the ZrO_2 supported catalyst and the peak at 878 cm^{-1} for the TiO_2 supported catalyst were used to determine the surface coverage of the adsorbed species, θ, under reaction conditions. This was done by integrating the peak intensities and normalizing the values to the peak area at saturation, at the highest ozone partial pressures and the lowest temperatures. Figure 5.7 presents the effect of ozone partial pressure on the Raman signal for the peroxide species as a function of ozone partial pressure for the MnO_x / ZrO_2 catalyst, at room temperature. Figure 5.8 presents the effect of temperature on the signal at the largest ozone partial pressure (3000 Pa) for the same catalyst. Figures 5.7 and 5.8 are drawn to scale.

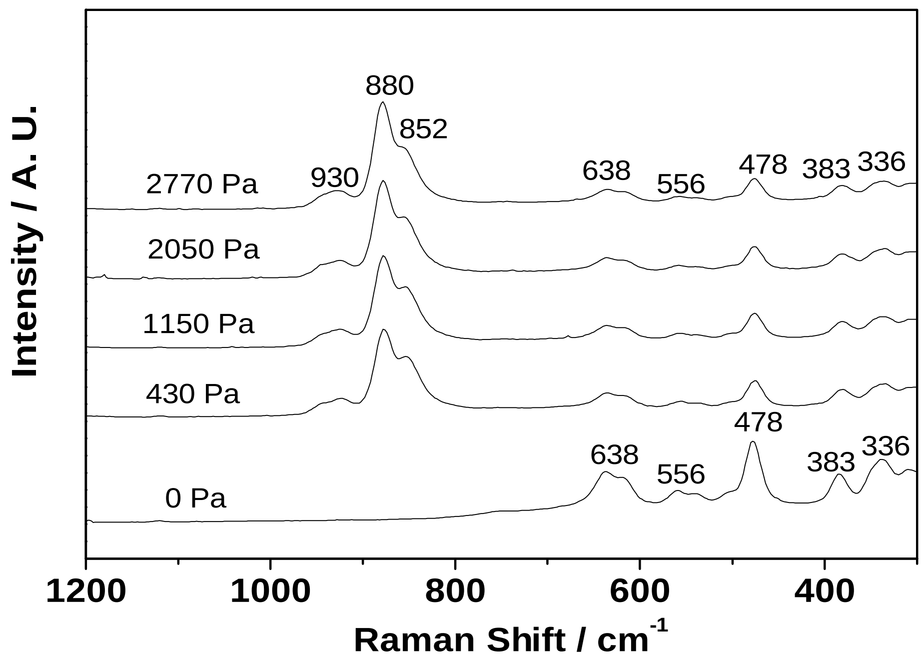

Figure 5.7 Effect of ozone partial pressure on peroxide species signal – MnO_x / ZrO_2 – 293 K

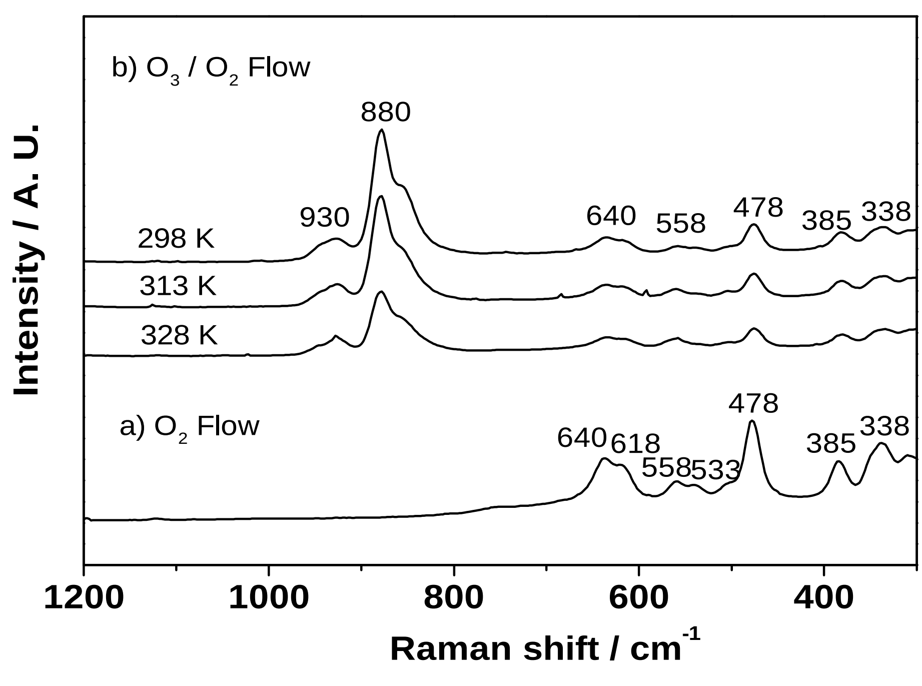

Figure 5.8 Effect of temperature on peroxide species signal – MnO_x / ZrO_2 – Ozone partial pressure 3000 Pa

Figures 5.9 and 5.10 present reaction isotherms of the surface coverage for ZrO_2 and TiO_2 supported manganese oxide catalysts. In both cases, the surface coverage increased with increasing ozone partial pressure eventually reaching saturation. Surface coverage values decreased with increasing temperature as expected.

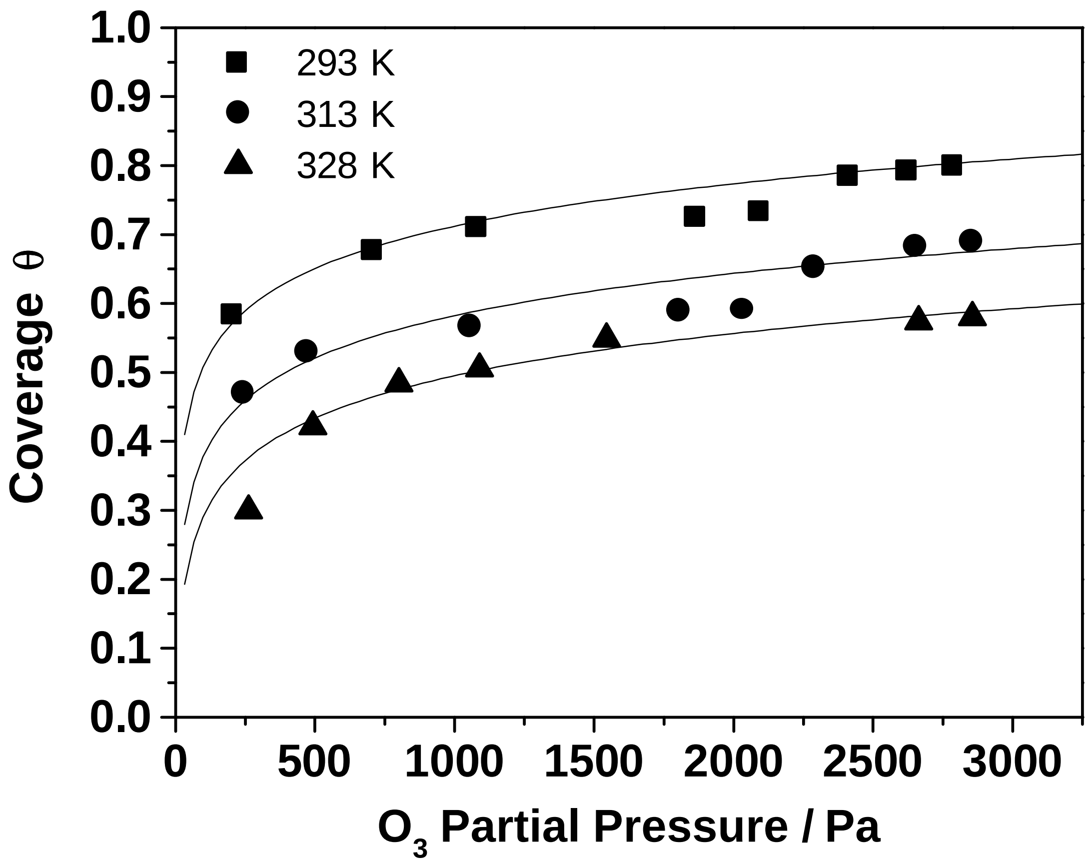

Figure 5.9 Peroxide species coverage vs ozone partial pressure – MnO_x / ZrO_2

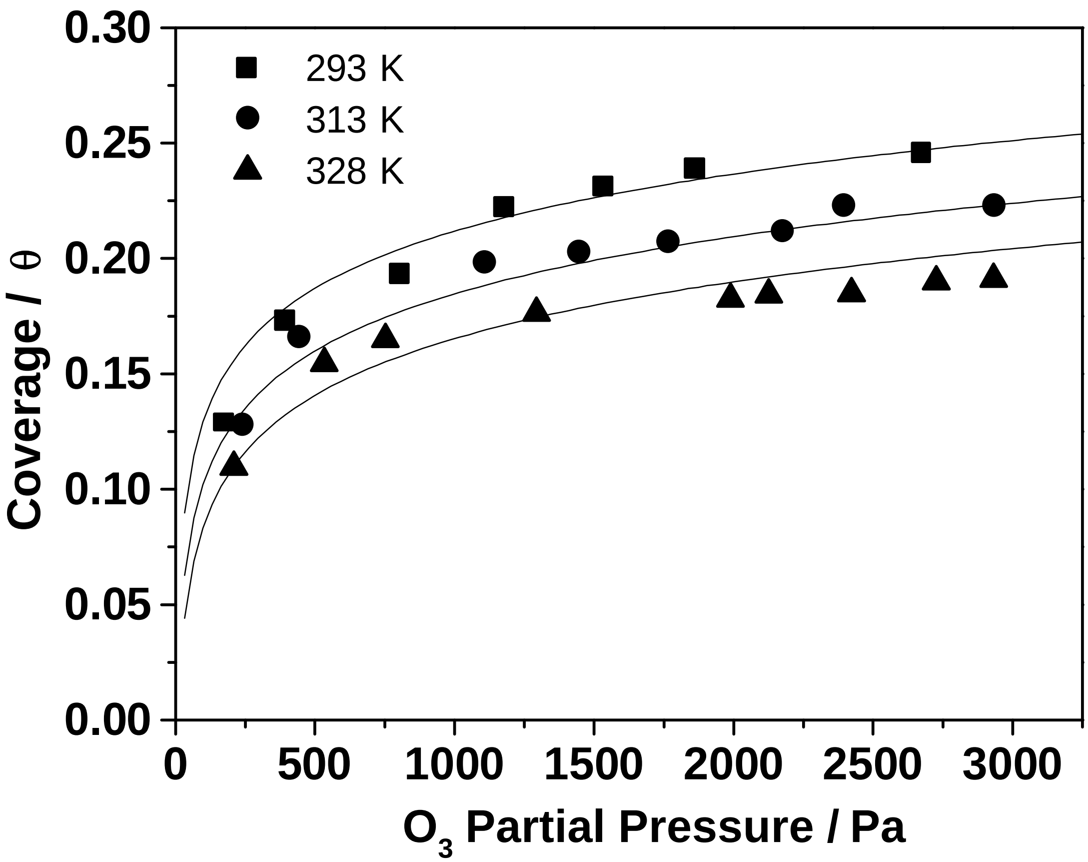

Figure 5.10 Peroxide species coverage vs ozone partial pressure – MnO_x / TiO_2

5.4.4 Uniform surface kinetics results

The acquired steady state data were analyzed with a uniform surface kinetic analysis using a Langmuirian expression for the coverage θ with an equilibrium constant K and a reaction rate constant k (Eqns 1, 2). The results of the analysis for the MnO_x / ZrO_2 and MnO_x / TiO_2 coverage fits are presented in Figures 5.11 and 5.12. The K values are tabulated in Table 5.2 along with the corresponding χ^2 values. The fits were not good and these results are discussed in detail later in this chapter.

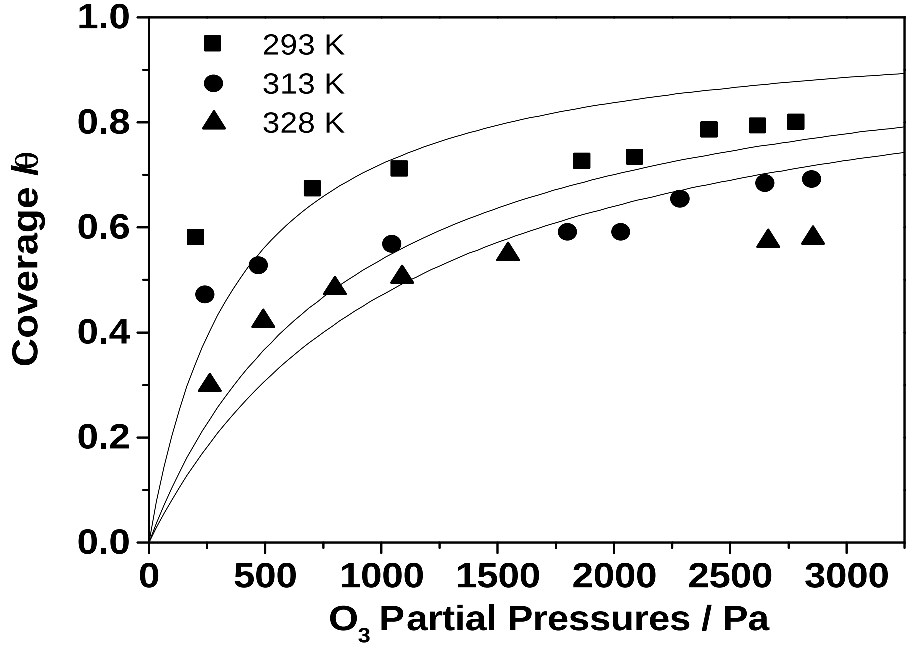

Figure 5.11 Uniform surface kinetics - Coverage analysis – MnO_x / ZrO_2

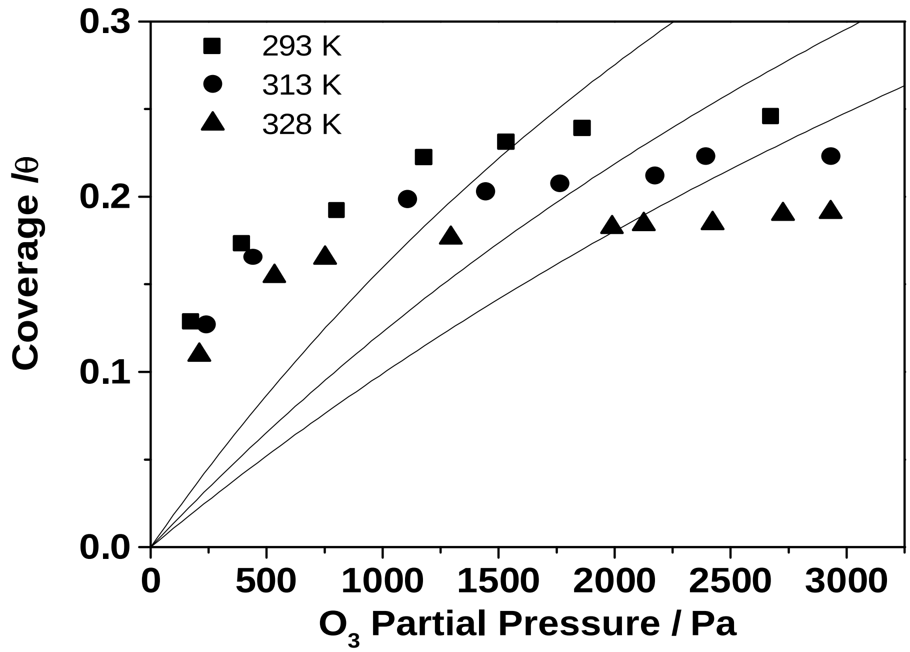

Figure 5.12 Uniform surface kinetics - Coverage analysis – MnO_x / TiO_2

Table 5.2: Uniform surface kinetics results

Catalyst	Temperature / K	K	χ^2
MnO_x / ZrO_2	293	$2.6*10^{-3}$	$1*10^{-2}$
	313	$1.1*10^{-3}$	$2*10^{-2}$
	328	$0.9*10^{-3}$	$1*10^{-2}$
MnO_x / TiO_2	293	$1.1*10^{-4}$	$6*10^{-3}$
	313	$1.4*10^{-4}$	$4*10^{-3}$
	328	$1.9*10^{-4}$	$4*10^{-3}$

5.4.5 Non uniform surface kinetics results

The values for the various non uniform surface kinetic parameters in equations 5 and 6 were obtained through a least-squares fitting of the experimental data. The linear fits of the steady state rate versus the ozone partial pressure (Figures 5.5, 5.6) and those of the steady state coverage of the peroxide species against the logarithm of the ozone partial pressure (Figures 5.13, 5.14) were used to simultaneously solve for the parameters in equations 5 and 6. The average χ^2 value for the coverage fits was 10^{-4} while the rate fits produced an average χ^2 value of 10^{-5}. The pre-exponential and activation energy values calculated for adsorption and desorption from the analysis are presented in Table 5.3 and are compared with the corresponding values obtained in the previous study for the Al_2O_3 supported catalyst.

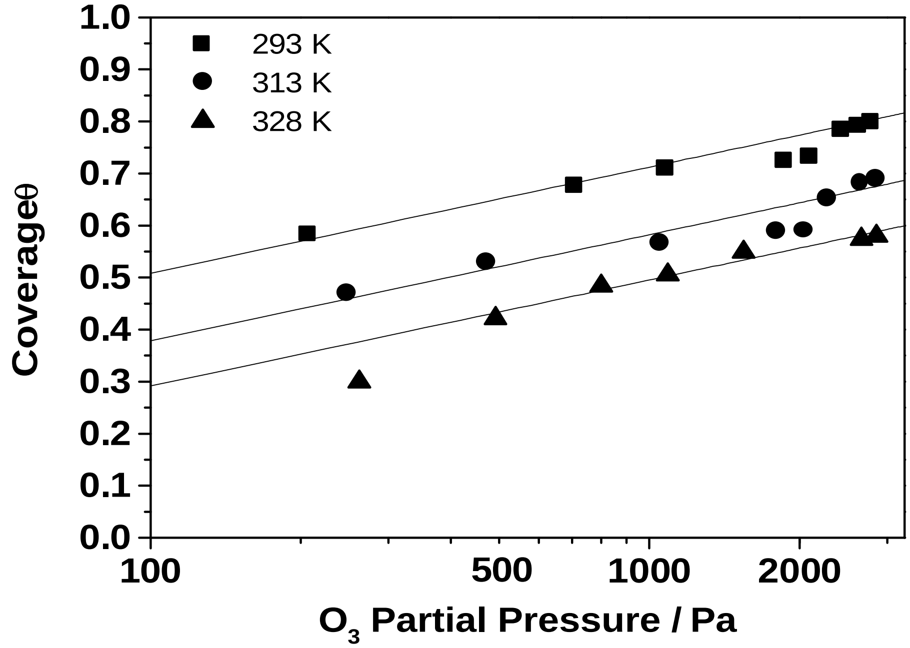

Figure 5.13 Non uniform surface kinetics – Coverage analysis – MnO_x / ZrO_2

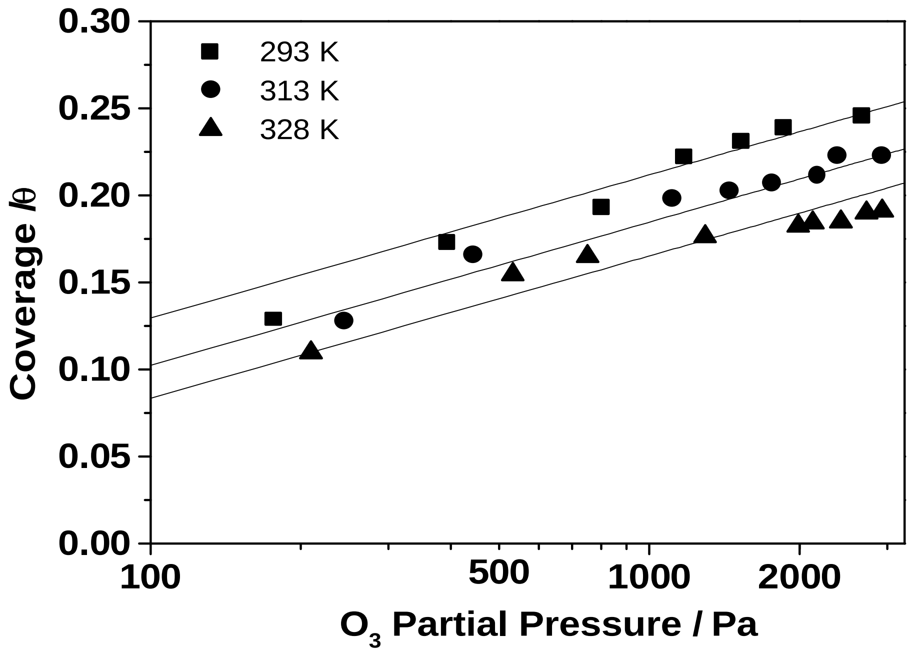

Figure 5.14 Non uniform surface kinetics – Coverage analysis – MnO_x / TiO_2

Table 5.3 : Kinetic parameters for ozone decomposition on supported manganese oxide catalysts

Parameter	Al_2O_3 support	ZrO_2 support	TiO_2 support
h	11.8	11.1	23.8
g	0.75	0.2	4.2
E_a^0	6 kJ/mol	6 kJ/mol	7 kJ/mol
E_d^0	69 kJ/mol	62 kJ/mol	44 kJ/mol
A_a^0	$3.1*10^{-18}$ cm^3s^{-1}	$1.1*10^{-18}$ cm^3s^{-1}	$1.2*10^{-18}$ cm^3s^{-1}
A_d^0	$1.6*10^7$ s^{-1}	$8*10^5$ s^{-1}	$1.9*10^3$ s^{-1}

5.5 Discussion

5.5.1 In situ Raman spectra

The Raman spectra obtained for each of the supported samples were indicative of dispersed species at the surface. In the absence of ozone for both the ZrO_2 and TiO_2 supported samples, the only peaks visible were those of the support. For the ZrO_2 supported sample, the peaks at 336 cm^{-1}, 383 cm^{-1}, 470 cm^{-1}, 552 cm^{-1} and 626 cm^{-1} belonged to ZrO_2. Similarly, for the TiO_2 supported sample, the peaks at 390 cm^{-1}, 509 cm^{-1} and 630 cm^{-1} could be assigned to TiO_2. Additonally, no XRD peaks (Fig 2.2) besides those of the support were observed in those samples. Nevertheless, the supported samples did undergo reduction, and chemisorb oxygen. This evidence suggests that the manganese oxide is in a dispersed state in the near surface of the support.

These conclusions are confirmed by studies conducted by Ma[11, 12] et al. for ZrO_2 and Al_2O_3 supported manganese oxide samples also using manganese acetate as a precursor. The catalysts were characterized using XPS, TPR and XRD, and it was deduced that the low loading catalysts prepared through incipient wetness resulted in well dispersed manganese oxide systems with oxidation states between +2 and +3. Kapteijn et al. have also studied the effect of precursor and metal loading on Al_2O_3 supported manganese oxide[13, 14] using XPS, TPR, Raman and IR spectroscopy. They observed that at low loadings (< 10 %), manganese oxide prepared from manganese acetate was a mixture of well dispersed manganese oxide phases, MnO and Mn_2O_3.

The new signals that appeared upon ozone exposure at 880 cm^{-1} and 878 cm^{-1} for the ZrO_2 and TiO_2 supported manganese catalysts can be attributed to an adsorbed peroxide species derived from ozone. The identification of the species as peroxide groups on the surface of the catalysts is based upon their band positions as obtained from their Raman spectra. The range of vibrational frequencies expected for neutral O_2 is 1460 – 1700 cm^{-1}, O_2^- is 1015 – 1180 cm^{-1} and O_2^{2-} is 640 – 970 cm^{-1} [15] and the observed bands clearly fall in the peroxide range. Also the bands are close to those of O_2^{2-} on MnO_x / Al_2O_3 where isotopic substitution has unambiguously identified the peroxide intermediate[5] at 884 cm^{-1}. According to these studies, the vibrational mode for the adsorbed species is highly localized. This could be the reason for the very small change in the vibrational frequency for the peroxide species on ZrO_2 and TiO_2 supported catalysts as compared to the Al_2O_3 supported catalyst. There are also smaller features at 930 cm^{-1} and 928 cm^{-1}, respectively, for the ZrO_2 and TiO_2 supported catalysts that accompany the main peaks. These are likely due to Mn = O vibrations formed from atomically adsorbed oxygen (Scheme 1, vide infra). These are consistent with the expected vibrational frequencies for such M = O as summarized by Che et al. [15] (900 – 1100 cm^{-1}). Atomically adsorbed oxygen species are more thermally stable than adsorbed peroxide species[16]. Table 5.4 presents the coverage of the two species as a function of increasing temperature at 3000 Pa and supports the assignment for the vibrations.These signals were not observed during blank experiments when the supports alone were used.

Table 5.4 : Effect of temperature on adsorbed species coverages

Temperature / K	θ_{O2*}	θ_{O*} (*)	Ratio (θ_{O*}/θ_{O2*})
293	0.80	0.05	0.06
313	0.69	0.06	0.09
328	0.58	0.12	0.21

* Coverages calculated using the calibration factor for the peroxide species

For the MnO_x / ZrO_2 catalyst, the peak at 880 cm^{-1} had a shoulder on the low wavenumber side at 852 cm^{-1} which is indicative of two different adsorbed peroxide species on the catalyst surface. The presence of these species was also indicated in the oxygen TPD results (Fig. 4.7d). It is likely that in the case of the MnO_x / ZrO_2 catalyst that, there are two peroxide species. The structure of these peroxide species is uncertain. They could be bidentate $\eta^2 – O_2$ complexes as likely on the monoatomic Mn center on MnO_x / Al_2O_3, or they could be bridging dioxygen species as possible on the multinuclear Mn center on the MnO_x / TiO_2 and MnO_x / SiO_2 catalysts (Fig 2.17). The bands on the MnO_x / ZrO_2 samples could also arise from different interactions of the peroxide species with the ZrO_2 support.

5.5.2 *Steady state rates*

The steady-state reaction rate data were analyzed using the expression

$r_{ss} = A_{app} \exp(\frac{-E_{app}}{RT})(O_3)^n$, where E_{app} is the apparent activation energy, T is the temperature, n is the reaction order and (O_3) represents the ozone partial pressure. This follows the non-uniform surface description of the kinetics as presented in an earlier work on the MnO_x / Al_2O_3 catalyst[6].

Table 5.5 summarizes the reaction orders and apparent activation energies for each of the catalysts. The fractional reaction order is consistent with that predicted by the non uniform surface kinetic analysis. There are no particular trends in the reaction orders. The apparent activation energies are derived from the Arrhenius plots for the catalysts which monitor steady-state rate at the largest ozone partial pressure (3000 Pa) as a function of temperature. These plots are presented in Figure 5.15.

Table 5.5 : Steady-state kinetic parameters

Catalyst	Reaction order	E_{app} / kJ mol^{-1}	A_{app}
MnO_x / Al_2O_3	0.99	3	$1.5*10^{-18}$
MnO_x / ZrO_2	0.98	7	$2.9*10^{-18}$
MnO_x / TiO_2	0.85	13	$1.6*10^{-14}$
MnO_x / SiO_2	0.92	15	$1.8*10^{-15}$

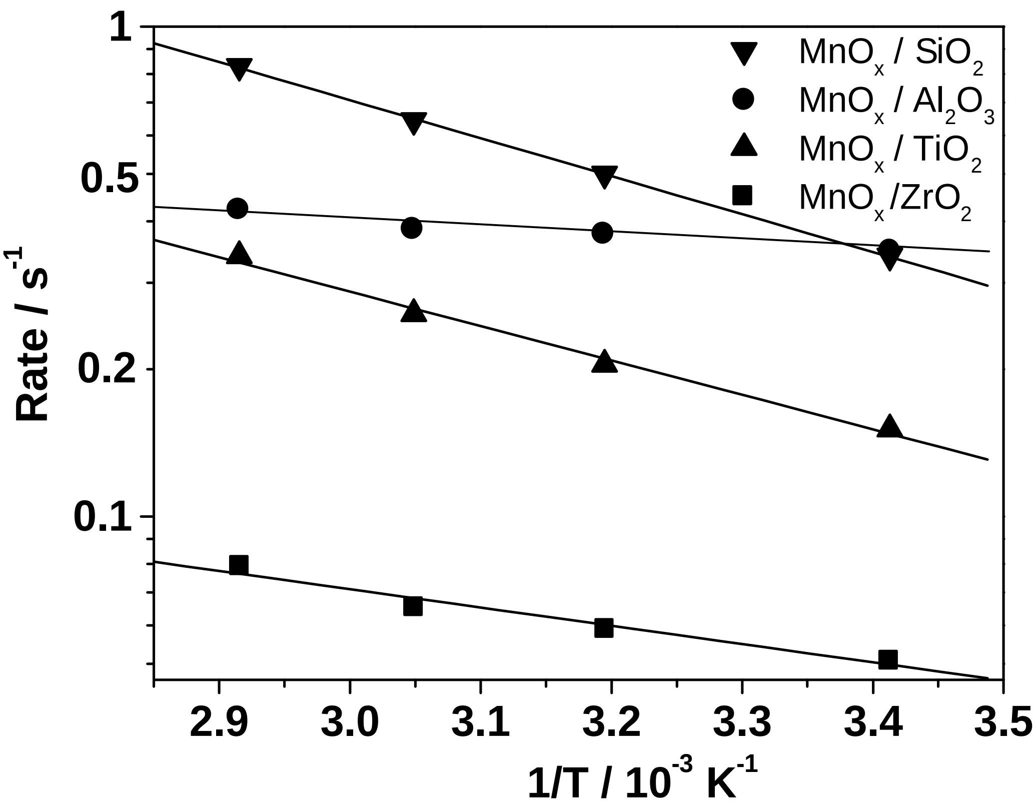

Figure 5.15 Arrhenius plots for the catalysts

It is clear from these plots that the apparent activation energy for ozone decomposition on MnO_x / Al_2O_3 catalyst is distinctively lower than those on the other catalysts. This is probably related to the structure of the MnO_x / Al_2O_3 catalyst which alone among the catalysts had a mononuclear manganese center. The trends in the apparent activation energies for reaction : $Al_2O_3 < ZrO_2 < TiO_2 < SiO_2$ mirror the trends in the NEXAFS shift, L_{III} /L_{II} ratios and shift in the L-edge features.

5.5.3 Kinetic analyses comparison

The uniform surface kinetic analysis (Fig. 5.11, 5.12) shows clearly that for the peroxide species coverages over the MnO_x / ZrO_2 and MnO_x / TiO_2, the quality of the fits is not good. The average χ^2 value for these fits was 10^{-2} compared to 10^{-4} for the non-uniform surface analysis. Figures 5.16 and 5.17 present the rate versus coverage plots for the two catalysts. From equation 2, a linear dependency of steady state rates on coverage is expected. The plots clearly show a non linear dependency of rates on coverage. It can be ascertained from these results that the experimental data are inadequately predicted by a uniform surface kinetic analysis.

The data fits for the equations deduced using non uniform surface kinetics, work very well throughout the entire range of variation of experimental conditions, for both the MnO_x / ZrO_2 and MnO_x / TiO_2 catalysts. As mentioned earlier, the average χ^2 value for the coverage fits 10^{-4} while the rate fits produced an average χ^2 value of 10^{-5}. The NEXAFS work presented in the earlier chapter confirmed the presence of mixed oxidation states for manganese on the support surface. This heterogeneity of the manganese oxide catalysts is further confirmed by the results of the non uniform surface kinetics analysis.

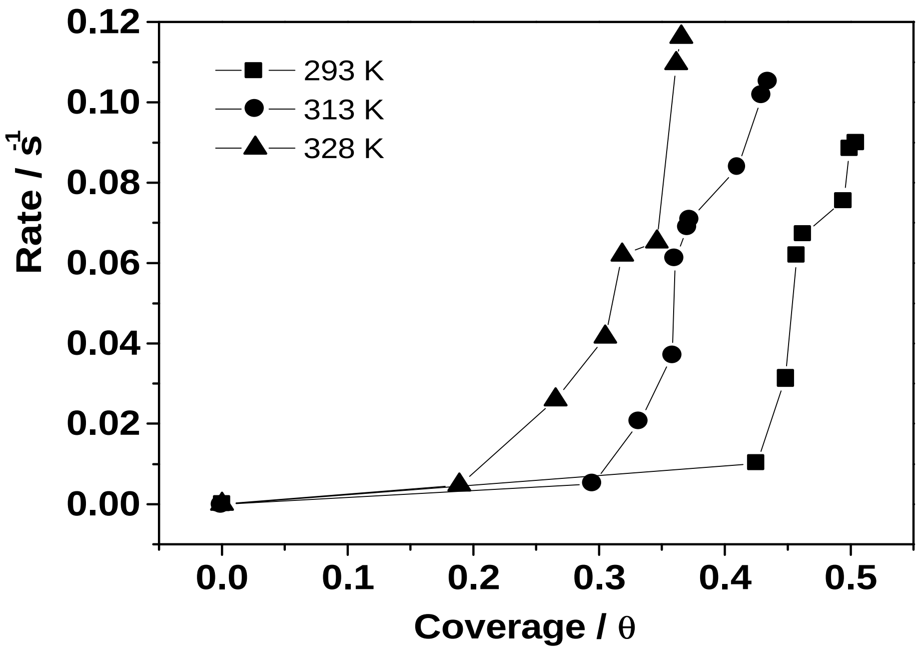

Figure 5.16 Rate vs coverage plot – MnO_x / ZrO_2

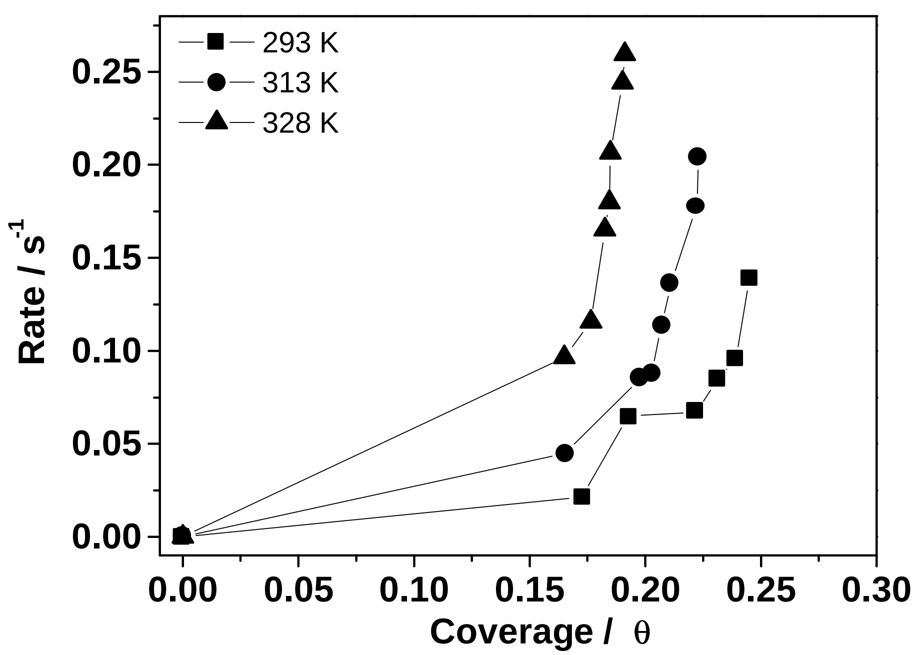

Figure 5.17 Rate vs coverage plot MnO_x / TiO_2

The steady-state rates for both catalysts had a fractional order dependency on ozone partial pressure which was independent of temperature. This is consistent with the fractional order h/(g+h) predicted by equation 3 with a value < 1. The kinetic parameters for ozone decomposition on the MnO_x / ZrO_2 and MnO_x / TiO_2 catalyst are compared to those obtained for MnO_x / Al_2O_3 in the earlier work[6] in Table 5.3.

The values for the pre-exponential for adsorption on each of the catalysts is in the range of 10^{-18} cm^3 s^{-1} and the activation energy for ozone adsorption on each of the catalysts is low (<10 kJ/mol). The activation energy for desorption is significantly larger than the activation energy of adsorption, for each catalyst. This could be the reason why a stable reaction intermediate was observed for the catalytic process. The activation energies and pre-exponentials for the desorption process follow the trend $Al_2O_3 > ZrO_2 > TiO_2$. This suggests that for the ozone decomposition process on supported manganese oxide catalysts, the desorption step is rate determining.

5.5.4 Effect of support on ozone decomposition reactivity

The effect of support on the ozone decomposition reactivity can be explained as follows : The Mn L-edge intensity shift ratios and chemical shifts indicated that oxidation state for Mn increased in the order : $Al_2O_3 < ZrO_2 < TiO_2 < SiO_2$. This trend follows the availability of empty d-states in the metal-support complex[17]. Kinetic data revealed that the values of the pre-exponential factors for the desorption step followed the same trend (Table 5.3). The desorption step involves electron transfer from the adsorbed species to the metal centers which thereby suggests that the empty d-states track the reducibility of the surface center. The difference in the pre-exponential value is probably a result of a difference in the electronic partition function of the activated complex as was suggested in earlier work for ethanol oxidation with supported molybdenum oxide[2, 18].

The relationship can be understood as follows. The pre-exponential factor is made up of contributions from the partition functions of the activated complex.

$$A = \frac{kT}{h}\frac{Q^{\#}}{Q_{react}} = \frac{kT}{h}\frac{q_{trans}q_{vib}q_{rot}q_{elec}}{q_{react,trans}q_{react,vib}q_{react,rot}q_{react,elec}}$$

For common intermediates (the peroxide species) in a common mechanism, the translational, vibrational and rotational partition functions are expected to be of a similar order of magnitude. The greatest variation cannot give rise to a difference of more than a factor of 2-3. Since, in addition, the kT/h is the same, the orders of magnitude differences in pre-exponential factor must reside in the electronic partition functions for the transition state and reactant $q_{elec}/q_{react,elec}$. These partition functions are associated with the density of unoccupied d-levels, which in turn is related to the reducibility of the metal oxide site.

The ozone decomposition activity trend for SiO_2, TiO_2 and ZrO_2 is identical to the trend in the pre-exponentials (Table 5.4). Only the position of Al_2O_3 is different from that predicted by the pre-exponentials and this is because of the compensation of its low pre-exponential by a low apparent activation energy. The unique behaviour of the Al_2O_3 supported manganese oxide is probably a consequence of its active site structure being different. As was seen earlier, the Mn center on Al_2O_3 was monoatomic, whereas it was multiatomic with the other supports.

5.6 Conclusions

The presence of an adsorbed peroxide species on the surface of ZrO_2 and TiO_2 during ozone decomposition was confirmed using *in situ* laser Raman spectroscopy. Simultaneous steady state kinetic measurements revealed a fractional order dependency of the turnover rates with respect to ozone partial pressure of 0.98 and 0.85 for the ZrO_2 and TiO_2 supported catalysts. The non-uniform surface kinetics analysis used in an earlier study on Al_2O_3 supported manganese oxide was found to work well for the catalysts in this study. There was substantial variation in the activation energy and pre-exponential values for the desorption step among the catalysts. The largest difference was in the pre-exponential factor for the desorption step rate constant during ozone decomposition. This step required the transfer of electrons from the adsorbed species to the active center. The trend in these pre-exponentials $Al_2O_3 > ZrO_2 > TiO_2$ seemed to follow the reducibility of the manganese active center. The reducibility of the catalysts was directly related to the number of empty d-states on Mn predicted by NEXAFS measurements.

REFERENCES:

[1] Stakheev, A. Y.; Kustov, L. M.; *Applied Catalysis A: General*., **1999**, *188*, 3.

[2] Zhang, W., Desikan, A., and Oyama, S. T., *J. Phys. Chem.* **1995**, *99*, 14468.

[3] Hu, H., and Wachs, I. E., *J. Phys. Chem.* **1995**, *99*, 10911.

[4] Deo, G., and Wachs, I. E., *J. Catal.* **1994**, *146*, 335.

[5] Li, W.; Oyama, S. T.; *J. Am. Chem. Soc.* **1998**, *120*, 9041.

[6] Li, W.; Oyama, S. T.; *J. Am. Chem. Soc.* **1998**, *120*, 9047.

[7] Boudart, M.; Mariadassou, G. D.; *Kinetics of Heterogeneous Catalytic Reactions*. **1984**, Princeton University Press.

[8] Thomas, J. M.; Thomas, W. M.; *Principles and Practice of Heterogeneous Catalysis.* **1997**, VCH Publishers Inc.

[9] Brunauer, S.; Love, K. S.; Kennan, R. G.; *J. Am. Chem. Soc.* **1942**, *64*, 751.

[10] Boudart, M.; Egawa, C.; Oyama, S. T.; Tamaru, K.; *J. Chim. Phys.* **1981**, *78*, 987.

[11] Ma, J.; Chuah, G. K.; Jaenicke, S.; Gopalakrishnan, R.; Tan, K. L.; *Ber.Bunsenges. Phys. Chem.* **1995**, *99*, 184.

[12] Ma, J.; Chuah, G. K.; Jaenicke, S.; Gopalakrishnan, R.; Tan, K. L.; *Ber.Bunsenges. Phys. Chem.* **1995**, *100*, 585.

[13] Kapteijn, F.; van Langeveld, A. D.; Moulijn, J. A.; Andreini, A; Vuurman, M. A.; Turek, M. A.; Jehng, J.M; Wachs, I. E.; *J. Catal.* **1994**, *150*, 9.

[14] Kapteijn, F.; Singoredjo, L.; van Driel, M.; Andreini, A.; Moulijn, J. A.; Ramis, G.; Busca G.; *J. Catal.* **1994**, *150*, 105.

[15] Che, M., and Tench, A. J., *Advances in Catalysis*, **1983**, *32*, 1.

[16]. Onishi, T. in *Dynamic Porcesses on Solid Surfaces*, ed. Tamaru, K., Plenum: New York, 237(1994).

[17] Chen, J. G.; *Surf. Sci. Rep.*, **1997**, *30(1-3)*, 1.

[18] Weber, R. S.; *J. Phys. Chem.*, **1994**, *98*, 2999.

CHAPTER 6

CONCLUSIONS AND RECOMMENDATIONS FOR FUTURE WORK

6.1 Conclusions

The main conclusions for this dissertation are as follows:

1) The support influenced the structure, oxidation state and ozone decomposition reactivity of the supported manganese oxides.
2) The manganese active center was mononuclear for the Al_2O_3 supported catalyst and was multinuclear for the other supports.
3) The oxidation state for the manganese on the supports followed the trend : Al_2O_3 < ZrO_2 < TiO_2 < SiO_2 as determined through NEXAFS spectroscopy.
4) The presence of an adsorbed peroxide on the surface of the manganese oxide catalysts during ozone decomposition was observed using *in situ* laser Raman spectroscopy and the results were confirmed through *ab initio* calculations.
5) The ozone reactant probe technique was deduced as a more reliable method than oxygen chemisorption for evaluating active site density for supported manganese oxide catalysts.
6) The pre-exponential for the desorption step during ozone decomposition for supported manganese oxides followed the trend : Al_2O_3 > ZrO_2 > TiO_2.

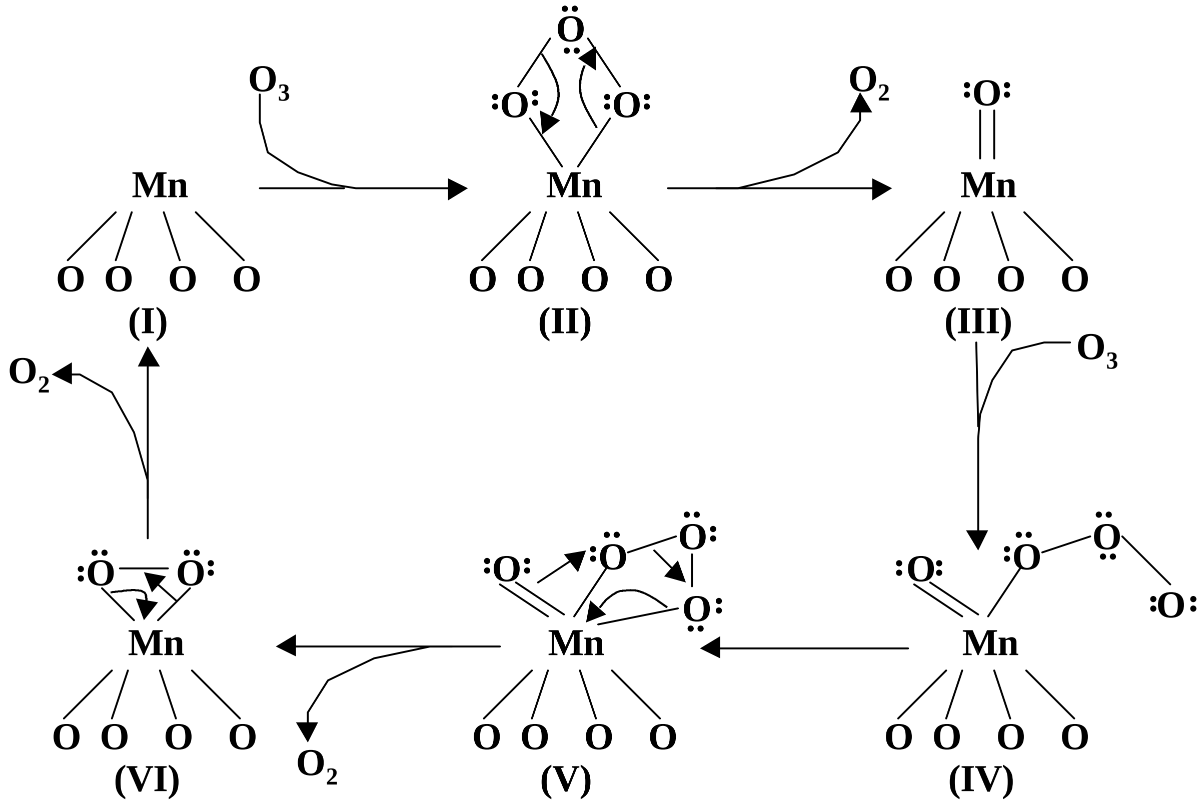

Figure 6.1 Catalytic cycle for ozone decomposition on MnO_x / Al_2O_3 catalyst

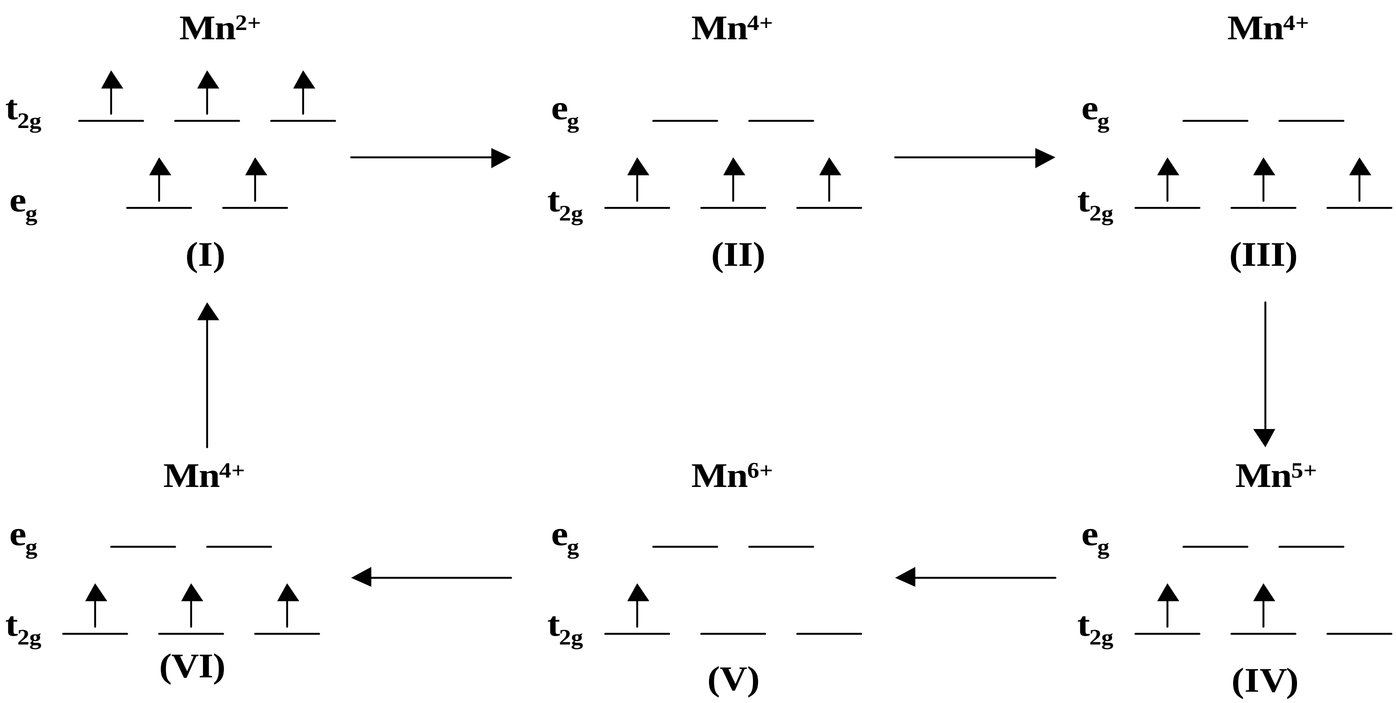

Fig 6.2 Energy level occupancies for d – orbitals during ozone decomposition on MnO_x / Al_2O_3

6.2 Ozone decomposition catalytic cycle

Figure 6.1 presented on the previous page shows a possible catalytic cycle for the ozone decomposition reaction on the MnO_x / Al_2O_3 catalyst. The transformation of the manganese site from species (I) to (III) is indicative of an oxidation reaction and represents the step $O_3 + * \longrightarrow O_2 + O*$ as shown in scheme 1 in Chapter 5 of this dissertation. This can also be depicted as a redox reaction : $O_3 + Mn^{2+} \longrightarrow O_2 + O^{2-} + Mn^{4+}$. The structure numbered (II) in Fig 6.1 is likely a transition state for this first step in the ozone decomposition process. The next step from scheme 1, $O_3 + O* \longrightarrow O_2* + O_2$ is represented by the transformation of species (III) to species (VI) in the proposed catalytic cycle. The redox reaction for this step is : $O_3 + Mn^{4+} + O^{2-} \longrightarrow O_2 + O_2^{2-} + Mn^{4+}$. The transition states for this reaction are species (IV) and (V) presented in the catalytic cycle. Finally, the desorption step represented by $O_2* \longrightarrow O_2 + *$ in scheme 1 is the transformation of species (VI) to (I) in the catalytic cycle. The redox reaction for this step is : $Mn^{4+} + O_2^{2-} \longrightarrow O_2 + Mn^{2+}$. The transition state (not shown) for this step is likely an O-O species bonded to the Mn site through a single bond with the Mn at a +3 oxidation state.

Figure 6.2 is an energy level diagram which indicates possible manganese oxide oxidation state changes during the catalytic cycle. The energy states for the d-orbitals of species (I) at an Mn oxidation state of +2 (d^5 configuration) have been depicted based on the assumption of a tetrahedral field (four co-ordinate geometry). The oxidation of Mn^{2+} in the presence of ozone results in the formation of a six co-ordinate species Mn^{4+} where energy separations are based on an octahedral field. The actual energy positions of the orbitals for the geometries presented can be estimated using ligand field theory[1].

Subsequent changes in the occupancy of the energy levels due to changes in manganese oxidation states have also been depicted in Fig. 6.2. An important observation gleaned from these energy level diagrams is that the Mn oxidation state for MnO_x / Al_2O_3 catalyst can vary from Mn^{2+} upto Mn^{6+}. The ability of the manganese species to reach several different oxidation states may be a possible reason for the high ozone decomposition activity of MnO_x / Al_2O_3 compared to the other catalysts.

6.3 Recommendations for future work

The *in situ* Raman spectra for the MnO_x / ZrO_2 catalyst (Fig. 5.1, Chapter 5), showed a well defined feature at 930 cm^{-1} which can be attributed to adsorbed atomic oxygen on the catalyst surface. The calibration factor used for the peroxide species was used to obtain coverages for this atomic oxygen species at various temperatures (Table 5.4, Chapter 5). The peak can be accurately calibrated using the TPD technique specified in Chapter 4 (Fig. 4.7) at a fixed temperature of ~500 K. At this temperature, the only adsorbed species on the catalyst surface would be adsorbed atomic oxygen species. Tracking the m/e = 32 signal for oxygen can provide a desorption curve which plots the concentration change in the adsorbed atomic oxygen species with time. A similar experiment using *in situ* Raman spectra for the adsorbed species can be performed. In this case, the desorption curve would be monitored by quantifying areas under the adsorbed atomic oxygen peak once O_3 flow is cut off. Comparing the two desorption curves would give a direct method of calibrating the coverages of the adsorbed atomic oxygen species.

An accurate calibration of the adsorbed atomic oxygen species will also help evaluate the reaction rate constant for step (i) presented for the ozone decomposition mechanism (Scheme 1). The analysis carried out to obtain this constant would be similar to the non uniform surface kinetics presented in Chapter 5. The main difference would be the use of two equations for the rates of adsorption r_{a1} and r_{a2} (with Brönsted parameters g1 and g2 respectively) and one rate of desorption r_d (with a Brönsted parameters h). Setting $r_{a2} = r_d$ and $r_{a1} = r_{a2}$ gives us three expressions which can be solved simultaneously to obtain all of the relevant rate constants and Brönsted parameters. These are:

$$r_{ss} = k_d^o \left[\frac{k_{a2}^o}{k_d^o} (O_3) \right]^{\frac{h}{g2+h}} \tag{1}$$

$$\theta_{ss,O2*} = \frac{1}{g2+h} \ln\left[\frac{k_{a2}^0}{k_d^0} (O_3) \right] \tag{2}$$

$$\theta_{ss,o*} = \frac{1}{g1} \ln\left[\frac{k_{a1}^0}{k_{a2}^0} \right] + \frac{g2}{g1} \theta_{SS,O2*} \tag{3}$$

Ab initio calculations have been carried out for the species labelled (I) and (IV) in Chapter 3. It is conceivable that similar calculations can be carried out on the rest of the species appearing in the catalytic cycle. Since these calculations are also accompanied by energy calculations, it is then possible to estimate the energetics (like enthalpy of reaction etc.) for each of the elementary steps.

Software (TheRate 1.1) (site address : http://therate.hec.utah.edu) developed by Duncan and Troung at the University of Utah allows the calculation of rate constants for bimolecular gas phase reactions from electronic structures and molecular orbital theory. This software might help calculate theoretical rate constants for the reactions presented in

Fig 6.1 and a direct comparison of calculated and experimental reaction rate constants may be possible.

Depending on the validity of the catalytic cycle and the structures involved, similar calculations could be performed with manganese structures for the other supports as well. Consequently, an alternative method involving *ab initio* calculations to determine the effect of support can be arrived at. This method would involve the calculation of electron densities around the (3,-1) critical point along a bond[2]. Software (XTREM.EXE) available through Dr G. V. Gibbs in the Geology department here at Virginia Tech performs such calculations. Consequently, comparing charge densities around the Mn-O bonds for various Mn – support clusters might provide theoretical insights into the effect of support on manganese oxide reactivity.

REFERENCES :

[1] Oxtoby, D. W.; Nachtrieb, N. M.; Freeman, W. A.; *Chemistry: Science of Change*, **1990**, Saunders College Publishing.

[2] Bader, R. F. W.; *Atoms in Molecules, A Quantum Theory*, **1990**, Oxford University Press, NY.

APPENDIX A1 : INPUT AND OUTPUT FILES FOR MnO_4Al_2O - FOUR COORDINATE

INPUT FILE

```
%chk = mn4al2

#p hf/6-311g opt = (cart, MaxCycle=100) scf=(direct,MaxCycle=400)
   Freq

mn4al

0 2
Mn1   .000000     .000000    1.697654
O1  -1.315561     .728334     .058901
O2   1.315561     .728334     .058901
O3  -1.315561    -.728334     .058901
O4   1.315561    -.728334     .058901
Al1   .000000    1.393192    -.970958
O5    .000000     .000000   -2.385158
Al2   .000000   -1.393192    -.970958
```

OUTPUT FILE

```
         Item               Value     Threshold  Converged?
 Maximum Force            .000078      .000450     YES
 RMS     Force            .000022      .000300     YES
 Maximum Displacement     .000243      .001800     YES
 RMS     Displacement     .000069      .001200     YES
 Predicted change in Energy=-2.002375D-08
 Optimization completed.
    -- Stationary point found.
 GradGradGradGradGradGradGradGradGradGradGradGradGradGradGradGradGradGrad

 Leave Link  103 at Thu Jul 20 22:50:10 2000, MaxMem=    6291456 cpu:        .2
 (Enter /apps/g98/l202.exe)
                          Input orientation:
 ---------------------------------------------------------------------
 Center     Atomic     Atomic              Coordinates (Angstroms)
 Number     Number      Type              X           Y           Z
 ---------------------------------------------------------------------
    1         25             0         .000000     .000000    1.390004
    2          8             0       -1.251707    1.100973     .238676
    3          8             0        1.251707    1.100973     .238676
    4          8             0       -1.251707   -1.100973     .238676
    5          8             0        1.251707   -1.100973     .238676
    6         13             0         .000000    1.328368    -.983805
    7          8             0         .000000     .000000   -2.101104
    8         13             0         .000000   -1.328368    -.983805
 ---------------------------------------------------------------------
```

```
                         Distance matrix (angstroms):
                   1          2          3          4          5
    1  Mn    .000000
    2  O    2.025949    .000000
    3  O    2.025949   2.503414    .000000
    4  O    2.025949   2.201946   3.334014    .000000
    5  O    2.025949   3.334014   2.201946   2.503414    .000000
    6  Al   2.720208   1.764352   1.764352   2.993815   2.993815
    7  O    3.491108   2.872888   2.872888   2.872888   2.872888
    8  Al   2.720208   2.993815   2.993815   1.764352   1.764352
                   6          7          8
    6  Al    .000000
    7  O    1.735776    .000000
    8  Al   2.656735   1.735776    .000000
                          Interatomic angles:
     O2-Mn1-O3= 76.3168      O2-Mn1-O4= 65.8357      O3-Mn1-O4=110.7378
      O3-O2-O4= 90.          O2-Mn1-O5=110.7378      O3-Mn1-O5= 65.8357
      O2-O3-O5= 90.          O4-Mn1-O5= 76.3168       O2-O4-O5= 90.
      O3-O5-O4= 90.         Mn1-O2-Al6= 91.4598     Mn1-O3-Al6= 91.4598
     O2-Al6-O3= 90.3792     O4-Mn1-Al6= 76.6708      O4-O2-Al6= 97.405
     O3-Al6-O4= 84.785      O5-Mn1-Al6= 76.6708      O2-Al6-O5= 84.785
     O5-O3-Al6= 97.405       O5-O4-Al6= 65.2855      Mn1-O2-O7= 89.1627
     Mn1-O3-O7= 89.1627       O3-O2-O7= 64.1704      Mn1-O4-O7= 89.1627
      O4-O2-O7= 67.4662       O3-O7-O4= 70.9369      Mn1-O5-O7= 89.1627
      O2-O7-O5= 70.9369       O5-O3-O7= 67.4662       O5-O4-O7= 64.1704
    Mn1-Al6-O7=100.8363      O2-Al6-O7=110.3263      O3-Al6-O7=110.3263
     O4-O7-Al6= 76.6463      O5-O7-Al6= 76.6463     O2-Mn1-Al8= 76.6708
    O3-Mn1-Al8= 76.6708      O3-O2-Al8= 65.2855     Mn1-O4-Al8= 91.4598
     O2-O4-Al8= 97.405       O3-Al8-O4= 84.785      Mn1-O5-Al8= 91.4598
     O2-Al8-O5= 84.785       O3-O5-Al8= 97.405       O4-Al8-O5= 90.3792
   Mn1-Al6-Al8= 60.7689     O2-Al6-Al8= 82.595      O3-Al6-Al8= 82.595
    O4-Al8-Al6= 82.595      O5-Al8-Al6= 82.595      Mn1-Al8-O7=100.8363
     O2-O7-Al8= 76.6463      O3-O7-Al8= 76.6463      O4-Al8-O7=110.3263
     O5-Al8-O7=110.3263     Al6-O7-Al8= 99.8652
Stoichiometry    Al2MnO5(2)
Framework group  C2V[C2(OMn),SGV(Al2),X(O4)]
Deg. of freedom    6
Full point group                 C2V     NOp   4
Largest Abelian subgroup         C2V     NOp   4
Largest concise Abelian subgroup C2V     NOp   4
                        Standard orientation:
---------------------------------------------------------------------
Center     Atomic     Atomic              Coordinates (Angstroms)
Number     Number      Type              X           Y           Z
---------------------------------------------------------------------
   1         25           0         .000000     .000000    1.390004
   2          8           0       -1.251707    1.100973     .238676
   3          8           0        1.251707    1.100973     .238676
   4          8           0       -1.251707   -1.100973     .238676
   5          8           0        1.251707   -1.100973     .238676
   6         13           0         .000000    1.328368    -.983805
   7          8           0         .000000     .000000   -2.101104
   8         13           0         .000000   -1.328368    -.983805
---------------------------------------------------------------------
Rotational constants (GHZ):      1.8511038      1.5188198      1.2469975
Isotopes: Mn-55,O-16,O-16,O-16,O-16,Al-27,O-16,Al-27
Leave Link  202 at Thu Jul 20 22:50:13 2000, MaxMem=    6291456 cpu:        .2
```

```
 (Enter /apps/g98/l601.exe)
 Copying SCF densities to generalized density rwf, ISCF=1 IROHF=0.

Condensed to atoms (all electrons):
              1          2          3          4          5          6
  1  Mn  23.318881    .040496    .040496    .040496    .040496   -.015933
  2  O     .040496   8.761652   -.047806   -.007218   -.002458    .163938
  3  O     .040496   -.047806   8.761652   -.002458   -.007218    .163938
  4  O     .040496   -.007218   -.002458   8.761652   -.047806    .009597
  5  O     .040496   -.002458   -.007218   -.047806   8.761652    .009597
  6  Al   -.015933    .163938    .163938    .009597    .009597  10.835698
  7  O     .009000   -.026017   -.026017   -.026017   -.026017    .177455
  8  Al   -.015933    .009597    .009597    .163938    .163938    .007496
              7          8
  1  Mn    .009000   -.015933
  2  O    -.026017    .009597
  3  O    -.026017    .009597
  4  O    -.026017    .163938
  5  O    -.026017    .163938
  6  Al    .177455    .007496
  7  O    9.009860    .177455
  8  Al    .177455  10.835698
 Total atomic charges:
              1
  1  Mn   1.542003
  2  O    -.892182
  3  O    -.892182
  4  O    -.892182
  5  O    -.892182
  6  Al   1.648215
  7  O   -1.269703
  8  Al   1.648215
 Sum of Mulliken charges=    .00000
 Atomic charges with hydrogens summed into heavy atoms:
              1
  1  Mn   1.542003
  2  O    -.892182
  3  O    -.892182
  4  O    -.892182
  5  O    -.892182
  6  Al   1.648215
  7  O   -1.269703
  8  Al   1.648215
 Sum of Mulliken charges=    .00000
          Atomic-Atomic Spin Densities.
              1          2          3          4          5          6
  1  Mn   1.013101   -.011742   -.011742   -.011742   -.011742    .000271
  2  O    -.011742    .090703    .005167   -.025612    .001913   -.017077
  3  O    -.011742    .005167    .090703    .001913   -.025612   -.017077
  4  O    -.011742   -.025612    .001913    .090703    .005167    .009045
  5  O    -.011742    .001913   -.025612    .005167    .090703    .009045
  6  Al    .000271   -.017077   -.017077    .009045    .009045   -.061000
  7  O    -.000585    .000305    .000305    .000305    .000305    .004979
  8  Al    .000271    .009045    .009045   -.017077   -.017077   -.015434
              7          8
  1  Mn   -.000585    .000271
  2  O     .000305    .009045
```

```
  3  O      .000305    .009045
  4  O      .000305   -.017077
  5  O      .000305   -.017077
  6  Al     .004979   -.015434
  7  O     -.013002    .004979
  8  Al     .004979   -.061000
Total atomic spin densities:
             1
  1  Mn     .966091
  2  O      .052703
  3  O      .052703
  4  O      .052703
  5  O      .052703
  6  Al    -.087247
  7  O     -.002409
  8  Al    -.087247
Sum of Mulliken spin densities=   1.00000
                      Isotropic Fermi Contact Couplings
    Atom                 a.u.       MegaHertz       Gauss      10(-4) cm-1
   1  Mn(55)            -.28439    -314.35195    -112.16862    -104.85652
   2  O(17)              .03297     -19.98857      -7.13242      -6.66747
   3  O(17)              .03297     -19.98857      -7.13242      -6.66747
   4  O(17)              .03297     -19.98857      -7.13242      -6.66747
   5  O(17)              .03297     -19.98857      -7.13242      -6.66747
   6  Al(27)             .00619       7.22062       2.57650       2.40854
   7  O(17)             -.00613       3.71604       1.32597       1.23954
   8  Al(27)             .00619       7.22062       2.57650       2.40854
Electronic spatial extent (au):  <R**2>=  1011.6996
Charge=      .0000 electrons
Dipole moment (Debye):
   X=      .0000    Y=      .0000    Z=     1.2194  Tot=     1.2194
Quadrupole moment (Debye-Ang):
  XX=   -81.1129   YY=   -51.5782   ZZ=   -49.3206
  XY=      .0000   XZ=      .0000   YZ=      .0000
Octapole moment (Debye-Ang**2):
 XXX=      .0000  YYY=      .0000  ZZZ=    77.7064  XYY=      .0000
 XXY=      .0000  XXZ=     1.7883  XZZ=      .0000  YZZ=      .0000
 YYZ=   -31.1930  XYZ=      .0000
Hexadecapole moment (Debye-Ang**3):
XXXX=  -344.2843 YYYY=  -391.6034 ZZZZ=  -479.7746 XXXY=      .0000
XXXZ=      .0000 YYYX=      .0000 YYYZ=      .0000 ZZZX=      .0000
ZZZY=      .0000 XXYY=  -152.7133 XXZZ=  -117.7027 YYZZ=   -96.7401
XXYZ=      .0000 YYXZ=      .0000 ZZXY=      .0000
N-N= 7.863869591795D+02 E-N=-6.357876936874D+03  KE= 2.008026997752D+03
Symmetry A1   KE= 6.253812443132D+02
Symmetry A2   KE= 4.698920364677D+01
Symmetry B1   KE= 1.143423556270D+02
Symmetry B2   KE= 2.208634111391D+02
Leave Link  601 at Thu Jul 20 22:50:18 2000, MaxMem=    6291456 cpu:       3.3
(Enter /apps/g98/l9999.exe)
1\1\GINC-SPIDER04\FOpt\UHF\6-311G\Al2Mn1O5(2)\RAKESH\20-Jul-2000\0\\#P
 HF/6-311G OPT = (CART, MAXCYCLE=100) SCF=(DIRECT,MAXCYCLE=400) FREQ G
EOM = CHECKPOINT\\mn4al\\0,2\Mn,0.,0.,1.3900044251\O,-1.2517069516,1.1
009731145,0.2386764829\O,1.2517069516,1.1009731145,0.2386764829\O,-1.2
517069516,-1.1009731145,0.2386764829\O,1.2517069516,-1.1009731145,0.23
86764829\Al,0.,1.3283677219,-0.9838048496\O,0.,0.,-2.1011039987\Al,0.,
-1.3283677219,-0.9838048496\\Version=IBM-RS6000-G98RevA.7\State=2-B2\H
```

```
F=-2007.6295365\S2=1.125419\S2-1=0.\S2A=0.812362\RMSD=5.202e-09\RMSF=2
.208e-05\Dipole=0.,0.,0.4797318\PG=C02V [C2(O1Mn1),SGV(Al2),X(O4)]\\@


IT IS A QUALITY OF REVOLUTIONS NOT TO GO BY OLD LINES OR OLD LAWS,
BUT TO BREAK UP BOTH, AND MAKE NEW ONES.
                                             -- A. LINCOLN (1848)
Leave Link 9999 at Thu Jul 20 22:50:30 2000, MaxMem=    6291456 cpu:        .2
Job cpu time:  0 days  8 hours 25 minutes  7.5 seconds.
File lengths (MBytes):  RWF=   23 Int=    0 D2E=    0 Chk=    5 Scr=    1
Normal termination of Gaussian 98.
(Enter /apps/g98/l1.exe)
Link1:  Proceeding to internal job step number  2.
---------------------------------------------
#P Geom=AllCheck Guess=TCheck UHF/6-311G Freq
---------------------------------------------
1/6=100,10=4,18=10,29=7,30=1,38=1/1,3;
2//2;
3/5=4,6=6,11=2,25=1,30=1/1,2,3;
4/5=101,7=2/1;
5/5=2,7=400/2;
8/6=4,11=11,23=2/1;
10/13=10/2;
11/6=2,8=1,9=11,15=111,16=11/1,2,10;
10/6=1/2;
6/7=2,8=2,9=2,10=2,18=1,28=1/1;
7/8=1,10=1,25=1/1,2,3,16;
1/6=100,10=4,18=10,30=1/3;
99//99;
Leave Link    1 at Thu Jul 20 22:50:33 2000, MaxMem=          0 cpu:        .4
(Enter /apps/g98/l101.exe)
-----
mn4al
-----
No Z-matrix found on checkpoint file.
Cartesian coordinates read from the checkpoint file:
 mn4al.chk
Charge =  0 Multiplicity = 2
Mn,0,0.,0.,1.3900044251
O,0,-1.2517069516,1.1009731145,0.2386764829
O,0,1.2517069516,1.1009731145,0.2386764829
O,0,-1.2517069516,-1.1009731145,0.2386764829
O,0,1.2517069516,-1.1009731145,0.2386764829
Al,0,0.,1.3283677219,-0.9838048496
O,0,0.,0.,-2.1011039987
Al,0,0.,-1.3283677219,-0.9838048496
Recover connectivity data from disk.
Leave Link  101 at Thu Jul 20 22:50:36 2000, MaxMem=    6291456 cpu:        .3
(Enter /apps/g98/l103.exe)

Leave Link  103 at Thu Jul 20 22:50:38 2000, MaxMem=    6291456 cpu:        .5
(Enter /apps/g98/l202.exe)
```

```
                         Input orientation:
 ---------------------------------------------------------------------
 Center     Atomic     Atomic              Coordinates (Angstroms)
 Number     Number      Type              X           Y           Z
 ---------------------------------------------------------------------
    1         25             0         .000000     .000000    1.390004
    2          8             0       -1.251707    1.100973     .238676
    3          8             0        1.251707    1.100973     .238676
    4          8             0       -1.251707   -1.100973     .238676
    5          8             0        1.251707   -1.100973     .238676
    6         13             0         .000000    1.328368    -.983805
    7          8             0         .000000     .000000   -2.101104
    8         13             0         .000000   -1.328368    -.983805
 ---------------------------------------------------------------------
                  Distance matrix (angstroms):
                   1          2          3          4          5
     1  Mn    .000000
     2  O    2.025949    .000000
     3  O    2.025949   2.503414    .000000
     4  O    2.025949   2.201946   3.334014    .000000
     5  O    2.025949   3.334014   2.201946   2.503414    .000000
     6  Al   2.720208   1.764352   1.764352   2.993815   2.993815
     7  O    3.491108   2.872888   2.872888   2.872888   2.872888
     8  Al   2.720208   2.993815   2.993815   1.764352   1.764352
                   6          7          8
     6  Al    .000000
     7  O    1.735776    .000000
     8  Al   2.656735   1.735776    .000000
                       Interatomic angles:
      O2-Mn1-O3= 76.3168      O2-Mn1-O4= 65.8357      O3-Mn1-O4=110.7378
       O3-O2-O4= 90.          O2-Mn1-O5=110.7378      O3-Mn1-O5= 65.8357
       O2-O3-O5= 90.          O4-Mn1-O5= 76.3168       O2-O4-O5= 90.
       O3-O5-O4= 90.         Mn1-O2-Al6= 91.4598     Mn1-O3-Al6= 91.4598
      O2-Al6-O3= 90.3792     O4-Mn1-Al6= 76.6708      O4-O2-Al6= 97.405
      O3-Al6-O4= 84.785      O5-Mn1-Al6= 76.6708      O2-Al6-O5= 84.785
      O5-O3-Al6= 97.405       O5-O4-Al6= 65.2855      Mn1-O2-O7= 89.1627
      Mn1-O3-O7= 89.1627       O3-O2-O7= 64.1704      Mn1-O4-O7= 89.1627
       O4-O2-O7= 67.4662       O3-O7-O4= 70.9369      Mn1-O5-O7= 89.1627
       O2-O7-O5= 70.9369       O5-O3-O7= 67.4662       O5-O4-O7= 64.1704
    Mn1-Al6-O7=100.8363       O2-Al6-O7=110.3263      O3-Al6-O7=110.3263
      O4-O7-Al6= 76.6463      O5-O7-Al6= 76.6463     O2-Mn1-Al8= 76.6708
     O3-Mn1-Al8= 76.6708      O3-O2-Al8= 65.2855     Mn1-O4-Al8= 91.4598
      O2-O4-Al8= 97.405       O3-Al8-O4= 84.785      Mn1-O5-Al8= 91.4598
      O2-Al8-O5= 84.785       O3-O5-Al8= 97.405       O4-Al8-O5= 90.3792
   Mn1-Al8-Al6= 60.7689     O2-Al6-Al8= 82.595      O3-Al6-Al8= 82.595
     O4-Al8-Al6= 82.595      O5-Al8-Al6= 82.595     Mn1-Al8-O7=100.8363
      O2-O7-Al8= 76.6463      O3-O7-Al8= 76.6463      O4-Al8-O7=110.3263
      O5-Al8-O7=110.3263     Al6-O7-Al8= 99.8652
 Stoichiometry    Al2MnO5(2)
 Framework group  C2V[C2(OMn),SGV(Al2),X(O4)]
 Deg. of freedom    6
 Full point group                C2V     NOp   4
 Largest Abelian subgroup        C2V     NOp   4
 Largest concise Abelian subgroup C2V     NOp   4
```

```
                        Standard orientation:
 ---------------------------------------------------------------------
 Center     Atomic     Atomic              Coordinates (Angstroms)
 Number     Number      Type              X           Y           Z
 ---------------------------------------------------------------------
    1         25           0         .000000     .000000    1.390004
    2          8           0       -1.251707    1.100973     .238676
    3          8           0        1.251707    1.100973     .238676
    4          8           0       -1.251707   -1.100973     .238676
    5          8           0        1.251707   -1.100973     .238676
    6         13           0         .000000    1.328368    -.983805
    7          8           0         .000000     .000000   -2.101104
    8         13           0         .000000   -1.328368    -.983805
 ---------------------------------------------------------------------
 Rotational constants (GHZ):      1.8511038      1.5188198      1.2469975
 Isotopes: Mn-55,O-16,O-16,O-16,O-16,Al-27,O-16,Al-27
 Leave Link  202 at Thu Jul 20 22:50:41 2000, MaxMem=    6291456 cpu:        .2
 (Enter /apps/g98/l301.exe)
 Standard basis: 6-311G (5D, 7F)
 There are    56 symmetry adapted basis functions of A1  symmetry.
 There are    21 symmetry adapted basis functions of A2  symmetry.
 There are    29 symmetry adapted basis functions of B1  symmetry.
 There are    40 symmetry adapted basis functions of B2  symmetry.
 Crude estimate of integral set expansion from redundant integrals=1.206.
 Integral buffers will be    262144 words long.
 Raffenetti 2 integral format.
 Two-electron integral symmetry is turned on.
   146 basis functions      281 primitive gaussians
    46 alpha electrons       45 beta electrons
       nuclear repulsion energy       786.3869591795 Hartrees.
 Leave Link  301 at Thu Jul 20 22:50:43 2000, MaxMem=    6291456 cpu:        .4
 (Enter /apps/g98/l302.exe)
 One-electron integrals computed using PRISM.
 One-electron integral symmetry used in STVInt
 NBasis=   146 RedAO= T  NBF=    56    21    29    40
 NBsUse=   146 1.00D-04 NBFU=    56    21    29    40
 Leave Link  302 at Thu Jul 20 22:50:50 2000, MaxMem=    6291456 cpu:       4.5
 (Enter /apps/g98/l303.exe)
 DipDrv:  MaxL=1.
 Leave Link  303 at Thu Jul 20 22:50:59 2000, MaxMem=    6291456 cpu:       1.0
 (Enter /apps/g98/l401.exe)
 Initial guess read from the checkpoint file:
  mn4al.chk
 Guess basis functions will be translated to current atomic coordinates.
 Initial guess orbital symmetries:

 SCF Done:  E(UHF) =  -2007.62953650     A.U. after    1 cycles
             Convg  =     .1591D-08             -V/T =  1.9998
             S**2   =   1.1254
 KE= 2.008026997916D+03 PE=-6.357876937039D+03 EE= 1.555833443443D+03
 Annihilation of the first spin contaminant:
 S**2 before annihilation     1.1254,   after      .8124
 Leave Link  502 at Thu Jul 20 22:52:25 2000, MaxMem=    6291456 cpu:      60.0
 (Enter /apps/g98/l801.exe)
 Range of M.O.s used for correlation:     1   146
 NBasis=   146 NAE=    46 NBE=    45 NFC=     0 NFV=     0
 NROrb=    146 NOA=    46 NOB=    45 NVA=   100 NVB=   101
```

```
Leave Link  801 at Thu Jul 20 22:52:30 2000, MaxMem=    6291456 cpu:        .1
(Enter /apps/g98/l1002.exe)
Minotr:  UHF wavefunction.
         Direct CPHF calculation.
         Solving linear equations simultaneously.
         Using symmetry in CPHF.
         Requested convergence is 1.0D-08 RMS, and 1.0D-07 maximum.
         Secondary convergence is 1.0D-12 RMS, and 1.0D-12 maximum.
         Differentiating once with respect to electric field.
               with respect to dipole field.
         NewPWx=F KeepS1=T KeepF1=T KeepIn=T MapXYZ=F.
         MDV=  6291456
         Using IRadAn=       2.
Integrals replicated using symmetry in FoFDir.
MinBra= 0 MaxBra= 2 Meth= 1.
IRaf=       0 NMat=   3 IRICut=       1 DoRegI=T DoRafI=F ISym2E= 2 JSym2E=2.
         There are   3 degrees of freedom in the 1st order CPHF.
  3 vectors were produced by pass  0.
AX will form   3 AO Fock derivatives at one time.
  3 vectors were produced by pass  1.
  3 vectors were produced by pass  2.
  3 vectors were produced by pass  3.
  3 vectors were produced by pass  4.
  3 vectors were produced by pass  5.
  3 vectors were produced by pass  6.
  3 vectors were produced by pass  7.
  3 vectors were produced by pass  8.
  3 vectors were produced by pass  9.
  3 vectors were produced by pass 10.
  3 vectors were produced by pass 11.
  3 vectors were produced by pass 12.
  3 vectors were produced by pass 13.
  3 vectors were produced by pass 14.
  3 vectors were produced by pass 15.
  1 vectors were produced by pass 16.
Inv2:  IOpt= 1 Iter= 1 AM= 1.00D-13 Conv= 1.00D-12.
Inverted reduced A of dimension  49 with in-core refinement.
Leave Link 1002 at Fri Jul 21 00:18:59 2000, MaxMem=    6291456 cpu:    5077.0
(Enter /apps/g98/l1101.exe)
Using compressed storage.
Will process   8 atoms per pass.
Leave Link 1101 at Fri Jul 21 00:19:09 2000, MaxMem=    6291456 cpu:       6.5
(Enter /apps/g98/l1102.exe)
Use density number 0.
Leave Link 1102 at Fri Jul 21 00:19:23 2000, MaxMem=    6291456 cpu:       1.2
(Enter /apps/g98/l1110.exe)
Forming Gx(P) for the SCF density.
Integral derivatives from FoFDir, PRISM(SPDF).
Do as many integral derivatives as possible in FoFDir.
G2DrvN: MDV=   6291456.
G2DrvN: will do    8 atoms at a time, making    1 passes doing MaxLOS=2.
Petite list used in FoFDir.
MinBra= 0 MaxBra= 2 Meth= 1.
IRaf=       0 NMat=   1 IRICut=       1 DoRegI=T DoRafI=F ISym2E= 1 JSym2E=1.
FoFDir used for L=0 through L=2.
Leave Link 1110 at Fri Jul 21 00:28:14 2000, MaxMem=    6291456 cpu:     523.3
(Enter /apps/g98/l1002.exe)
```

```
 Minotr:  UHF wavefunction.
          Direct CPHF calculation.
          Solving linear equations simultaneously.
          Using symmetry in CPHF.
          Requested convergence is 1.0D-08 RMS, and 1.0D-07 maximum.
          Secondary convergence is 1.0D-12 RMS, and 1.0D-12 maximum.
          Differentiating once with respect to electric field.
                with respect to dipole field.
          Differentiating once with respect to nuclear coordinates.
          NewPWx=T KeepS1=F KeepF1=F KeepIn=F MapXYZ=F.
          MDV=  6291456
          Using IRadAn=       2.
 Integrals replicated using symmetry in FoFDir.
 MinBra= 0 MaxBra= 2 Meth= 1.
 IRaf=       0 NMat=  15 IRICut=      15 DoRegI=T DoRafI=T ISym2E= 2 JSym2E=2.
          There are  15 degrees of freedom in the 1st order CPHF.
  15 vectors were produced by pass  0.
 AX will form  15 AO Fock derivatives at one time.
  15 vectors were produced by pass  1.
  15 vectors were produced by pass  2.
  15 vectors were produced by pass  3.
  15 vectors were produced by pass  4.
  15 vectors were produced by pass  5.
  15 vectors were produced by pass  6.
  15 vectors were produced by pass  7.
  15 vectors were produced by pass  8.
  14 vectors were produced by pass  9.
   9 vectors were produced by pass 10.
   4 vectors were produced by pass 11.
   2 vectors were produced by pass 12.
   1 vectors were produced by pass 13.
 Inv2:  IOpt= 1 Iter= 1 AM= 9.58D-14 Conv= 1.00D-12.
 Inverted reduced A of dimension 165 with in-core refinement.
 Leave Link 1002 at Fri Jul 21 02:19:12 2000, MaxMem=    6291456 cpu:    6405.3
 (Enter /apps/g98/l601.exe)
 Copying SCF densities to generalized density rwf, ISCF=1 IROHF=0.

Condensed to atoms (all electrons):
               1           2           3           4           5           6
  1  Mn  23.318881    .040496    .040496    .040496    .040496   -.015933
  2  O     .040496   8.761652   -.047806   -.007218   -.002458    .163938
  3  O     .040496   -.047806   8.761652   -.002458   -.007218    .163938
  4  O     .040496   -.007218   -.002458   8.761652   -.047806    .009597
  5  O     .040496   -.002458   -.007218   -.047806   8.761652    .009597
  6  Al   -.015933    .163938    .163938    .009597    .009597  10.835698
  7  O     .009000   -.026017   -.026017   -.026017   -.026017    .177455
  8  Al   -.015933    .009597    .009597    .163938    .163938    .007496
               7           8
  1  Mn    .009000   -.015933
  2  O    -.026017    .009597
  3  O    -.026017    .009597
  4  O    -.026017    .163938
  5  O    -.026017    .163938
  6  Al    .177455    .007496
  7  O    9.009860    .177455
  8  Al    .177455  10.835698
```

```
Total atomic charges:
             1
 1  Mn   1.542003
 2  O    -.892182
 3  O    -.892182
 4  O    -.892182
 5  O    -.892182
 6  Al   1.648215
 7  O   -1.269703
 8  Al   1.648215
Sum of Mulliken charges=    .00000
Atomic charges with hydrogens summed into heavy atoms:
             1
 1  Mn   1.542003
 2  O    -.892182
 3  O    -.892182
 4  O    -.892182
 5  O    -.892182
 6  Al   1.648215
 7  O   -1.269703
 8  Al   1.648215
Sum of Mulliken charges=    .00000
         Atomic-Atomic Spin Densities.
             1          2          3          4          5          6
 1  Mn   1.013101   -.011742   -.011742   -.011742   -.011742    .000271
 2  O    -.011742    .090703    .005167   -.025612    .001913   -.017077
 3  O    -.011742    .005167    .090703    .001913   -.025612   -.017077
 4  O    -.011742   -.025612    .001913    .090703    .005167    .009045
 5  O    -.011742    .001913   -.025612    .005167    .090703    .009045
 6  Al    .000271   -.017077   -.017077    .009045    .009045   -.061000
 7  O    -.000585    .000305    .000305    .000305    .000305    .004979
 8  Al    .000271    .009045    .009045   -.017077   -.017077   -.015434
             7          8
 1  Mn   -.000585    .000271
 2  O     .000305    .009045
 3  O     .000305    .009045
 4  O     .000305   -.017077
 5  O     .000305   -.017077
 6  Al    .004979   -.015434
 7  O    -.013002    .004979
 8  Al    .004979   -.061000
Total atomic spin densities:
             1
 1  Mn    .966091
 2  O     .052703
 3  O     .052703
 4  O     .052703
 5  O     .052703
 6  Al   -.087247
 7  O    -.002409
 8  Al   -.087247
Sum of Mulliken spin densities=   1.00000
```

```
                      Isotropic Fermi Contact Couplings
     Atom                 a.u.       MegaHertz       Gauss      10(-4) cm-1
   1  Mn(55)             -.28439    -314.35196    -112.16863    -104.85653
   2  O(17)               .03297     -19.98861      -7.13244      -6.66748
   3  O(17)               .03297     -19.98861      -7.13244      -6.66748
   4  O(17)               .03297     -19.98861      -7.13244      -6.66748
   5  O(17)               .03297     -19.98861      -7.13244      -6.66748
   6  Al(27)              .00619       7.22066       2.57651       2.40855
   7  O(17)              -.00613       3.71603       1.32597       1.23954
   8  Al(27)              .00619       7.22066       2.57651       2.40855
 Electronic spatial extent (au):  <R**2>=  1011.6996
 Charge=      .0000 electrons
 Dipole moment (Debye):
    X=      .0000    Y=      .0000    Z=     1.2194  Tot=     1.2194
 Quadrupole moment (Debye-Ang):
   XX=   -81.1129   YY=   -51.5782   ZZ=   -49.3206
   XY=      .0000   XZ=      .0000   YZ=      .0000
 Octapole moment (Debye-Ang**2):
  XXX=      .0000  YYY=      .0000  ZZZ=    77.7064  XYY=      .0000
  XXY=      .0000  XXZ=     1.7883  XZZ=      .0000  YZZ=      .0000
  YYZ=   -31.1930  XYZ=      .0000
 Hexadecapole moment (Debye-Ang**3):
 XXXX=  -344.2843 YYYY=  -391.6034 ZZZZ=  -479.7746 XXXY=      .0000
 XXXZ=      .0000 YYYX=      .0000 YYYZ=      .0000 ZZZX=      .0000
 ZZZY=      .0000 XXYY=  -152.7133 XXZZ=  -117.7027 YYZZ=   -96.7401
 XXYZ=      .0000 YYXZ=      .0000 ZZXY=      .0000
 N-N= 7.863869591795D+02 E-N=-6.357876937580D+03  KE= 2.008026997916D+03
 Symmetry A1   KE= 6.253812443709D+02
 Symmetry A2   KE= 4.698920367971D+01
 Symmetry B1   KE= 1.143423556924D+02
 Symmetry B2   KE= 2.208634111122D+02
  Exact polarizability: 142.748    .002 129.673    .001   -.001  59.559
 Approx polarizability:  96.767    .000 113.520    .000    .000  48.270
 Leave Link  601 at Fri Jul 21 02:19:29 2000, MaxMem=    6291456 cpu:       5.0
 (Enter /apps/g98/l701.exe)
 Compute integral second derivatives.
 ... and contract with generalized density number  0.
 Leave Link  701 at Fri Jul 21 02:19:47 2000, MaxMem=    6291456 cpu:       9.8
 (Enter /apps/g98/l702.exe)
 L702 exits ... SP integral derivatives will be done elsewhere.
 Leave Link  702 at Fri Jul 21 02:19:56 2000, MaxMem=    6291456 cpu:        .0
 (Enter /apps/g98/l703.exe)
 Compute integral second derivatives.
 Integral derivatives from FoFDir, PRISM(SPDF).
 Petite list used in FoFDir.
 MinBra= 0 MaxBra= 2 Meth= 1.
 IRaf=       0 NMat=   1 IRICut=       1 DoRegI=T DoRafI=F ISym2E= 1 JSym2E=1.
 Leave Link  703 at Fri Jul 21 02:35:09 2000, MaxMem=    6291456 cpu:     904.2
 (Enter /apps/g98/l716.exe)
 Dipole        =-1.46545632D-14 7.10542736D-15 4.79731616D-01
 Polarizability= 1.42747863D+02 1.51873984D-03 1.29672657D+02
                 9.92336716D-04-7.91181128D-04 5.95586545D+01
 HyperPolar    = 1.42269539D+00-3.60240033D+00-1.13202176D+00
                -2.82586543D-01-2.56963564D+01 1.97443206D-01
                -5.22564120D+02-1.02626881D+00 1.11173228D-01
                -9.60978298D+02
 Full mass-weighted force constant matrix:
```

```
Low frequencies --- -928.1965 -196.8892  -22.9496   -4.8858   -4.0199    -.0727
Low frequencies ---    3.0941    8.8309  150.2733
******    2 imaginary frequencies (negative Signs) ******
Harmonic frequencies (cm**-1), IR intensities (KM/Mole),
Raman scattering activities (A**4/AMU), Raman depolarization ratios,
reduced masses (AMU), force constants (mDyne/A) and normal coordinates:
                     1                      2                      3
                    B1                     B2                     ?A
Frequencies --  -928.1965              -196.8889               150.2713
Red. masses --    17.0824                26.9279                16.9124
Frc consts  --     8.6712                  .6150                  .2250
IR Inten    --  2869.8200                63.1433                70.5901
Raman Activ --    20.6945                50.7479               561.9881
Depolar     --      .7500                  .7500                  .1539
Atom AN      X      Y      Z        X      Y      Z        X      Y      Z
  1  25      .09    .00    .00      .00    .42    .00      .00    .00   -.15
  2   8     -.20   -.43    .02     -.18   -.28    .03      .10    .47    .11
  3   8     -.20    .43   -.02      .18   -.28    .03     -.10    .47    .11
  4   8     -.20    .43    .02      .18   -.28   -.03      .10   -.47    .11
  5   8     -.20   -.43   -.02     -.18   -.28   -.03     -.10   -.47    .11
  6  13      .19    .00    .00      .00   -.13    .41      .00    .06    .00
  7   8     -.13    .00    .00      .00    .10    .00      .00    .00    .08
  8  13      .19    .00    .00      .00   -.13   -.41      .00   -.06    .00
                     4                      5                      6
                    ?A                     B2                     A1
Frequencies --   217.7180               221.7966               300.3449
Red. masses --    18.6406                19.2016                27.0967
Frc consts  --      .5206                  .5565                 1.4401
IR Inten    --      .0001                40.7342                11.9505
Raman Activ --     6.3956                43.1047               137.1537
Depolar     --      .7499                  .7500                  .0406
Atom AN      X      Y      Z        X      Y      Z        X      Y      Z
  1  25      .00    .00    .00      .00    .00    .00      .00    .00    .48
  2   8      .00    .31    .30      .02    .33    .24      .24    .12   -.03
  3   8      .00   -.31   -.30     -.02    .33    .24     -.24    .12   -.03
  4   8      .00    .31   -.30     -.02    .33   -.24      .24   -.12   -.03
  5   8      .00   -.31    .30      .02    .33   -.24     -.24   -.12   -.03
  6  13     -.35    .00    .00      .00   -.34    .16      .00   -.15   -.29
  7   8      .00    .00    .00      .00   -.17    .00      .00    .00   -.52
  8  13      .35    .00    .00      .00   -.34   -.16      .00    .15   -.29
                     7                      8                      9
                    ?B                     ?B                     B2
Frequencies --   362.9947               385.6616               436.6941
Red. masses --    18.2527                16.0041                17.5882
Frc consts  --     1.4170                 1.4025                 1.9762
IR Inten    --    25.9679                  .0000                70.2468
Raman Activ --     3.6305               103.4937                  .9331
Depolar     --      .7500                  .7500                  .7500
Atom AN      X      Y      Z        X      Y      Z        X      Y      Z
  1  25     -.14    .00    .00      .00    .00    .00      .00    .17    .00
  2   8      .12    .07   -.08      .29   -.27    .31      .36   -.16    .28
  3   8      .12   -.07    .08      .29    .27   -.31     -.36   -.16    .28
  4   8      .12   -.07   -.08     -.29   -.27   -.31     -.36   -.16   -.28
  5   8      .12    .07    .08     -.29    .27    .31      .36   -.16   -.28
  6  13      .26    .00    .00      .02    .00    .00      .00    .02   -.14
  7   8     -.86    .00    .00      .00    .00    .00      .00   -.01    .00
  8  13      .26    .00    .00     -.02    .00    .00      .00    .02    .14
```

	10			11			12		
	A1			?C			?C		
Frequencies --	462.0714			542.8450			594.9107		
Red. masses --	24.2706			17.8561			20.4615		
Frc consts --	3.0532			3.1002			4.2667		
IR Inten --	2.6085			158.0127			72.4595		
Raman Activ --	127.0738			1332.0278			50.6899		
Depolar --	.1205			.3594			.7500		
Atom AN	X	Y	Z	X	Y	Z	X	Y	Z
1 25	.00	.00	.19	.00	.00	-.18	.33	.00	.00
2 8	.04	.00	-.13	.33	-.19	.28	-.18	.11	-.41
3 8	-.04	.00	-.13	-.33	-.19	.28	-.18	-.11	.41
4 8	.04	.00	-.13	.33	.19	.28	-.18	-.11	-.41
5 8	-.04	.00	-.13	-.33	.19	.28	-.18	.11	.41
6 13	.00	.53	-.18	.00	.11	-.12	-.07	.00	.00
7 8	.00	.00	.51	.00	.00	-.10	-.18	.00	.00
8 13	.00	-.53	-.18	.00	-.11	-.12	-.07	.00	.00

	13			14			15		
	?C			?C			?C		
Frequencies --	641.7780			715.4397			720.7095		
Red. masses --	17.8280			18.2313			17.3890		
Frc consts --	4.3264			5.4981			5.3216		
IR Inten --	.6984			.0004			3.6006		
Raman Activ --	7.4671			1136.1148			317.6451		
Depolar --	.7500			.7500			.0765		
Atom AN	X	Y	Z	X	Y	Z	X	Y	Z
1 25	-.07	.00	.00	.00	.00	.00	.00	.00	.01
2 8	.31	-.27	-.21	.33	-.01	-.30	-.27	.02	.19
3 8	.31	.27	.21	.33	.01	.30	.27	.02	.19
4 8	.31	.27	-.21	-.33	-.01	.30	-.27	-.02	.19
5 8	.31	-.27	.21	-.33	.01	-.30	.27	-.02	.19
6 13	-.28	.00	.00	-.32	.00	.00	.00	.25	-.04
7 8	-.08	.00	.00	.00	.00	.00	.00	.00	-.66
8 13	-.28	.00	.00	.32	.00	.00	.00	-.25	-.04

	16			17			18		
	B2			B2			A1		
Frequencies --	764.9724			841.1608			851.9607		
Red. masses --	17.0951			18.6649			20.2821		
Frc consts --	5.8940			7.7810			8.6737		
IR Inten --	29.7351			.1302			201.1720		
Raman Activ --	13.3702			.4178			323.6935		
Depolar --	.7500			.7490			.0667		
Atom AN	X	Y	Z	X	Y	Z	X	Y	Z
1 25	.00	.02	.00	.00	.02	.00	.00	.00	.00
2 8	-.31	-.04	.28	-.16	-.03	.08	.22	.01	-.22
3 8	.31	-.04	.28	.16	-.03	.08	-.22	.01	-.22
4 8	.31	-.04	-.28	.16	-.03	-.08	.22	-.01	-.22
5 8	-.31	-.04	-.28	-.16	-.03	-.08	-.22	-.01	-.22
6 13	.00	.15	-.16	.00	-.22	-.27	.00	.18	.40
7 8	.00	-.43	.00	.00	.79	.00	.00	.00	-.47
8 13	.00	.15	.16	.00	-.22	.27	.00	-.18	.40

```
-------------------
- Thermochemistry -
-------------------
Temperature   298.150 Kelvin.  Pressure   1.00000 Atm.
Atom  1 has atomic number 25 and mass  54.93805
Atom  2 has atomic number  8 and mass  15.99491
Atom  3 has atomic number  8 and mass  15.99491
Atom  4 has atomic number  8 and mass  15.99491
Atom  5 has atomic number  8 and mass  15.99491
Atom  6 has atomic number 13 and mass  26.98154
Atom  7 has atomic number  8 and mass  15.99491
Atom  8 has atomic number 13 and mass  26.98154
Molecular mass:   188.87570 amu.
Principal axes and moments of inertia in atomic units:
                          1         2         3
    EIGENVALUES --   974.954081188.252331447.26923
          X             .00000    .00000   1.00000
          Y             .00000   1.00000    .00000
          Z            1.00000    .00000    .00000
THIS MOLECULE IS AN ASYMMETRIC TOP.
ROTATIONAL SYMMETRY NUMBER  2.
WARNING-- ASSUMPTION OF CLASSICAL BEHAVIOR FOR ROTATION
          MAY CAUSE SIGNIFICANT ERROR
ROTATIONAL TEMPERATURES (KELVIN)       .08884      .07289      .05985
ROTATIONAL CONSTANTS (GHZ)            1.85110     1.51882     1.24700
   2 IMAGINARY FREQUENCIES IGNORED.
Zero-point vibrational energy      49114.7 (Joules/Mol)
                                  11.73869 (Kcal/Mol)
WARNING-- EXPLICIT CONSIDERATION OF  10 DEGREES OF FREEDOM AS
          VIBRATIONS MAY CAUSE SIGNIFICANT ERROR
VIBRATIONAL TEMPERATURES:    216.21   313.25   319.11   432.13   522.27
         (KELVIN)            554.88   628.30   664.81   781.03   855.94
                             923.37  1029.35  1036.93  1100.62  1210.24
                            1225.77

Zero-point correction=                           .018707 (Hartree/Particle)
Thermal correction to Energy=                    .025790
Thermal correction to Enthalpy=                  .026735
Thermal correction to Gibbs Free Energy=        -.013559
Sum of electronic and zero-point Energies=        -2007.610830
Sum of electronic and thermal Energies=           -2007.603746
Sum of electronic and thermal Enthalpies=         -2007.602802
Sum of electronic and thermal Free Energies=      -2007.643096
```

APPENDIX A2 : INPUT AND OUTPUT FILES FOR $MnO_4Al_2O(O_2)^+$

INPUT FILE

```
%chk = mn4alo22

#p hf/6-311G opt = (cart, MaxCycle=100) scf=(direct,MaxCycle=400)
   Freq

mn4alo2

1 1
Mn1    .000000     .000000    1.228754
O1   -1.290164     .768332    -.406828
O2    1.290164     .768332    -.406828
O3   -1.290164    -.768332    -.406828
O4    1.290164    -.768332    -.406828
Al1    .000000    1.215154   -1.569243
O5     .000000     .000000   -2.742515
Al2    .000000   -1.215154   -1.569243
O6    -.731904     .000000    2.815006
O7     .731904     .000000    2.815006
```

^{18}O - ^{18}O ISOTOPE CALCULATION

```
--Link1--
%chk = mn4alo22
%Nosave
#p hf/6-311G Freq(ReadIso,ReadFC) Geom = AllCheck Test

298.15 1.0
55
16
16
16
16
27
16
27
18
18
```

OUTPUT FILE

```
         Item               Value     Threshold  Converged?
 Maximum Force            .000296      .000450     YES
 RMS     Force            .000066      .000300     YES
 Maximum Displacement     .000785      .001800     YES
 RMS     Displacement     .000265      .001200     YES
 Predicted change in Energy=-1.593659D-07
 Optimization completed.
    -- Stationary point found.
```

```
GradGradGradGradGradGradGradGradGradGradGradGradGradGradGradGradGradGrad

Leave Link  103 at Tue Jul 25 14:18:20 2000, MaxMem=    6291456 cpu:        .1
(Enter /apps/g98/l202.exe)

                       Input orientation:
---------------------------------------------------------------------
Center     Atomic     Atomic              Coordinates (Angstroms)
Number     Number      Type              X           Y           Z
---------------------------------------------------------------------
   1         25           0          .000000     .000000    1.241518
   2          8           0        -1.250961     .753246    -.386133
   3          8           0         1.250961     .753246    -.386133
   4          8           0        -1.250961    -.753246    -.386133
   5          8           0         1.250961    -.753246    -.386133
   6         13           0          .000000    1.289146   -1.616691
   7          8           0          .000000     .000000   -2.744930
   8         13           0          .000000   -1.289146   -1.616691
   9          8           0         -.733426     .000000    2.831982
  10          8           0          .733426     .000000    2.831982
---------------------------------------------------------------------
                   Distance matrix (angstroms):
                    1          2          3          4          5
    1  Mn    .000000
    2  O    2.186672    .000000
    3  O    2.186672   2.501923    .000000
    4  O    2.186672   1.506492   2.920468    .000000
    5  O    2.186672   2.920468   1.506492   2.501923    .000000
    6  Al   3.135484   1.834766   1.834766   2.692683   2.692683
    7  O    3.986448   2.774204   2.774204   2.774204   2.774204
    8  Al   3.135484   2.692683   2.692683   1.834766   1.834766
    9  O    1.751425   3.345368   3.855054   3.345368   3.855054
   10  O    1.751425   3.855054   3.345368   3.855054   3.345368
                    6          7          8          9         10
    6  Al    .000000
    7  O    1.713132    .000000
    8  Al   2.578292   1.713132    .000000
    9  O    4.689404   5.624932   4.689404    .000000
   10  O    4.689404   5.624932   4.689404   1.466852    .000000
                      Interatomic angles:
     O2-Mn1-O3= 69.7914      Mn1-O2-O4= 69.8505      O3-Mn1-O4= 83.7932
      O3-O2-O4= 90.          O2-Mn1-O5= 83.7932      Mn1-O3-O5= 69.8505
      O2-O3-O5= 90.          O4-Mn1-O5= 69.7914       O2-O4-O5= 90.
      O3-O5-O4= 90.         Mn1-O2-Al6=102.11       Mn1-O3-Al6=102.11
     O2-Al6-O3= 85.9705     Mn1-O4-Al6= 79.2287      O4-O2-Al6=106.9826
     O3-Al6-O4= 77.8018     Mn1-O5-Al6= 79.2287      O2-Al6-O5= 77.8018
     O5-O3-Al6=106.9826      O5-O4-Al6= 62.3171      Mn1-O2-O7=106.3434
     Mn1-O3-O7=106.3434       O3-O2-O7= 63.1969      Mn1-O4-O7=106.3434
      O4-O2-O7= 74.2454       O3-O7-O4= 63.5199      Mn1-O5-O7=106.3434
      O2-O7-O5= 63.5199       O5-O3-O7= 74.2454       O5-O4-O7= 63.1969
     O2-Al6-O7=102.8213      O3-Al6-O7=102.8213      O4-Al6-O7= 74.3475
     O5-Al6-O7= 74.3475     Mn1-O2-Al8= 79.2287     Mn1-O3-Al8= 79.2287
     O3-O2-Al8= 62.3171     Mn1-O4-Al8=102.11        O2-O4-Al8=106.9826
     O3-Al8-O4= 77.8018     Mn1-O5-Al8=102.11        O2-Al8-O5= 77.8018
     O3-O5-Al8=106.9826      O4-Al8-O5= 85.9705     O2-Al6-Al8= 73.0174
    O3-Al6-Al8= 73.0174     O4-Al8-Al6= 73.0174     O5-Al8-Al6= 73.0174
     O2-Al8-O7= 74.3475      O3-Al8-O7= 74.3475      O4-Al8-O7=102.8213
```

```
     O5-Al8-O7=102.8213     Al6-O7-Al8= 97.6163      O2-Mn1-O9=115.873
     O3-Mn1-O9=156.2781      O4-Mn1-O9=115.873       O5-Mn1-O9=156.2781
    O2-Mn1-O10=156.2781     O3-Mn1-O10=115.873      O4-Mn1-O10=156.2781
    O5-Mn1-O10=115.873      Mn1-O9-O10= 65.2437
Stoichiometry    Al2MnO7(1+)
Framework group  C2V[C2(OMn),SGV(Al2),SGV'(O2),X(O4)]
Deg. of freedom    8
Full point group                C2V     NOp   4
Largest Abelian subgroup        C2V     NOp   4
Largest concise Abelian subgroup C2V     NOp   4
                        Standard orientation:
---------------------------------------------------------------------
Center     Atomic     Atomic              Coordinates (Angstroms)
Number     Number      Type              X           Y           Z
---------------------------------------------------------------------
   1        25           0         .000000     .000000    1.241518
   2         8           0       -1.250961     .753246    -.386133
   3         8           0        1.250961     .753246    -.386133
   4         8           0       -1.250961    -.753246    -.386133
   5         8           0        1.250961    -.753246    -.386133
   6        13           0         .000000    1.289146   -1.616691
   7         8           0         .000000     .000000   -2.744930
   8        13           0         .000000   -1.289146   -1.616691
   9         8           0        -.733426     .000000    2.831982
  10         8           0         .733426     .000000    2.831982
---------------------------------------------------------------------
Rotational constants (GHZ):      2.0770850       .6926506       .6845333
Isotopes: Mn-55,O-16,O-16,O-16,O-16,Al-27,O-16,Al-27,O-16,O-16
Leave Link  202 at Tue Jul 25 14:18:23 2000, MaxMem=    6291456 cpu:        .2
(Enter /apps/g98/l601.exe)
Copying SCF densities to generalized density rwf, ISCF=0 IROHF=0.
         Condensed to atoms (all electrons):
             1          2          3          4          5          6
 1  Mn  23.022378    .011057    .011057    .011057    .011057   -.003034
 2  O      .011057   8.685676   -.063444   -.053851    .007787    .127429
 3  O      .011057   -.063444   8.685676    .007787   -.053851    .127429
 4  O      .011057   -.053851    .007787   8.685676   -.063444   -.019004
 5  O      .011057    .007787   -.053851   -.063444   8.685676   -.019004
 6  Al   -.003034    .127429    .127429   -.019004   -.019004  10.530356
 7  O      .002042   -.027981   -.027981   -.027981   -.027981    .198567
 8  Al   -.003034   -.019004   -.019004    .127429    .127429    .017539
 9  O      .134704    .000353   -.000765    .000353   -.000765    .000928
10  O      .134704   -.000765    .000353   -.000765    .000353    .000928
             7          8          9         10
 1  Mn     .002042   -.003034    .134704    .134704
 2  O    -.027981   -.019004    .000353   -.000765
 3  O    -.027981   -.019004   -.000765    .000353
 4  O    -.027981    .127429    .000353   -.000765
 5  O    -.027981    .127429   -.000765    .000353
 6  Al    .198567    .017539    .000928    .000928
 7  O    8.904785    .198567    .000000    .000000
 8  Al    .198567  10.530356    .000928    .000928
 9  O      .000000    .000928   8.368277   -.062673
10  O      .000000    .000928   -.062673   8.368277
Total atomic charges:
             1
 1  Mn   1.668011
```

```
 2  O    -.667257
 3  O    -.667257
 4  O    -.667257
 5  O    -.667257
 6  Al   2.037865
 7  O   -1.192037
 8  Al   2.037865
 9  O    -.441339
10  O    -.441339
Sum of Mulliken charges=   1.00000
Atomic charges with hydrogens summed into heavy atoms:
             1
 1  Mn   1.668011
 2  O    -.667257
 3  O    -.667257
 4  O    -.667257
 5  O    -.667257
 6  Al   2.037865
 7  O   -1.192037
 8  Al   2.037865
 9  O    -.441339
10  O    -.441339
Sum of Mulliken charges=   1.00000
Electronic spatial extent (au):  <R**2>=  1643.7015
Charge=     1.0000 electrons
Dipole moment (Debye):
   X=      .0000    Y=      .0000    Z=   -14.5976  Tot=    14.5976
Quadrupole moment (Debye-Ang):
  XX=   -83.9526   YY=   -31.0173   ZZ=   -78.9556
  XY=      .0000   XZ=      .0000   YZ=      .0000
Octapole moment (Debye-Ang**2):
 XXX=      .0000  YYY=      .0000  ZZZ=   -54.7828  XYY=      .0000
 XXY=      .0000  XXZ=    -2.7554  XZZ=      .0000  YZZ=      .0000
 YYZ=   -64.1678  XYZ=      .0000
Hexadecapole moment (Debye-Ang**3):
XXXX=  -349.3323 YYYY=  -122.2186 ZZZZ= -1618.0233 XXXY=      .0000
XXXZ=      .0000 YYYX=      .0000 YYYZ=      .0000 ZZZX=      .0000
ZZZY=      .0000 XXYY=  -102.5755 XXZZ=  -278.7293 YYZZ=  -126.6544
XXYZ=      .0000 YYXZ=      .0000 ZZXY=      .0000
N-N= 1.053147733232D+03 E-N=-7.219626022710D+03  KE= 2.157214188819D+03
Symmetry A1   KE= 1.326260175013D+03
Symmetry A2   KE= 1.005677083155D+02
Symmetry B1   KE= 3.002663094955D+02
Symmetry B2   KE= 4.301199959953D+02
Leave Link  601 at Tue Jul 25 14:18:28 2000, MaxMem=    6291456 cpu:       1.8
(Enter /apps/g98/l9999.exe)
1\1\GINC-SPIDER02\FOpt\RHF\6-311G\Al2Mn1O7(1+)\RAKESH\25-Jul-2000\0\\#
P HF/6-311G OPT = (CART, MAXCYCLE=100) SCF=(DIRECT,MAXCYCLE=400) FREQ
OUTPUT = WFN\\mn4alo2\\1,1\Mn,0.,0.,1.2415184449\O,-1.2509612871,0.753
2461349,-0.3861332897\O,1.2509612871,0.7532461349,-0.3861332897\O,-1.2
509612871,-0.7532461349,-0.3861332897\O,1.2509612871,-0.7532461349,-0.
3861332897\Al,0.,1.2891461719,-1.6166912192\O,0.,0.,-2.74493001\Al,0.,
-1.2891461719,-1.6166912192\O,-0.7334260971,0.,2.8319822455\O,0.733426
0971,0.,2.8319822455\\Version=IBM-RS6000-G98RevA.7\State=1-A1\HF=-2156
.9170862\RMSD=7.339e-09\RMSF=6.559e-05\Dipole=0.,0.,-5.743082\PG=C02V
[C2(O1Mn1),SGV(Al2),SGV'(O2),X(O4)]\\@
```

```
Writing a WFN file to mn4alo2.wfn.


A BIRD IN THE HAND IS SAFER THAN ONE OVERHEAD.

                      -- NEWTON'S SEVENTH LAW
Leave Link 9999 at Tue Jul 25 14:18:43 2000, MaxMem=    6291456 cpu:        .4
Job cpu time:  0 days  1 hours 32 minutes 43.7 seconds.
File lengths (MBytes):  RWF=   25 Int=    0 D2E=    0 Chk=    4 Scr=    1
Normal termination of Gaussian 98.
(Enter /apps/g98/l1.exe)
Link1:  Proceeding to internal job step number  2.
---------------------------------------------
#P Geom=AllCheck Guess=TCheck RHF/6-311G Freq
---------------------------------------------
1/6=100,10=4,18=10,29=7,30=1,38=1/1,3;
2//2;
3/5=4,6=6,11=1,25=1,30=1/1,2,3;
4/5=101,7=1/1;
5/5=2,7=400/2;
8/6=4,11=11,23=2/1;
10/13=10/2;
11/6=2,8=1,9=11,15=111,16=11/1,2,10;
10/6=1/2;
6/7=2,8=2,9=2,10=2,18=1,28=1/1;
7/8=1,10=1,25=1/1,2,3,16;
1/6=100,10=4,18=10,30=1/3;
99//99;
Leave Link    1 at Tue Jul 25 14:18:48 2000, MaxMem=          0 cpu:        .4
(Enter /apps/g98/l101.exe)

-------
mn4alo2
-------
No Z-matrix found on checkpoint file.
Cartesian coordinates read from the checkpoint file:
 mn4alo26.chk
Charge =  1 Multiplicity = 1
Mn,0,0.,0.,1.2415184449
O,0,-1.2509612871,0.7532461349,-0.3861332897
O,0,1.2509612871,0.7532461349,-0.3861332897
O,0,-1.2509612871,-0.7532461349,-0.3861332897
O,0,1.2509612871,-0.7532461349,-0.3861332897
Al,0,0.,1.2891461719,-1.6166912192
O,0,0.,0.,-2.74493001
Al,0,0.,-1.2891461719,-1.6166912192
O,0,-0.7334260971,0.,2.8319822455
O,0,0.7334260971,0.,2.8319822455
Recover connectivity data from disk.
Leave Link  101 at Tue Jul 25 14:18:51 2000, MaxMem=    6291456 cpu:        .3
(Enter /apps/g98/l103.exe)

Trust Radius=3.00D-01 FncErr=1.00D-07 GrdErr=1.00D-07
Number of steps in this run= 100 maximum allowed number of steps= 100.
GradGradGradGradGradGradGradGradGradGradGradGradGradGradGradGradGradGradGrad

Leave Link  103 at Tue Jul 25 14:18:53 2000, MaxMem=    6291456 cpu:        .5
```

```
(Enter /apps/g98/l202.exe)
                         Input orientation:
---------------------------------------------------------------------
Center     Atomic     Atomic              Coordinates (Angstroms)
Number     Number      Type              X           Y           Z
---------------------------------------------------------------------
   1         25           0         .000000     .000000    1.241518
   2          8           0       -1.250961     .753246    -.386133
   3          8           0        1.250961     .753246    -.386133
   4          8           0       -1.250961    -.753246    -.386133
   5          8           0        1.250961    -.753246    -.386133
   6         13           0         .000000    1.289146   -1.616691
   7          8           0         .000000     .000000   -2.744930
   8         13           0         .000000   -1.289146   -1.616691
   9          8           0        -.733426     .000000    2.831982
  10          8           0         .733426     .000000    2.831982
---------------------------------------------------------------------
                   Distance matrix (angstroms):
                    1          2          3          4          5
    1  Mn    .000000
    2  O    2.186672    .000000
    3  O    2.186672   2.501923    .000000
    4  O    2.186672   1.506492   2.920468    .000000
    5  O    2.186672   2.920468   1.506492   2.501923    .000000
    6  Al   3.135484   1.834766   1.834766   2.692683   2.692683
    7  O    3.986448   2.774204   2.774204   2.774204   2.774204
    8  Al   3.135484   2.692683   2.692683   1.834766   1.834766
    9  O    1.751425   3.345368   3.855054   3.345368   3.855054
   10  O    1.751425   3.855054   3.345368   3.855054   3.345368


                    6          7          8          9         10
    6  Al    .000000
    7  O    1.713132    .000000
    8  Al   2.578292   1.713132    .000000
    9  O    4.689404   5.624932   4.689404    .000000
   10  O    4.689404   5.624932   4.689404   1.466852    .000000
                         Interatomic angles:
     O2-Mn1-O3= 69.7914      Mn1-O2-O4= 69.8505      O3-Mn1-O4= 83.7932
      O3-O2-O4= 90.           O2-Mn1-O5= 83.7932      Mn1-O3-O5= 69.8505
      O2-O3-O5= 90.           O4-Mn1-O5= 69.7914       O2-O4-O5= 90.
      O3-O5-O4= 90.          Mn1-O2-Al6=102.11       Mn1-O3-Al6=102.11
     O2-Al6-O3= 85.9705     Mn1-O4-Al6= 79.2287      O4-O2-Al6=106.9826
     O3-Al6-O4= 77.8018     Mn1-O5-Al6= 79.2287      O2-Al6-O5= 77.8018
     O5-O3-Al6=106.9826      O5-O4-Al6= 62.3171      Mn1-O2-O7=106.3434
     Mn1-O3-O7=106.3434       O3-O2-O7= 63.1969      Mn1-O4-O7=106.3434
      O4-O2-O7= 74.2454       O3-O7-O4= 63.5199      Mn1-O5-O7=106.3434
      O2-O7-O5= 63.5199       O5-O3-O7= 74.2454       O5-O4-O7= 63.1969
     O2-Al6-O7=102.8213      O3-Al6-O7=102.8213      O4-Al6-O7= 74.3475
     O5-Al6-O7= 74.3475     Mn1-O2-Al8= 79.2287     Mn1-O3-Al8= 79.2287
     O3-O2-Al8= 62.3171     Mn1-O4-Al8=102.11        O2-O4-Al8=106.9826
     O3-Al8-O4= 77.8018     Mn1-O5-Al8=102.11        O2-Al8-O5= 77.8018
     O3-O5-Al8=106.9826      O4-Al8-O5= 85.9705     O2-Al6-Al8= 73.0174
    O3-Al6-Al8= 73.0174     O4-Al8-Al6= 73.0174     O5-Al8-Al6= 73.0174
     O2-Al8-O7= 74.3475      O3-Al8-O7= 74.3475      O4-Al8-O7=102.8213
     O5-Al8-O7=102.8213     Al6-O7-Al8= 97.6163      O2-Mn1-O9=115.873
     O3-Mn1-O9=156.2781      O4-Mn1-O9=115.873       O5-Mn1-O9=156.2781
```

```
    O2-Mn1-O10=156.2781     O3-Mn1-O10=115.873      O4-Mn1-O10=156.2781
    O5-Mn1-O10=115.873      Mn1-O9-O10= 65.2437
Stoichiometry    Al2MnO7(1+)
Framework group  C2V[C2(OMn),SGV(Al2),SGV'(O2),X(O4)]
Deg. of freedom    8
Full point group                C2V     NOp   4
Largest Abelian subgroup        C2V     NOp   4
Largest concise Abelian subgroup C2V     NOp   4
                        Standard orientation:
---------------------------------------------------------------------
Center     Atomic     Atomic              Coordinates (Angstroms)
Number     Number      Type              X           Y           Z
---------------------------------------------------------------------
   1         25           0         .000000     .000000    1.241518
   2          8           0       -1.250961     .753246    -.386133
   3          8           0        1.250961     .753246    -.386133
   4          8           0       -1.250961    -.753246    -.386133
   5          8           0        1.250961    -.753246    -.386133
   6         13           0         .000000    1.289146   -1.616691
   7          8           0         .000000     .000000   -2.744930
   8         13           0         .000000   -1.289146   -1.616691
   9          8           0        -.733426     .000000    2.831982
  10          8           0         .733426     .000000    2.831982
---------------------------------------------------------------------
Rotational constants (GHZ):      2.0770850       .6926506       .6845333
Isotopes: Mn-55,O-16,O-16,O-16,O-16,Al-27,O-16,Al-27,O-16,O-16
Leave Link  202 at Tue Jul 25 14:18:56 2000, MaxMem=    6291456 cpu:        .2
(Enter /apps/g98/l301.exe)
Standard basis: 6-311G (5D, 7F)
There are    66 symmetry adapted basis functions of A1  symmetry.
There are    24 symmetry adapted basis functions of A2  symmetry.
There are    39 symmetry adapted basis functions of B1  symmetry.
There are    43 symmetry adapted basis functions of B2  symmetry.
Crude estimate of integral set expansion from redundant integrals=1.142.
Integral buffers will be    262144 words long.
Raffenetti 1 integral format.
Two-electron integral symmetry is turned on.
  172 basis functions      333 primitive gaussians
   53 alpha electrons       53 beta electrons
      nuclear repulsion energy      1053.1477332317 Hartrees.
Leave Link  301 at Tue Jul 25 14:18:58 2000, MaxMem=    6291456 cpu:        .3
(Enter /apps/g98/l302.exe)
One-electron integrals computed using PRISM.
One-electron integral symmetry used in STVInt
NBasis=   172 RedAO= T  NBF=    66    24    39    43
NBsUse=   172 1.00D-04 NBFU=    66    24    39    43
Leave Link  302 at Tue Jul 25 14:19:08 2000, MaxMem=    6291456 cpu:       4.0
(Enter /apps/g98/l303.exe)
DipDrv:  MaxL=1.
Leave Link  303 at Tue Jul 25 14:19:20 2000, MaxMem=    6291456 cpu:        .8
(Enter /apps/g98/l401.exe)
Initial guess read from the checkpoint file:
 mn4alo26.chk
Guess basis functions will be translated to current atomic coordinates.
SCF Done:  E(RHF) =  -2156.91708621     A.U. after    1 cycles
            Convg  =     .2464D-08             -V/T =  1.9999
            S**2   =    .0000
```

```
KE= 2.157214188158D+03 PE=-7.219626022049D+03 EE= 1.852347014451D+03
Leave Link  502 at Tue Jul 25 14:20:51 2000, MaxMem=    6291456 cpu:      35.4
(Enter /apps/g98/l801.exe)
Range of M.O.s used for correlation:     1   172
NBasis=   172 NAE=    53 NBE=    53 NFC=     0 NFV=     0
NROrb=    172 NOA=    53 NOB=    53 NVA=   119 NVB=   119
Leave Link  801 at Tue Jul 25 14:21:00 2000, MaxMem=    6291456 cpu:        .0
(Enter /apps/g98/l1002.exe)
Minotr:  Closed-shell wavefunction.
         Direct CPHF calculation.
         Solving linear equations simultaneously.
         Using symmetry in CPHF.
         Requested convergence is 1.0D-08 RMS, and 1.0D-07 maximum.
         Secondary convergence is 1.0D-12 RMS, and 1.0D-12 maximum.
         Differentiating once with respect to electric field.
               with respect to dipole field.
         NewPWx=F KeepS1=T KeepF1=T KeepIn=T MapXYZ=F.
         MDV=  6291456
         Using IRadAn=       2.
Integrals replicated using symmetry in FoFDir.
MinBra= 0 MaxBra= 2 Meth= 1.
IRaf=       0 NMat=   3 IRICut=       1 DoRegI=T DoRafI=F ISym2E= 2 JSym2E=2.
         There are   3 degrees of freedom in the 1st order CPHF.
  3 vectors were produced by pass  0.
AX will form   3 AO Fock derivatives at one time.
  3 vectors were produced by pass  1.
  3 vectors were produced by pass  2.
  3 vectors were produced by pass  3.
  3 vectors were produced by pass  4.
  3 vectors were produced by pass  5.
  3 vectors were produced by pass  6.
  3 vectors were produced by pass  7.
  3 vectors were produced by pass  8.
  3 vectors were produced by pass  9.
  3 vectors were produced by pass 10.
  3 vectors were produced by pass 11.
  3 vectors were produced by pass 12.
  2 vectors were produced by pass 13.
  1 vectors were produced by pass 14.
Inv2:  IOpt= 1 Iter= 1 AM= 1.61D-12 Conv= 1.00D-12.
Inv2:  IOpt= 1 Iter= 2 AM= 1.26D-26 Conv= 1.00D-12.
Inverted reduced A of dimension  42 with in-core refinement.
Leave Link 1002 at Tue Jul 25 15:14:05 2000, MaxMem=    6291456 cpu:    1718.8
(Enter /apps/g98/l1101.exe)
Using compressed storage.
Will process  10 atoms per pass.
Leave Link 1101 at Tue Jul 25 15:14:25 2000, MaxMem=    6291456 cpu:       5.9
(Enter /apps/g98/l1102.exe)
Use density number 0.
Leave Link 1102 at Tue Jul 25 15:14:42 2000, MaxMem=    6291456 cpu:        .9
(Enter /apps/g98/l1110.exe)
Forming Gx(P) for the SCF density.
Integral derivatives from FoFDir, PRISM(SPDF).
Do as many integral derivatives as possible in FoFDir.
G2DrvN: MDV=   6291456.
G2DrvN: will do   10 atoms at a time, making    1 passes doing MaxLOS=2.
Petite list used in FoFDir.
```

```
MinBra= 0 MaxBra= 2 Meth= 1.
IRaf=       0 NMat=   1 IRICut=       1 DoRegI=T DoRafI=F ISym2E= 1 JSym2E=1.
FoFDir used for L=0 through L=2.
Leave Link 1110 at Tue Jul 25 15:22:38 2000, MaxMem=    6291456 cpu:     253.3
(Enter /apps/g98/l1002.exe)
Minotr:  Closed-shell wavefunction.
         Direct CPHF calculation.
         Solving linear equations simultaneously.
         Using symmetry in CPHF.
         Requested convergence is 1.0D-08 RMS, and 1.0D-07 maximum.
         Secondary convergence is 1.0D-12 RMS, and 1.0D-12 maximum.
         Differentiating once with respect to electric field.
               with respect to dipole field.
         Differentiating once with respect to nuclear coordinates.
         NewPWx=T KeepS1=F KeepF1=F KeepIn=F MapXYZ=F.
         MDV=  6291456
         Using IRadAn=       2.
Integrals replicated using symmetry in FoFDir.
MinBra= 0 MaxBra= 2 Meth= 1.
IRaf=       0 NMat=  18 IRICut=      18 DoRegI=T DoRafI=T ISym2E= 2 JSym2E=2.
         There are  18 degrees of freedom in the 1st order CPHF.
 18 vectors were produced by pass  0.
AX will form  18 AO Fock derivatives at one time.
 18 vectors were produced by pass  1.
 18 vectors were produced by pass  2.
 18 vectors were produced by pass  3.
 18 vectors were produced by pass  4.
 18 vectors were produced by pass  5.
 18 vectors were produced by pass  6.
 18 vectors were produced by pass  7.
 16 vectors were produced by pass  8.
  5 vectors were produced by pass  9.
  3 vectors were produced by pass 10.
Inv2:  IOpt= 1 Iter= 1 AM= 6.44D-12 Conv= 1.00D-12.
Inv2:  IOpt= 1 Iter= 2 AM= 2.42D-25 Conv= 1.00D-12.
Inverted reduced A of dimension 168 with in-core refinement.
Leave Link 1002 at Tue Jul 25 17:18:17 2000, MaxMem=    6291456 cpu:    3666.6
(Enter /apps/g98/l601.exe)
Copying SCF densities to generalized density rwf, ISCF=0 IROHF=0.
         Condensed to atoms (all electrons):
              1          2          3          4          5          6
 1  Mn  23.022378    .011057    .011057    .011057    .011057   -.003034
 2  O     .011057   8.685676   -.063444   -.053851    .007787    .127429
 3  O     .011057   -.063444   8.685676    .007787   -.053851    .127429
 4  O     .011057   -.053851    .007787   8.685676   -.063444   -.019004
 5  O     .011057    .007787   -.053851   -.063444   8.685676   -.019004
 6  Al   -.003034    .127429    .127429   -.019004   -.019004  10.530356
 7  O     .002042   -.027981   -.027981   -.027981   -.027981    .198567
 8  Al   -.003034   -.019004   -.019004    .127429    .127429    .017539
 9  O     .134704    .000353   -.000765    .000353   -.000765    .000928
10  O     .134704   -.000765    .000353   -.000765    .000353    .000928
              7          8          9         10
 1  Mn    .002042   -.003034    .134704    .134704
 2  O    -.027981   -.019004    .000353   -.000765
 3  O    -.027981   -.019004   -.000765    .000353
 4  O    -.027981    .127429    .000353   -.000765
 5  O    -.027981    .127429   -.000765    .000353
```

```
 6  Al    .198567    .017539    .000928    .000928
 7  O    8.904785    .198567    .000000    .000000
 8  Al    .198567  10.530356    .000928    .000928
 9  O     .000000    .000928   8.368277   -.062673
10  O     .000000    .000928   -.062673   8.368277
Total atomic charges:
             1
 1  Mn   1.668011
 2  O    -.667257
 3  O    -.667257
 4  O    -.667257
 5  O    -.667257
 6  Al   2.037865
 7  O   -1.192037
 8  Al   2.037865
 9  O    -.441339
10  O    -.441339
Sum of Mulliken charges=   1.00000
Atomic charges with hydrogens summed into heavy atoms:
             1
 1  Mn   1.668011
 2  O    -.667257
 3  O    -.667257
 4  O    -.667257
 5  O    -.667257
 6  Al   2.037865
 7  O   -1.192037
 8  Al   2.037865
 9  O    -.441339
10  O    -.441339
Sum of Mulliken charges=   1.00000
Electronic spatial extent (au):  <R**2>=  1643.7015
Charge=     1.0000 electrons
Dipole moment (Debye):
   X=      .0000    Y=      .0000    Z=   -14.5976  Tot=    14.5976
Quadrupole moment (Debye-Ang):
  XX=   -83.9526   YY=   -31.0173   ZZ=   -78.9556
  XY=      .0000   XZ=      .0000   YZ=      .0000
Octapole moment (Debye-Ang**2):
 XXX=      .0000  YYY=      .0000  ZZZ=   -54.7828  XYY=      .0000
 XXY=      .0000  XXZ=    -2.7554  XZZ=      .0000  YZZ=      .0000
 YYZ=   -64.1678  XYZ=      .0000
Hexadecapole moment (Debye-Ang**3):
XXXX=  -349.3323 YYYY=  -122.2186 ZZZZ= -1618.0233 XXXY=      .0000
XXXZ=      .0000 YYYX=      .0000 YYYZ=      .0000 ZZZX=      .0000
ZZZY=      .0000 XXYY=  -102.5755 XXZZ=  -278.7293 YYZZ=  -126.6544
XXYZ=      .0000 YYXZ=      .0000 ZZXY=      .0000
N-N= 1.053147733232D+03 E-N=-7.219626020337D+03  KE= 2.157214188158D+03
Symmetry A1   KE= 1.326260174761D+03
Symmetry A2   KE= 1.005677081562D+02
Symmetry B1   KE= 3.002663092493D+02
Symmetry B2   KE= 4.301199959918D+02
 Exact polarizability:  41.232    .000  59.114    .000    .000  64.137
Approx polarizability:  38.782    .000  55.474    .000    .000  51.217
Leave Link  601 at Tue Jul 25 17:18:33 2000, MaxMem=    6291456 cpu:       2.1
(Enter /apps/g98/l701.exe)
Compute integral second derivatives.
```

```
... and contract with generalized density number  0.
Leave Link  701 at Tue Jul 25 17:18:55 2000, MaxMem=    6291456 cpu:       8.7
(Enter /apps/g98/l702.exe)
L702 exits ... SP integral derivatives will be done elsewhere.
Leave Link  702 at Tue Jul 25 17:19:02 2000, MaxMem=    6291456 cpu:        .0
(Enter /apps/g98/l703.exe)
Compute integral second derivatives.
Integral derivatives from FoFDir, PRISM(SPDF).
Petite list used in FoFDir.
MinBra= 0 MaxBra= 2 Meth= 1.
IRaf=       0 NMat=   1 IRICut=       1 DoRegI=T DoRafI=F ISym2E= 1 JSym2E=1.
Leave Link  703 at Tue Jul 25 17:35:20 2000, MaxMem=    6291456 cpu:     526.5
(Enter /apps/g98/l716.exe)
Dipole        = 0.00000000D+00-1.15719151D-14-5.74308201D+00
Polarizability= 4.12321596D+01 3.53043816D-05 5.91138909D+01
                1.04396512D-07 9.98826294D-06 6.41369532D+01
HyperPolar    = 1.06588096D-04 6.74513025D-03 2.50365856D-03
                2.62820854D-02 2.40028389D+00 5.98795723D-04
               -2.30358756D+02-1.23178541D-04-3.14869447D-03
               -1.84317128D+02
Full mass-weighted force constant matrix:
Low frequencies --- -807.1059 -184.4962   -1.6312    -.5362    -.3960    -.0016
Low frequencies ---    2.6543    3.2413  126.7251
******    2 imaginary frequencies (negative Signs) ******
Harmonic frequencies (cm**-1), IR intensities (KM/Mole),
Raman scattering activities (A**4/AMU), Raman depolarization ratios,
reduced masses (AMU), force constants (mDyne/A) and normal coordinates:

                    1                      2                      3
                   B2                     A2                     ?A
Frequencies --  -807.1059              -184.4961               126.7251
Red. masses --    25.8733                16.1674                17.6647
Frc consts  --     9.9303                  .3242                  .1671
IR Inten    --   147.1434                  .0000                  .0602
Raman Activ --   498.1372                 1.1008                 5.1018
Depolar     --      .7500                  .7500                  .7500
Atom AN      X      Y      Z        X      Y      Z        X      Y      Z
  1  25      .00    .50    .00      .00    .00    .00      .00    .05    .00
  2   8      .20   -.19   -.02      .38   -.24    .15      .08   -.31    .18
  3   8     -.20   -.19   -.02      .38    .24   -.15     -.08   -.31    .18
  4   8     -.20   -.19    .02     -.38   -.24   -.15     -.08   -.31   -.18
  5   8      .20   -.19    .02     -.38    .24    .15      .08   -.31   -.18
  6  13      .00    .00   -.03      .09    .00    .00      .00    .03    .27
  7   8      .00   -.01    .00      .00    .00    .00      .00    .28    .00
  8  13      .00    .00    .03     -.09    .00    .00      .00    .03   -.27
  9   8      .00   -.47    .00      .00   -.21    .00      .00    .35    .00
 10   8      .00   -.47    .00      .00    .21    .00      .00    .35    .00
```

			4			5			6	
			?A			A2			B1	
Frequencies --			137.0861			140.8173			220.8628	
Red. masses --			16.5616			16.0456			23.3135	
Frc consts --			.1834			.1875			.6700	
IR Inten --			3.0834			.0000			7.6025	
Raman Activ --			.0750			2.0895			.3458	
Depolar --			.7500			.7500			.7500	
Atom	AN	X	Y	Z	X	Y	Z	X	Y	Z
1	25	.12	.00	.00	.00	.00	.00	.42	.00	.00
2	8	.20	.00	.24	-.06	.19	-.02	-.25	.00	-.19
3	8	.20	.00	-.24	-.06	-.19	.02	-.25	.00	.19
4	8	.20	.00	.24	.06	.19	.02	-.25	.00	-.19
5	8	.20	.00	-.24	.06	-.19	-.02	-.25	.00	.19
6	13	-.03	.00	.00	.05	.00	.00	-.16	.00	.00
7	8	-.36	.00	.00	.00	.00	.00	.31	.00	.00
8	13	-.03	.00	.00	-.05	.00	.00	-.16	.00	.00
9	8	-.38	.00	-.29	.00	-.65	.00	-.12	.00	-.37
10	8	-.38	.00	.29	.00	.65	.00	-.12	.00	.37

			7			8			9	
			A1			A2			B2	
Frequencies --			239.0881			260.7820			361.1459	
Red. masses --			23.2631			18.8673			17.3837	
Frc consts --			.7835			.7560			1.3358	
IR Inten --			8.5203			.0000			60.5772	
Raman Activ --			4.2786			.1025			.8124	
Depolar --			.1817			.7500			.7500	
Atom	AN	X	Y	Z	X	Y	Z	X	Y	Z
1	25	.00	.00	.37	.00	.00	.00	.00	.03	.00
2	8	.05	.00	-.20	-.10	-.24	-.34	.14	.23	.37
3	8	-.05	.00	-.20	-.10	.24	.34	-.14	.23	.37
4	8	.05	.00	-.20	.10	-.24	.34	-.14	.23	-.37
5	8	-.05	.00	-.20	.10	.24	-.34	.14	.23	-.37
6	13	.00	-.06	-.29	.36	.00	.00	.00	-.24	.07
7	8	.00	.00	-.39	.00	.00	.00	.00	-.19	.00
8	13	.00	.06	-.29	-.36	.00	.00	.00	-.24	-.07
9	8	.02	.00	.43	.00	-.05	.00	.00	-.03	.00
10	8	-.02	.00	.43	.00	.05	.00	.00	-.03	.00

			10			11			12	
			B2			B1			A1	
Frequencies --			368.9549			410.6606			438.8443	
Red. masses --			21.0289			16.7257			16.8142	
Frc consts --			1.6866			1.6619			1.9079	
IR Inten --			37.6520			162.5168			166.1045	
Raman Activ --			.4361			.9598			7.2443	
Depolar --			.7500			.7500			.4605	
Atom	AN	X	Y	Z	X	Y	Z	X	Y	Z
1	25	.00	.17	.00	.05	.00	.00	.00	.00	-.05
2	8	-.37	.08	-.10	.00	-.01	-.29	.33	.01	.30
3	8	.37	.08	-.10	.00	.01	.29	-.33	.01	.30
4	8	.37	.08	.10	.00	.01	-.29	.33	-.01	.30
5	8	-.37	.08	.10	.00	-.01	.29	-.33	-.01	.30
6	13	.00	-.23	.36	.17	.00	.00	.00	-.08	-.16
7	8	.00	.04	.00	-.77	.00	.00	.00	.00	-.33
8	13	.00	-.23	-.36	.17	.00	.00	.00	.08	-.16
9	8	.00	-.08	.00	.01	.00	-.03	-.03	.00	-.08
10	8	.00	-.08	.00	.01	.00	.03	.03	.00	-.08

			13			14			15	
			A1			B1			A2	
Frequencies --			504.6204			566.2173			572.8971	
Red. masses --			21.4032			18.0350			17.5969	
Frc consts --			3.2111			3.4067			3.4028	
IR Inten --			83.8815			.0903			.0000	
Raman Activ --			1.5821			2.0951			.2836	
Depolar --			.6103			.7500			.7500	
Atom	AN	X	Y	Z	X	Y	Z	X	Y	Z
1	25	.00	.00	.01	.22	.00	.00	.00	.00	.00
2	8	.23	.00	-.06	.06	-.03	-.06	-.26	-.08	.37
3	8	-.23	.00	-.06	.06	.03	.06	-.26	.08	-.37
4	8	.23	.00	-.06	.06	.03	-.06	.26	-.08	-.37
5	8	-.23	.00	-.06	.06	-.03	.06	.26	.08	.37
6	13	.00	.48	-.14	-.10	.00	.00	.27	.00	.00
7	8	.00	.00	.52	.01	.00	.00	.00	.00	.00
8	13	.00	-.48	-.14	-.10	.00	.00	-.27	.00	.00
9	8	.00	.00	.07	-.34	.00	.58	.00	.02	.00
10	8	.00	.00	.07	-.34	.00	-.58	.00	-.02	.00

			16			17			18	
			B1			B2			A1	
Frequencies --			653.2912			679.2080			692.9174	
Red. masses --			19.0696			17.8489			18.2335	
Frc consts --			4.7952			4.8514			5.1580	
IR Inten --			275.4570			142.0659			120.5999	
Raman Activ --			2.6260			4.9448			41.1363	
Depolar --			.7500			.7500			.0579	
Atom	AN	X	Y	Z	X	Y	Z	X	Y	Z
1	25	-.10	.00	.00	.00	-.07	.00	.00	.00	.03
2	8	.31	-.15	-.23	.33	.12	-.29	.33	-.16	-.25
3	8	.31	.15	.23	-.33	.12	-.29	-.33	-.16	-.25
4	8	.31	.15	-.23	-.33	.12	.29	.33	.16	-.25
5	8	.31	-.15	.23	.33	.12	.29	-.33	.16	-.25
6	13	-.35	.00	.00	.00	-.11	.25	.00	-.20	.24
7	8	.08	.00	.00	.00	.05	.00	.00	.00	.16
8	13	-.35	.00	.00	.00	-.11	-.25	.00	.20	.24
9	8	.09	.00	-.12	.00	.05	.00	-.02	.00	-.05
10	8	.09	.00	.12	.00	.05	.00	.02	.00	-.05

			19			20			21	
			A1			A1			B2	
Frequencies --			723.4912			828.9438			884.3345	
Red. masses --			20.5846			19.8130			18.5955	
Frc consts --			6.3483			8.0214			8.5682	
IR Inten --			29.8929			161.6000			158.3936	
Raman Activ --			38.8300			2.8769			.6316	
Depolar --			.5688			.0651			.7500	
Atom	AN	X	Y	Z	X	Y	Z	X	Y	Z
1	25	.00	.00	.34	.00	.00	.01	.00	.00	.00
2	8	-.04	.01	-.01	-.02	.11	.03	.00	.02	-.01
3	8	.04	.01	-.01	.02	.11	.03	.00	.02	-.01
4	8	-.04	-.01	-.01	-.02	-.11	.03	.00	.02	.01
5	8	.04	-.01	-.01	.02	-.11	.03	.00	.02	.01
6	13	.00	.05	-.03	.00	-.32	-.27	.00	-.28	-.21
7	8	.00	.00	-.02	.00	.00	.78	.00	.87	.00
8	13	.00	-.05	-.03	.00	.32	-.27	.00	-.28	.21
9	8	-.42	.00	-.51	-.02	.00	.00	.00	.00	.00
10	8	.42	.00	-.51	.02	.00	.00	.00	.00	.00

```
                    22                     23                     24
                    B1                     A1                     A1
Frequencies --   931.9663               951.4367               1010.8768
Red. masses --    16.2143                16.3475                 17.2651
Frc consts  --     8.2976                 8.7189                 10.3948
IR Inten    --    21.0174               106.6786                159.4245
Raman Activ --      .4809                51.2258                 27.9887
Depolar     --      .7500                  .5302                   .2664
Atom AN      X      Y      Z        X      Y      Z        X      Y      Z
  1  25     .01    .00    .00      .00    .00    .02      .00    .00    .18
  2   8    -.09   -.48    .07      .09    .47   -.08      .00   -.05    .02
  3   8    -.09    .48   -.07     -.09    .47   -.08      .00   -.05    .02
  4   8    -.09    .48    .07      .09   -.47   -.08      .00    .05    .02
  5   8    -.09   -.48   -.07     -.09   -.47   -.08      .00    .05    .02
  6  13     .10    .00    .00      .00    .00    .12      .00    .01   -.03
  7   8    -.01    .00    .00      .00    .00   -.09      .00    .00    .03
  8  13     .10    .00    .00      .00    .00    .12      .00   -.01   -.03
  9   8    -.01    .00    .00      .07    .00   -.03      .62    .00   -.30
 10   8    -.01    .00    .00     -.07    .00   -.03     -.62    .00   -.30

-------------------
- Thermochemistry -
-------------------
Temperature   298.150 Kelvin.  Pressure   1.00000 Atm.
Atom  1 has atomic number 25 and mass  54.93805
Atom  2 has atomic number  8 and mass  15.99491
Atom  3 has atomic number  8 and mass  15.99491
Atom  4 has atomic number  8 and mass  15.99491
Atom  5 has atomic number  8 and mass  15.99491
Atom  6 has atomic number 13 and mass  26.98154
Atom  7 has atomic number  8 and mass  15.99491
Atom  8 has atomic number 13 and mass  26.98154
Atom  9 has atomic number  8 and mass  15.99491
Atom 10 has atomic number  8 and mass  15.99491
Molecular mass:   220.86553 amu.
Principal axes and moments of inertia in atomic units:
                          1         2         3
    EIGENVALUES --   868.881722605.557662636.45482
          X             .00000    .00000   1.00000
          Y             .00000   1.00000    .00000
          Z            1.00000    .00000    .00000
THIS MOLECULE IS AN ASYMMETRIC TOP.
ROTATIONAL SYMMETRY NUMBER  2.
WARNING-- ASSUMPTION OF CLASSICAL BEHAVIOR FOR ROTATION
          MAY CAUSE SIGNIFICANT ERROR
ROTATIONAL TEMPERATURES (KELVIN)       .09968      .03324      .03285
ROTATIONAL CONSTANTS (GHZ)            2.07708      .69265      .68453
   2 IMAGINARY FREQUENCIES IGNORED.
Zero-point vibrational energy      70012.5 (Joules/Mol)
                                  16.73338 (Kcal/Mol)
WARNING-- EXPLICIT CONSIDERATION OF  13 DEGREES OF FREEDOM AS
          VIBRATIONS MAY CAUSE SIGNIFICANT ERROR
VIBRATIONAL TEMPERATURES:    182.33   197.24   202.60   317.77   343.99
         (KELVIN)            375.20   519.61   530.84   590.85   631.40
                             726.03   814.66   824.27   939.93   977.22
                             996.95  1040.94  1192.66  1272.35  1340.88
                            1368.90  1454.42
```

```
 Zero-point correction=                           .026666 (Hartree/Particle)
 Thermal correction to Energy=                    .035578
 Thermal correction to Enthalpy=                  .036523
 Thermal correction to Gibbs Free Energy=        -.007421
 Sum of electronic and zero-point Energies=          -2156.890420
 Sum of electronic and thermal Energies=             -2156.881508
 Sum of electronic and thermal Enthalpies=           -2156.880564
 Sum of electronic and thermal Free Energies=        -2156.924507
```

ISOTOPE FREQUENCY CALCULATION

```
%chk = mn4alo22
 %Nosave
 -----------------------------------------------------
 #p hf/6-311G Freq(ReadIso,ReadFC) Geom = AllCheck Test
 -----------------------------------------------------
 1/29=7,38=1/1;
 2//2;
 7/8=2,25=11/16;
 99/5=2/99;
 Leave Link    1 at Wed Oct  4 19:04:06 2000, MaxMem=         0 cpu:        .7
 (Enter /apps/g98/l101.exe)
 -------
 mn4alo2
 -------
 No Z-matrix found on checkpoint file.
 Cartesian coordinates read from the checkpoint file:
  mn4alo22.chk
 Charge =  1 Multiplicity = 1
 Mn,0,0.,0.,1.2415184449
 O,0,-1.2509612871,0.7532461349,-0.3861332897
 O,0,1.2509612871,0.7532461349,-0.3861332897
 O,0,-1.2509612871,-0.7532461349,-0.3861332897
 O,0,1.2509612871,-0.7532461349,-0.3861332897
 Al,0,0.,1.2891461719,-1.6166912192
 O,0,0.,0.,-2.74493001
 Al,0,0.,-1.2891461719,-1.6166912192
 O,0,-0.7334260971,0.,2.8319822455
 O,0,0.7334260971,0.,2.8319822455
 Recover connectivity data from disk.
 Leave Link  101 at Wed Oct  4 19:04:09 2000, MaxMem=   6291456 cpu:        .3
 (Enter /apps/g98/l202.exe)
```

```
                         Input orientation:
---------------------------------------------------------------------
Center     Atomic     Atomic              Coordinates (Angstroms)
Number     Number      Type              X           Y           Z
---------------------------------------------------------------------
   1         25           0         .000000     .000000    1.241518
   2          8           0       -1.250961     .753246    -.386133
   3          8           0        1.250961     .753246    -.386133
   4          8           0       -1.250961    -.753246    -.386133
   5          8           0        1.250961    -.753246    -.386133
   6         13           0         .000000    1.289146   -1.616691
   7          8           0         .000000     .000000   -2.744930
   8         13           0         .000000   -1.289146   -1.616691
   9          8           0        -.733426     .000000    2.831982
  10          8           0         .733426     .000000    2.831982
---------------------------------------------------------------------
                   Distance matrix (angstroms):
                      1          2          3          4          5
    1  Mn    .000000
    2  O    2.186672    .000000
    3  O    2.186672   2.501923    .000000
    4  O    2.186672   1.506492   2.920468    .000000
    5  O    2.186672   2.920468   1.506492   2.501923    .000000
    6  Al   3.135484   1.834766   1.834766   2.692683   2.692683
    7  O    3.986448   2.774204   2.774204   2.774204   2.774204
    8  Al   3.135484   2.692683   2.692683   1.834766   1.834766
    9  O    1.751425   3.345368   3.855054   3.345368   3.855054
   10  O    1.751425   3.855054   3.345368   3.855054   3.345368
                      6          7          8          9         10
    6  Al    .000000
    7  O    1.713132    .000000
    8  Al   2.578292   1.713132    .000000
    9  O    4.689404   5.624932   4.689404    .000000
   10  O    4.689404   5.624932   4.689404   1.466852    .000000
                        Interatomic angles:
     O2-Mn1-O3= 69.7914      Mn1-O2-O4= 69.8505      O3-Mn1-O4= 83.7932
      O3-O2-O4= 90.          O2-Mn1-O5= 83.7932      Mn1-O3-O5= 69.8505
      O2-O3-O5= 90.          O4-Mn1-O5= 69.7914       O2-O4-O5= 90.
      O3-O5-O4= 90.         Mn1-O2-Al6=102.11       Mn1-O3-Al6=102.11
     O2-Al6-O3= 85.9705     Mn1-O4-Al6= 79.2287      O4-O2-Al6=106.9826
     O3-Al6-O4= 77.8018     Mn1-O5-Al6= 79.2287      O2-Al6-O5= 77.8018
     O5-O3-Al6=106.9826      O5-O4-Al6= 62.3171      Mn1-O2-O7=106.3434
     Mn1-O3-O7=106.3434       O3-O2-O7= 63.1969      Mn1-O4-O7=106.3434
      O4-O2-O7= 74.2454       O3-O7-O4= 63.5199      Mn1-O5-O7=106.3434
      O2-O7-O5= 63.5199       O5-O3-O7= 74.2454       O5-O4-O7= 63.1969
     O2-Al6-O7=102.8213      O3-Al6-O7=102.8213      O4-Al6-O7= 74.3475
     O5-Al6-O7= 74.3475     Mn1-O2-Al8= 79.2287     Mn1-O3-Al8= 79.2287
     O2-O3-Al8= 62.3171     Mn1-O4-Al8=102.11        O2-O4-Al8=106.9826
     O3-Al8-O4= 77.8018     Mn1-O5-Al8=102.11        O2-Al8-O5= 77.8018
     O3-O5-Al8=106.9826      O4-Al8-O5= 85.9705     O2-Al6-Al8= 73.0174
    O3-Al6-Al8= 73.0174     O4-Al8-Al6= 73.0174     O5-Al8-Al6= 73.0174
     O2-Al8-O7= 74.3475      O3-Al8-O7= 74.3475      O4-Al8-O7=102.8213
     O5-Al8-O7=102.8213     Al6-O7-Al8= 97.6163      O2-Mn1-O9=115.873
     O3-Mn1-O9=156.2781      O4-Mn1-O9=115.873       O5-Mn1-O9=156.2781
    O2-Mn1-O10=156.2781     O3-Mn1-O10=115.873      O4-Mn1-O10=156.2781
    O5-Mn1-O10=115.873      Mn1-O9-O10= 65.2437
Stoichiometry    Al2MnO7(1+)
```

```
Framework group  C2V[C2(OMn),SGV(Al2),SGV'(O2),X(O4)]
Deg. of freedom    8
Full point group                C2V     NOp   4
Largest Abelian subgroup        C2V     NOp   4
Largest concise Abelian subgroup C2V     NOp   4
                        Standard orientation:
---------------------------------------------------------------------
Center     Atomic     Atomic              Coordinates (Angstroms)
Number     Number      Type              X           Y           Z
---------------------------------------------------------------------
   1         25             0         .000000     .000000    1.241518
   2          8             0       -1.250961     .753246    -.386133
   3          8             0        1.250961     .753246    -.386133
   4          8             0       -1.250961    -.753246    -.386133
   5          8             0        1.250961    -.753246    -.386133
   6         13             0         .000000    1.289146   -1.616691
   7          8             0         .000000     .000000   -2.744930
   8         13             0         .000000   -1.289146   -1.616691
   9          8             0        -.733426     .000000    2.831982
  10          8             0         .733426     .000000    2.831982
---------------------------------------------------------------------
Rotational constants (GHZ):      2.0770850       .6926506       .6845333
Isotopes: Mn-55,O-16,O-16,O-16,O-16,Al-27,O-16,Al-27,O-16,O-16
Leave Link  202 at Wed Oct  4 19:04:11 2000, MaxMem=    6291456 cpu:        .2
(Enter /apps/g98/l716.exe)
Electric field and nuclear coordinate derivatives read from checkpoint file.
Rotating electric field derivatives to standard orientation.
Dipole        = 6.72107685D-16-1.25239869D-14-5.74308201D+00
Polarizability= 4.12321596D+01 3.53043816D-05 5.91138909D+01
                1.04396510D-07 9.98826294D-06 6.41369532D+01
HyperPolar    = 1.06588096D-04 6.74513025D-03 2.50365856D-03
                2.62820854D-02 2.40028389D+00 5.98795723D-04
               -2.30358756D+02-1.23178541D-04-3.14869447D-03
               -1.84317128D+02
Rotating nuclear coordinate derivatives to standard orientation.
Atom  1 has atomic number 25 and mass  54.93805
Atom  2 has atomic number  8 and mass  15.99491
Atom  3 has atomic number  8 and mass  15.99491
Atom  4 has atomic number  8 and mass  15.99491
Atom  5 has atomic number  8 and mass  15.99491
Atom  6 has atomic number 13 and mass  26.98154
Atom  7 has atomic number  8 and mass  15.99491
Atom  8 has atomic number 13 and mass  26.98154
Atom  9 has atomic number  8 and mass  17.99916
Atom 10 has atomic number  8 and mass  17.99916
Full mass-weighted force constant matrix:
```

			1			2			3	
			B2			A2			?A	
Frequencies --			-794.5973			-183.5896			125.1201	
Red. masses --			27.7046			16.3235			18.1354	
Frc consts --			10.3062			.3242			.1673	
IR Inten --			141.5065			.0000			.1052	
Raman Activ --			485.9934			1.0459			5.0250	
Depolar --			.7500			.7500			.7500	
Atom	AN	X	Y	Z	X	Y	Z	X	Y	Z
1	25	.00	.53	.00	.00	.00	.00	.00	.03	.00
2	8	.21	-.20	-.02	.38	-.24	.16	.08	-.31	.19
3	8	-.21	-.20	-.02	.38	.24	-.16	-.08	-.31	.19
4	8	-.21	-.20	.02	-.38	-.24	-.16	-.08	-.31	-.19
5	8	.21	-.20	.02	-.38	.24	.16	.08	-.31	-.19
6	13	.00	-.01	-.03	.09	.00	.00	.00	.03	.27
7	8	.00	-.01	.00	.00	.00	.00	.00	.29	.00
8	13	.00	-.01	.03	-.09	.00	.00	.00	.03	-.27
9	8	.00	-.44	.00	.00	-.19	.00	.00	.33	.00
10	8	.00	-.44	.00	.00	.19	.00	.00	.33	.00

			4			5			6	
			?A			A2			B1	
Frequencies --			133.5809			134.0289			218.2458	
Red. masses --			17.6442			17.7148			23.6805	
Frc consts --			.1855			.1875			.6646	
IR Inten --			2.7420			.0000			6.7537	
Raman Activ --			.0799			1.9261			.3292	
Depolar --			.7500			.7500			.7500	
Atom	AN	X	Y	Z	X	Y	Z	X	Y	Z
1	25	.14	.00	.00	.00	.00	.00	.41	.00	.00
2	8	.20	.00	.25	-.06	.20	-.02	-.25	.00	-.20
3	8	.20	.00	-.25	-.06	-.20	.02	-.25	.00	.20
4	8	.20	.00	.25	.06	.20	.02	-.25	.00	-.20
5	8	.20	.00	-.25	.06	-.20	-.02	-.25	.00	.20
6	13	-.04	.00	.00	.06	.00	.00	-.16	.00	.00
7	8	-.37	.00	.00	.00	.00	.00	.32	.00	.00
8	13	-.04	.00	.00	-.06	.00	.00	-.16	.00	.00
9	8	-.35	.00	-.30	.00	-.64	.00	-.09	.00	-.35
10	8	-.35	.00	.30	.00	.64	.00	-.09	.00	.35

			7			8			9	
			A1			A2			B2	
Frequencies --			235.3875			260.7102			361.1057	
Red. masses --			23.7136			18.8770			17.4395	
Frc consts --			.7741			.7560			1.3398	
IR Inten --			7.8251			.0000			61.8534	
Raman Activ --			4.2639			.0935			.7913	
Depolar --			.1817			.7500			.7500	
Atom	AN	X	Y	Z	X	Y	Z	X	Y	Z
1	25	.00	.00	.36	.00	.00	.00	.00	.04	.00
2	8	.05	.00	-.20	-.10	-.24	-.34	.14	.23	.37
3	8	-.05	.00	-.20	-.10	.24	.34	-.14	.23	.37
4	8	.05	.00	-.20	.10	-.24	.34	-.14	.23	-.37
5	8	-.05	.00	-.20	.10	.24	-.34	.14	.23	-.37
6	13	.00	-.06	-.29	.36	.00	.00	.00	-.24	.08
7	8	.00	.00	-.40	.00	.00	.00	.00	-.19	.00
8	13	.00	.06	-.29	-.36	.00	.00	.00	-.24	-.08
9	8	.03	.00	.42	.00	-.05	.00	.00	-.03	.00
10	8	-.03	.00	.42	.00	.05	.00	.00	-.03	.00

```
                      10                     11                     12
                      B2                     B1                     A1
Frequencies --   368.7335               410.5909               438.4499
Red. masses --    21.0341                16.7236                16.8295
Frc consts  --     1.6850                 1.6611                 1.9062
IR Inten    --    36.6898               161.8690               162.6976
Raman Activ --      .4633                  .9835                 7.1454
Depolar     --      .7500                  .7500                  .4563
Atom AN      X      Y      Z        X      Y      Z        X      Y      Z
  1  25     .00    .17    .00      .05    .00    .00      .00    .00   -.04
  2   8    -.37    .07   -.11      .00   -.01   -.29      .33    .01    .30
  3   8     .37    .07   -.11      .00    .01    .29     -.33    .01    .30
  4   8     .37    .07    .11      .00    .01   -.29      .33   -.01    .30
  5   8    -.37    .07    .11      .00   -.01    .29     -.33   -.01    .30
  6  13     .00   -.22    .36      .17    .00    .00      .00   -.08   -.16
  7   8     .00    .04    .00     -.77    .00    .00      .00    .00   -.33
  8  13     .00   -.22   -.36      .17    .00    .00      .00    .08   -.16
  9   8     .00   -.08    .00      .02    .00   -.04     -.03    .00   -.08
 10   8     .00   -.08    .00      .02    .00    .04      .03    .00   -.08
                      13                     14                     15
                      A1                     B1                     A2
Frequencies --   504.3883               540.2146               572.8825
Red. masses --    21.4123                20.4012                17.5981
Frc consts  --     3.2096                 3.5078                 3.4029
IR Inten    --    86.6680                  .4896                  .0000
Raman Activ --     1.5223                 2.0931                  .2797
Depolar     --      .6097                  .7500                  .7500
Atom AN      X      Y      Z        X      Y      Z        X      Y      Z
  1  25     .00    .00    .01      .25    .00    .00      .00    .00    .00
  2   8     .23    .00   -.06      .05   -.02   -.05     -.26   -.08    .37
  3   8    -.23    .00   -.06      .05    .02    .05     -.26    .08   -.37
  4   8     .23    .00   -.06      .05    .02   -.05      .26   -.08   -.37
  5   8    -.23    .00   -.06      .05   -.02    .05      .26    .08    .37
  6  13     .00    .48   -.14     -.09    .00    .00      .27    .00    .00
  7   8     .00    .00    .52      .00    .00    .00      .00    .00    .00
  8  13     .00   -.48   -.14     -.09    .00    .00     -.27    .00    .00
  9   8     .00    .00    .07     -.34    .00    .58      .00    .01    .00
 10   8     .00    .00    .07     -.34    .00   -.58      .00   -.01    .00
                      16                     17                     18
                      B1                     B2                     A1
Frequencies --   652.2104               679.0511               691.3156
Red. masses --    19.1264                17.8660                19.4072
Frc consts  --     4.7936                 4.8538                 5.4647
IR Inten    --   275.0968               141.5854               145.9620
Raman Activ --     2.3298                 5.0606                53.9568
Depolar     --      .7500                  .7500                  .1336
Atom AN      X      Y      Z        X      Y      Z        X      Y      Z
  1  25    -.09    .00    .00      .00   -.07    .00      .00    .00    .20
  2   8     .32   -.15   -.23      .33    .12   -.29      .27   -.13   -.23
  3   8     .32    .15    .23     -.33    .12   -.29     -.27   -.13   -.23
  4   8     .32    .15   -.23     -.33    .12    .29      .27    .13   -.23
  5   8     .32   -.15    .23      .33    .12    .29     -.27    .13   -.23
  6  13    -.36    .00    .00      .00   -.11    .25      .00   -.16    .20
  7   8     .08    .00    .00      .00    .05    .00      .00    .00    .14
  8  13    -.36    .00    .00      .00   -.11   -.25      .00    .16    .20
  9   8     .07    .00   -.08      .00    .04    .00     -.22    .00   -.26
 10   8     .07    .00    .08      .00    .04    .00      .22    .00   -.26
```

```
                     19                     20                     21
                     A1                     A1                     B2
Frequencies --   696.8206               828.9069               884.3345
Red. masses --    21.4026                19.8158                18.5955
Frc consts  --     6.1229                 8.0218                 8.5682
IR Inten    --     1.1490               164.8494               158.3917
Raman Activ --    21.9689                 2.7015                  .6317
Depolar     --      .6785                  .0602                  .7500
Atom AN      X      Y      Z        X      Y      Z        X      Y      Z
  1  25      .00    .00    .29      .00    .00    .00      .00    .00    .00
  2   8     -.21    .09    .12     -.02    .11    .03      .00    .02   -.01
  3   8      .21    .09    .12      .02    .11    .03      .00    .02   -.01
  4   8     -.21   -.09    .12     -.02   -.11    .03      .00    .02    .01
  5   8      .21   -.09    .12      .02   -.11    .03      .00    .02    .01
  6  13      .00    .15   -.16      .00   -.32   -.27      .00   -.28   -.21
  7   8      .00    .00   -.09      .00    .00    .78      .00    .87    .00
  8  13      .00   -.15   -.16      .00    .32   -.27      .00   -.28    .21
  9   8     -.36    .00   -.37     -.02    .00    .00      .00    .00    .00
 10   8      .36    .00   -.37      .02    .00    .00      .00    .00    .00
                     22                     23                     24
                     B1                     A1                     A1
Frequencies --   931.9622               948.3531               962.5981
Red. masses --    16.2143                17.0601                18.7160
Frc consts  --     8.2975                 9.0401                10.2177
IR Inten    --    20.9632               207.5607                44.8379
Raman Activ --      .4842                53.6415                23.0483
Depolar     --      .7500                  .7091                  .0255
Atom AN      X      Y      Z        X      Y      Z        X      Y      Z
  1  25      .01    .00    .00      .00    .00    .10      .00    .00    .18
  2   8     -.09   -.48    .07      .09    .42   -.07     -.05   -.26    .05
  3   8     -.09    .48   -.07     -.09    .42   -.07      .05   -.26    .05
  4   8     -.09    .48    .07      .09   -.42   -.07     -.05    .26    .05
  5   8     -.09   -.48   -.07     -.09   -.42   -.07      .05    .26    .05
  6  13      .10    .00    .00      .00    .01    .10      .00    .01   -.09
  7   8     -.01    .00    .00      .00    .00   -.06      .00    .00    .07
  8  13      .10    .00    .00      .00   -.01    .10      .00   -.01   -.09
  9   8     -.01    .00    .00      .29    .00   -.15      .51    .00   -.26
 10   8     -.01    .00    .00     -.29    .00   -.15     -.51    .00   -.26

-------------------
- Thermochemistry -
-------------------
Temperature   298.150 Kelvin.  Pressure   1.00000 Atm.
Atom  1 has atomic number 25 and mass  54.93805
Atom  2 has atomic number  8 and mass  15.99491
Atom  3 has atomic number  8 and mass  15.99491
Atom  4 has atomic number  8 and mass  15.99491
Atom  5 has atomic number  8 and mass  15.99491
Atom  6 has atomic number 13 and mass  26.98154
Atom  7 has atomic number  8 and mass  15.99491
Atom  8 has atomic number 13 and mass  26.98154
Atom  9 has atomic number  8 and mass  17.99916
Atom 10 has atomic number  8 and mass  17.99916
Molecular mass:   224.87402 amu.
Principal axes and moments of inertia in atomic units:
```

```
                           1         2         3
    EIGENVALUES --   876.581732724.954772748.15193
          X            .00000    .00000   1.00000
          Y            .00000   1.00000    .00000
          Z           1.00000    .00000    .00000
THIS MOLECULE IS AN ASYMMETRIC TOP.
ROTATIONAL SYMMETRY NUMBER  2.
WARNING-- ASSUMPTION OF CLASSICAL BEHAVIOR FOR ROTATION
          MAY CAUSE SIGNIFICANT ERROR
ROTATIONAL TEMPERATURES (KELVIN)       .09881      .03179      .03152
ROTATIONAL CONSTANTS (GHZ)            2.05884      .66230      .65671
   2 IMAGINARY FREQUENCIES IGNORED.
Zero-point vibrational energy      69257.8 (Joules/Mol)
                                  16.55300 (Kcal/Mol)
WARNING-- EXPLICIT CONSIDERATION OF  13 DEGREES OF FREEDOM AS
          VIBRATIONS MAY CAUSE SIGNIFICANT ERROR
VIBRATIONAL TEMPERATURES:    180.02   192.19   192.84   314.01   338.67
         (KELVIN)            375.10   519.55   530.52   590.75   630.83
                             725.70   777.24   824.25   938.38   977.00
                             994.64  1002.56  1192.61  1272.35  1340.88
                            1364.46  1384.96

Zero-point correction=                           .026379 (Hartree/Particle)
Thermal correction to Energy=                    .035358
Thermal correction to Enthalpy=                  .036302
Thermal correction to Gibbs Free Energy=        -.007868
Sum of electronic and zero-point Energies=         -2156.890707
Sum of electronic and thermal Energies=            -2156.881728
Sum of electronic and thermal Enthalpies=          -2156.880784
Sum of electronic and thermal Free Energies=       -2156.924954
```

VITA

Rakesh Radhakrishnan was born in Thrissur, Kerala, India in 1973. He moved to Dubai, United Arab Emirates in 1978 and did his 1st to 12th grade schooling at the Indian High School in Dubai. He arrived in the U.S in 1991 for his undergraduate education at the University of Virginia, Charlottesville, VA. After the completion of his BS in chemical engineering at UVA, he entered the graduate program in chemical engineering at Virginia Polytechnic Institute and State University, Blacksburg, VA in 1995. Shortly thereafter, he joined the Environmental Catalysis and Materials Laboratory headed up by Dr S. Ted Oyama in the chemical engineering department at VPI. He was awarded an M. Eng degree in chemical engineering from VPI in 1999. His dissertation deals with the study of the structure and ozone decomposition reactivity of supported manganese oxides. This dissertation completes the requirements for his PhD degree and he is expected to officially graduate from VPI in May 2001. He is expected to join the research group headed up by Bill Thomson at Washington State University, Pullman, WA as a postdoctoral research associate in March 2001.